

## **INFORMATION TO USERS**

**This manuscript has been reproduced from the microfilm master. UMI films the text directly from the original or copy submitted. Thus, some thesis and dissertation copies are in typewriter face, while others may be from any type of computer printer.**

**The quality of this reproduction is dependent upon the quality of the copy submitted. Broken or indistinct print, colored or poor quality illustrations and photographs, print bleedthrough, substandard margins, and improper alignment can adversely affect reproduction.**

**In the unlikely event that the author did not send UMI a complete manuscript and there are missing pages, these will be noted. Also, if unauthorized copyright material had to be removed, a note will indicate the deletion.**

**Oversize materials (e.g., maps, drawings, charts) are reproduced by sectioning the original, beginning at the upper left-hand corner and continuing from left to right in equal sections with small overlaps.**

**Photographs included in the original manuscript have been reproduced xerographically in this copy. Higher quality 6" x 9" black and white photographic prints are available for any photographs or illustrations appearing in this copy for an additional charge. Contact UMI directly to order.**

**Bell & Howell Information and Learning  
300 North Zeeb Road, Ann Arbor, MI 48106-1346 USA  
800-521-0600**

**UMI<sup>®</sup>**



# **RECOVERING GOLD FROM HIGH DENSITY GANGUES WITH KNELSON CONCENTRATORS**

***Bo Zhang***

**Department of Mining and Metallurgical Engineering  
McGill University  
Montreal, Canada**

**March, 1998**

**A thesis submitted to the Faculty of Graduate Studies and Research  
in partial fulfilment of the requirements for the degree of Master of Engineering**

**©Bo Zhang, 1998**



National Library  
of Canada

Acquisitions and  
Bibliographic Services

395 Wellington Street  
Ottawa ON K1A 0N4  
Canada

Bibliothèque nationale  
du Canada

Acquisitions et  
services bibliographiques

395, rue Wellington  
Ottawa ON K1A 0N4  
Canada

*Your file* *Votre référence*

*Our file* *Notre référence*

The author has granted a non-exclusive licence allowing the National Library of Canada to reproduce, loan, distribute or sell copies of this thesis in microform, paper or electronic formats.

The author retains ownership of the copyright in this thesis. Neither the thesis nor substantial extracts from it may be printed or otherwise reproduced without the author's permission.

L'auteur a accordé une licence non exclusive permettant à la Bibliothèque nationale du Canada de reproduire, prêter, distribuer ou vendre des copies de cette thèse sous la forme de microfiche/film, de reproduction sur papier ou sur format électronique.

L'auteur conserve la propriété du droit d'auteur qui protège cette thèse. Ni la thèse ni des extraits substantiels de celle-ci ne doivent être imprimés ou autrement reproduits sans son autorisation.

0-612-50680-0

**Canada**

## **ABSTRACT**

**This research documents the use of a 7.6 cm laboratory Knelson Concentrator (LKC) to determine the amount of gravity recoverable gold (GRG) content in ores and evaluate the performance of gravity circuits, with an emphasis on high gangue density. Two approaches were used to minimize the effect of the high gangue density in estimating the GRG content, oversize removal and 2 : 1 ratio dilution with silica flour.**

**The amount of GRG was determined in four ore samples with an established protocol, yielding values of 35% to 78% of total gold. Lower density auriferous silver (kustelite) and high density pyrite gangue lower the amount of GRG in Aur's Louvicourt ore, 29 - 35%, mostly below 300 µm. Gangue density is somewhat lower at Agnico-Eagle La Ronde Division (AELRD), about 50% sulphide, and its GRG content is 50%, also mostly below 300 µm. The ore of Snip contains more GRG, 58 - 61%, of only slightly coarser size, but in a lower density gangue. Barrick Gold's East Malartic contains very coarse gold, and as a result the GRG content cannot be determined accurately. It stands in the range of 60 to 75%. East Malartic has a gangue density similar to AELRD's.**

**Kustelite and the high density gangue at Louvicourt explain the very poor performance of gravity recovery, only 1.8% stage recovery and 4.2% total recovery. Overload of the Plant Knelson Concentrator (PKC) was detected at AELRD and frequent concentrate removal was suggested. At East Malartic, only the table tails were investigated, and contained a very high amount of GRG, 91%. Table recovery was itself high, above 95%. This suggests that the high density of the ore and coarse PKC feed (screened at 1.7 mm) only make it possible for the PKC to recover highly recoverable GRG. Samples from the Chimo gravity circuit were also processed, but results were marred by very unreliable fire assays. Nevertheless, it was concluded that the 76 cm PKC was very probably underfed, which limited its ability to recover gold.**

**Results from the AELRD, Louvicourt and East Malartic mills suggest that the typical**

**Knelson-based gravity circuit which can recover one half to two thirds of GRG from low density gangues will only recover one third to two fifths of the GRG from high density gangues. Simulation of gold recovery at AELRD showed that the high circulating loads - 1100%, were a significant factor in reducing gold recovery by gravity.**

## RÉSUMÉ

Ce projet porte sur l'utilisation d'un concentrateur Knelson de laboratoire (CKL) de 7,6 cm de diamètre pour déterminer la quantité d'or récupérable par gravimétrie (ORG) présent dans les minerais et évaluer la performance de circuits gravimétriques d'or, surtout pour des minerais à gangue de densité élevée. Pour minimiser l'effet de la densité de gangue élevée, on a utilisé deux procédés, l'élimination des particules plus grossières et la dilution avec de la farine de silice.

On a déterminé la quantité d'ORG de quatre échantillons de minerais en utilisant un protocole reconnu; ces échantillons contenaient de 35 à 78% d'ORG. Dans le minerai Louvicourt d'Aur, la densité moins élevée du minéral porteur d'or, la kustelite, et la densité élevée de la gangue (surtout de la pyrite) limitent la quantité d'ORG à 29-35%, surtout au-dessous de 300 µm. La densité de la gangue est moins élevée pour le minerai de la division La Ronde d'Agnico Eagle (DLRAE), qui contient 50% de pyrite, et qui contient 50% d'ORG, également en grande partie plus fin que 300 µm. Le minerai de Snip contient plus d'ORG, 58-61%, légèrement plus grossier, et dans une gangue moins dense. Le minerai d'Est Malartic, dont la densité de la gangue se rapproche de celle de DLRAE, contient de l'or très grossier, ce qui rend très ardue la détermination de la quantité d'ORG, qui de l'ordre de 60 à 75%.

A Louvicourt, la présence de kustelite et la densité élevée de la gangue permettent d'expliquer la récupération gravimétrique très basse, 1.8% de l'alimentation du Knelson et 4.2% de l'or total. A DLRAE, on a pu déterminer que le concentrateur Knelson d'usine (CKU) était moins efficace en fin de cycle de récupération; nous avons recommandé d'en raccourcir la durée. A Est Malartic, la récupération de la table à secousses est élevée, plus de 95%, et le CKL récupère des rejets de cette table 91% de l'or présent. Ces deux observations permettent de conclure que le CKU ne récupère que de l'ORG très facilement récupérable. L'étude du circuit de Chimo a permis de conclure que le CKU de 76 cm était probablement sous-alimenté, et pourrait récupérer plus d'or à taux d'alimentation plus élevé.

Les études de DLRAE, Louvicourt et Est Malartic suggèrent que le circuit de récupération gravimétrique Knelson typique, qui permet de récupérer de 50 à 67% de l'ORG de minerais à densité de gangue peu élevée, ne récupérera que du tiers aux deux cinquièmes de l'ORG d'un minerai dont la gangue est de densité élevée. A DLRAE, une simulation du circuit de récupération gravimétrique a permis de conclure que la charge circulante, élevée (700 - 1100%) du circuit de broyage affectait l'efficacité du circuit gravimétrique.



## 摘要

本论文阐明了使用 7.6 cm 试验室尼尔森选矿机来测定金的重选可回收金的含量和评价黄金选厂的重选回路效率的研究。本试验着重于对含高比重脉石的金矿选矿。为了最大限度地减小高比重脉石在重选可回收金测定过程中的影响，本研究应用了两种新方法，即：筛除给矿中过粗级别法和用石英粉按 2:1 稀释法。本试验还模拟了 Agnico Eagle 金矿重选回路的黄金回收工艺。

对四种金矿石的试验室研究结果表明，重选可回收金的含量在 35 - 78% 范围。在 Aur's Louvicourt 矿石中，由于低于纯金比重的金银矿石 (kustelie) 和高比重的黄铁矿脉石的影响，重选可回收金仅为 29 - 35%，而且大部分是在小于 300 微米级别。对于 Agnico Eagle 矿石，硫化矿含量占 50%，重选可回收金主要在细粒级别。Cominco's snip 矿石含可重选金较高，达 58 - 61%，且稍细，脉石比重较低。相反于 Snip 矿石，Barrick Gold's East Malartic 含有很粗的金，它的脉石比重相近于 Agnico Eagle，重选可回收金约为 60 - 70%。

在 Aur's Louvicourt 金矿，由于金银矿石的存在和高比重的脉石矿物影响，现厂重选回路的效率非常差，作业回收率为 1.8%，总回收率为 4.2%。在 Agnico Eagle，现厂尼尔森给矿过量，建议增加排精矿的次数。对于 Barrick Gold's East Malartic，本研究仅对摇床尾矿进行了试验，发现很高的可重选回收金，达 91%。现厂摇床本身回收率可达 95%。这些结果说明了现厂尼尔森可有效地处理高比重和粗粒给料(达 1.7 mm)。同时对 Chimo 金矿重选回路的矿进行了试验，但是由于不可靠的品位化验数据，使得整体结果难以分析。然而，可以认为现厂 76 cm 尼尔森回收率低的主要原因很可能是由于它的给矿量太低。

## **ACKNOWLEDGEMENTS**

First of all I would like to express my sincerest gratitude and my deepest appreciation to my supervisor Prof. Dr. A.R. Laplante for his wise guidance, thoughtful advice, constant encouragement and financial assistance throughout the course of this research.

I acknowledge Prof. J.A. Finch, Z. Xu and R. Rao for their suggestions and invaluable discussions.

I thank Mr. R. Langlois, for both his technical expertise in the laboratory and friendship; my fellow colleagues and graduate students, Mr. L. Huang and Mr. J. Lin, for their endless technical discussions; Dr. M. Noaparast, for his helpful advice on both laboratory techniques and slide preparation; Mr. A. Farzanegan, for his suggestion to improve my computer skill; J. Paventi, for his help in sampling at Agnico-Eagle (La Ronde Division); and all the mineral processing group, for countless discussions at group meetings and seminars and their friendship.

I would like to extend my appreciation to the people of Cominco's Snip, Barrick Gold's East Malartic, Aur's Louvicourt, and Agnico-Eagle's La Ronde Division for their support and provision of gold samples and fire assaying services. I shall always be thankful to the Natural Sciences and Engineering Research Council of Canada for the generous research funding.

Finally, I am very grateful to my parents, F. Wu and P. Zhang, for their love and encouragement; to my lovely five-year old son, Michael Liu, for his kind cooperation during my study and to my husband, Dr. Qingxia Liu, for his thought-provoking discussions, and unfailing support, encouragement and understanding.

# TABLE OF CONTENTS

ABSTRACT .....	i
RESUME .....	iii
ZAIYAO .....	v
ACKNOWLEDGEMENTS .....	vi
TABLE OF CONTENTS .....	vii
LIST OF FIGURES .....	x
LIST OF TABLES .....	xii
LIST OF ABBREVIATIONS .....	xiii
LIST OF VARIABLES .....	xiv
<b>CHAPTER 1</b>	
<b>INTRODUCTION</b> .....	1
1.1 Background .....	1
1.2 Objectives .....	3
1.3 Structure of the Thesis .....	4
<b>CHAPTER 2</b>	
<b>LITERATURE REVIEW</b> .....	5
2.1 Knelson Concentrator .....	5
2.2 Applications of the 7.5 cm Knelson Concentrator .....	9
2.2.1 Measuring GRG in ore samples .....	9
2.2.2 A Methodology for Studying Gravity Circuits .....	11
2.2.3 Predicting GRG Recovery .....	12
2.3 Previous Studies of Gold Gravity Circuits with LKC Methodology .....	15
2.3.1 Studying circuits with a low density gangue .....	15
2.3.2 Studies of gravity circuits with a high density gangue .....	16
2.3.3 Upgrading of Primary Concentrates .....	16

<b>CHAPTER 3</b>	
<b>CHARACTERIZING ORES FOR GRAVITY RECOVERABLE GOLD</b> .....	18
3.1 Introduction .....	18
3.2 Cominco's Snip Operations .....	18
3.2.1 Description of Snip .....	18
3.2.2 Materials and experiments .....	20
3.2.3 Results and discussion .....	21
3.3 Aur Louvicourt .....	28
3.3.1 Information .....	28
3.3.2 Results and discussion .....	28
3.4 East Malartic .....	30
3.4.1 Information .....	30
3.4.2 Results and discussion .....	31
3.5 Agnico-Eagle La Ronde Division .....	33
3.5.1 Introduction .....	33
3.5.2 Results and discussion .....	33
3.6 Discussion and conclusion .....	34
<b>CHAPTER 4</b>	
<b>STUDYING GOLD GRAVITY CIRCUITS</b> .....	36
4.1 Introduction .....	36
4.1.1 Gravity circuits .....	36
4.1.2 Objectives .....	37
4.2 Aur Louvicourt .....	37
4.2.1 Introduction .....	37
4.2.2 Materials and method .....	38
4.2.3 Results and discussion .....	39
4.3 Agnico-Eagle La Ronde Division .....	43
4.3.1 Introduction .....	43
4.3.2 Sampling procedure .....	43
4.3.3 Results and discussion .....	44
4.3.4 Conclusions .....	50
4.4 Barrick's Est Malartic .....	51
4.4.1 Introduction .....	51
4.4.2 Previous work on the 76 cm (30") CD Knelson .....	53
4.4.3 Materials and Method .....	53
4.4.4 Results and discussion .....	54
4.5 Cambior's Chimo Mine .....	57
4.5.1 Description of grinding and gravity circuit .....	57
4.5.2 Sampling and processing with a laboratory Knelson .....	58
4.5.3 Results and discussion .....	59

<b>CHAPTER 5</b>	
<b>SIMULATION OF GOLD GRAVITY RECOVERY AT AELRD</b> .....	<b>62</b>
<b>CHAPTER 6</b>	
<b>CONCLUSIONS AND FUTURE WORK</b> .....	<b>69</b>
6.1 Summary and Conclusions .....	69
6.1.1 Gravity Recoverable Gold .....	69
6.1.2 Plant Work .....	70
6.1.3 Recovering gold from high gangue density ores .....	72
6.2 Recommendations .....	72
6.3 Future Work .....	73
<b>REFERENCES</b> .....	<b>74</b>
<b>APPENDIX A</b>	
<b>TEST RESULTS OF GRAVITY RECOVERABLE</b>	
<b>GOLD DETERMINATIONS</b> .....	<b>1-1</b>
Appendix A-1 GRG tests of Snip2 Ball mill feed .....	1-2
Appendix A-2 GRG tests of Aur Louvicourt2 .....	1-5
Appendix A-3 GRG tests of Barrick East Malartic .....	1-8
<b>APPENDIX B</b>	
<b>TESTS RESULTS OF THE GRAVITY CIRCUIT INVESTIGATIONS</b> .....	<b>2-1</b>
Appendix B-1 Aur Louvicourt .....	2-2
Appendix B-2 Agnico-Eagle La Ronde Division .....	2-6
Appendix B-3 Table tail at Barrick East Malartic .....	2-11
Appendix B-4 Cambior's Chimo .....	2-14
<b>APPENDIX C</b>	
<b>MASS BALANCE OF SIZE DISTRIBUTIONS AT</b>	
<b>THE GRAVITY CIRCUIT OF CHIMO MINE</b> .....	<b>3-1</b>

## LIST OF FIGURES

Figure 1-1. Different routes for gold extraction .....	2
Figure 2-1 A schematic diagram of the laboratory Knelson Concentrator with a conventional bowl .....	6
Figure 2-2 The supply of fluidizing water .....	7
Figure 2-3 Schematic of a gold recovery circuit within a grinding circuit .....	14
Figure 3-1 The flowsheet of Cominco's Snip gold operations .....	19
Figure 3-2 Procedure for measuring GRG content with a LKC .....	21
Figure 3-3 Cumulative passing as a function of particle size for Snip2 .....	22
Figure 3-4 Size-by-size recoveries for each stage for Snip2 .....	23
Figure 3-5 Cumulative gold recoveries for each of the three stages for Snip2 .....	24
Figure 3-6 GRG content as a function of $F_{80}$ for Snip1 and Snip2 .....	24
Figure 3-7 Size-by-size cumulative recoveries for Snip1 and Snip2 .....	25
Figure 3-8 Cumulative gold recovery as a function of particle size for Hemlo2 .....	26
Figure 3-9 Comparison of the GRG content for both Hemlo1 and Hemlo2 .....	27
Figure 3-10 Cumulative recovery for each of the three stages of Aur2 .....	29
Figure 3-11 Comparison of GRG between Aur1 and Aur2 .....	30
Figure 3-12 Cumulative recovery for each of the three stages of Est Malartic .....	32
Figure 3-13 Cumulative gold recovery as a function of particle size for AELRD .....	34
Figure 3-14 Comparison of the GRG in ores .....	35
Figure 4 - 1 A general flowsheet of KC-based or jig-based gravity circuit .....	37
Figure 4-2 Size-by-size gold recoveries for PKC feeds of Aur Louvicourt .....	39
Figure 4-3 Size-by-size gold recoveries for PKC concentrates of Aur Louvicourt ...	40

Figure 4-4	Size-by-size gold recoveries for PKC tails of Aur Louvicourt	40
Figure 4-5	Size-by-size head grades of the PKC tail samples of Aur Louvicourt	41
Figure 4-6	Sampling of Agnico-Eagle La Ronde Division	44
Figure 4-7	Size-by-size gold recoveries of diluted and undiluted PKC feed of AELRD	47
Figure 4-8	Size-by-size gold recoveries of diluted and undiluted PKC tail of AELRD	47
Figure 4-9	GRG content of PKC feed and tails over a three-hour recovery cycle of AELRD	49
Figure 4-10	Size distributions of PKC feed of AELRD	50
Figure 4-11	Block flowsheet of Barrick's Est Malartic	52
Figure 4-12	Size-by-size gold recovery of table tails of Barrick's Est Malartic	55
Figure 4-13	Size distributions of the table tails of Barrick's Est Malartic	56
Figure 4-14	A flowsheet of the grinding and gravity circuit of Chimo Mine	57
Figure 4-15	Size distributions of PKC feed, tail and flash cell tail of Chimo Mine	60
Figure 4-16	GRG content of PKC feed, tail and flash cell tail of Chimo Mine	61
Figure 5-1	Schematic of a gold gravity circuit (recovery from cyclone underflow)	62
Figure 5-2	Selection function vs. particle size	64
Figure 5-3	Cumulative GRG size distribution of simulated and measured gravity stage recovery	68

## LIST OF TABLES

Table 3-1 Processing conditions of LKC for GRG measurement for Aur2 .....	28
Table 3-2 Processing conditions of LKC for GRG measurement for East Malartic ...	31
Table 3-3 Processing conditions of LKC for GRG measurement for AELRD .....	33
Table 4-1 Processing conditions and recovery of the LKC tests for Aur Louvicourt ..	38
Table 4-2 Processing conditions of LKC tests for AELRD .....	44
Table 4-3 The LKC test results for AELRD .....	45
Table 4-4 Table tails test results for Barrick East Malartic .....	54
Table 4-5 Processing conditions with LKC for Chimo .....	58
Table 4-6 Overall results of LKC tests for Chimo .....	59
Table 5-1 R, P, and GRG matrix F (% of the total gold in feed) and main diagonal of C matrices .....	63
Table 5-2 Uncorrected H matrix .....	66
Table 5-3 Correction factors for the H matrix .....	66
Table 5-4 Measured and simulated recovery .....	67
Table 6-1 Recommendations for gold plants .....	73



## **LIST OF ABBREVIATIONS AND ACRONYMS**

**adj. - adjusted**

**AELRD - Agnico-Eagle La Ronde Division**

**C/O, Cyclone O/F - cyclone overflow**

**C/U - Cyclone underflow**

**calc. - calculated**

**Conc. - Concentrate**

**Cyclone U2 - Cyclone under flow2**

**Cyclone U1 - Cyclone under flow1**

**dis. - distribution**

**Dist'n - distribution of total gold**

**GRG - Gravity recoverable gold**

**KC - Knelson Concentrator**

**LKC - Laboratory Knelson Concentrator**

**meas. - measured**

**PCU - Plant cyclone underflow**

**PKC - Plant Knelson Concentrator**

**Rec. - gold recovery**

**S.D. - Standard deviation**

**SAG disc. - SAG mill discharge**

**Screen o/s - screen oversize**

**Screen u/s - screen undersize**

**Wt. - weight**

## LIST OF VARIABLES

- C - the classification efficiency curve of the cyclones for GRG
- D - a column matrix of the free gold flowrate into the concentrate
- F - a column matrix representing what amount of gold of the ore reports as GRG in each size class (in %, g/t or oz/st)
- $G_c$  - PKC concentrate grade, g/t
- $G_f$  - PKC feed grade, g/t
- $G_{ff}$  - fresh feed grade, g/t
- $G_t$  - PKC tails grade, g/t
- H - a matrix representing the breakage of GRG into finer size classes
- I - identify matrix
- $L^{GRG}$  - GRG loss, %
- $M_c$  - the mass of PKC concentrate, kg
- P - a diagonal matrix expressing the probability that free gold in size class  $i$  will be pre-concentrated to be fed to the separator
- $Q_f$  - PKC dry feed rate, t/h
- R - a diagonal matrix of free gold recovery in size class  $i$
- $R$  - gold recovery, %
- $R_f$  - GRG content of feed
- $R_{PKC}$  - PKC gold gravity recovery, %
- $R_t$  - GRG content of tails
- $R_{Total}$  - total gold recovery, %
- $\sigma$  - standard deviation
- $\sigma^2$  - variance
- $T_c$  - PKC cycle time, hour

# **CHAPTER 1**

## **INTRODUCTION**

### **1.1 Background**

The dramatic rise in the price of gold over the past twenty years has been the driving force of intense exploration and production activity all over the world. This activity has resulted not only in the development of many new conventional ore bodies, but also in the delineation and development of more refractory ores and the continuing search for improvements in the economics of existing operations [Prasad et al., 1991].

Processes for the extraction of gold have improved significantly over the years. The latest developments in gold processing technology have not only focused on the economics in terms of increased efficiency and reduced costs but also on environmental aspects, particularly with regard to gaseous emissions and liquid effluent discharges from gold plants. There is also wide spread interest in replacing cyanide by lixivants which are nontoxic and environmentally safe.

On the basis of mineralogy, gold ores can be classified as two main types: non refractory (oxides, clay minerals) and refractory (sulfides, carbonaceous) [Haque, 1987]. The various process treatment options available for gold processing are illustrated in Figure 1-1.

Many refractory gold ores do not respond very well to gravity separation and conventional cyanidation. Such ores are characterized by low gold recoveries and high cyanide consumptions when subjected to direct cyanide leaching. These ores are subjected to oxidation pretreatments such as roasting, chemical oxidation, pressure oxidation and bio-oxidation prior to cyanidation.

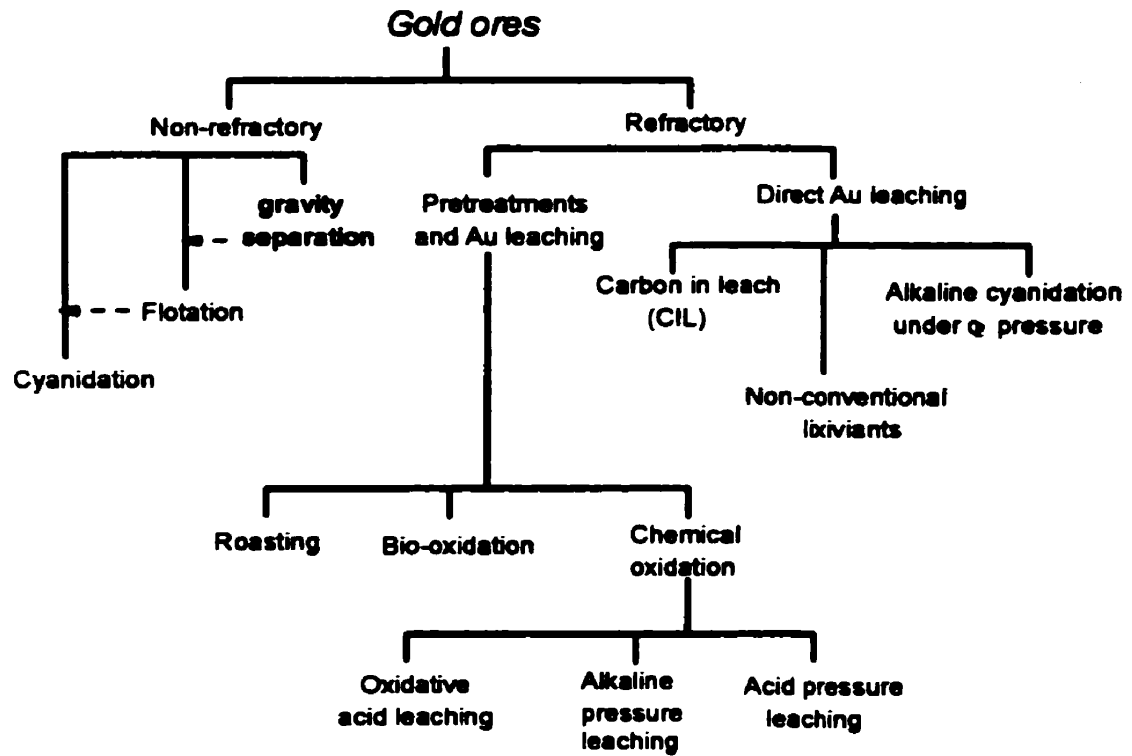


Figure 1-1. Different routes for gold extraction

Non-refractory ores have been economically processed by gravity, flotation, and conventional cyanidation, or a combination there of. More recently, gold gravity separation has experienced a resurgence in popularity, because of a number of technological innovations. Of these, the Knelson Concentrators<sup>1</sup>, semi-continuous centrifuge units, are easily the most significant. These are characterized by high gold recoveries over a wide size range [Knelson, 1992; Laplante, 1993; Poulter, Fitzmaurice and Steward, 1994].

Knelsons have been used in gravity separation in gold plants for over fifteen years and at laboratory scale for gold ore and circuit evaluations for over nine years [Laplante, Shu and

<sup>1</sup>For the sake of brevity, Knelson Concentrators will in this monograph be referred to as Knelsons, KC, or PKC for plant units and LKC for laboratory units.

Marois, 1992; Liu, 1989]. The Laboratory Knelson Concentrator (LKC) methodology developed at McGill University has been used for determining the amount of gravity recoverable gold (GRG) in relatively large samples and evaluate the performance of gravity circuits in gold plants [Liu, 1989; Laplante and Shu, 1992].

The efficiency of the LKC has been systematically studied with both natural<sup>2</sup> and synthetic<sup>3</sup> feeds, varying operating variables such as feed rate, density, size distribution and fluidizing water pressure [Laplante, Shu, Marois, 1996; Laplante, Huang and Harris, 1996]. It was demonstrated that gangue density is the most significant variable. High density gold ores containing massive sulphide minerals or tramp iron may also yield a lower gold recovery with a PKC. Although this is partly offset by the effect of the high gold circulating load, the net effect may well be that different design criteria must be used to achieve the same efficiency as that reported for low density gangues. Alternatively, it may prove necessary to lower projected gravity recoveries.

## **1.2 Objectives**

Previous studies of gold gravity circuits at McGill have used and progressively improved the LKC methodology. The objectives of this work are to take advantage of these tools developed in house to:

- (1). determine the GRG content in a few selected ores, most of which have a high density;
- (2). evaluate existing gravity circuits, most of which process ores with a high density gangue;
- (3). apply and evaluate proposed improvements of the LKC methodology for high density gangues;
- (4). investigate further the effect of high density gangues using a gravity circuit simulator developed at McGill.

---

<sup>2</sup>Natural feeds: samples obtained from gold plants or mines.

<sup>3</sup>Synthetic feeds: silica (80% passing 100 and 600  $\mu\text{m}$ ) and magnetite (to mimic low and high density gangue) of various size distributions with fine (8-75  $\mu\text{m}$ ) or coarse (8-425  $\mu\text{m}$ ) tungsten (to mimic gold).

In order to achieve these, both existing but yet unpublished data and new data will be used.

### **1.3 Structure of the Thesis**

After this introduction, the use of the LKC to measure GRG in ores and study gold gravity circuits will be reviewed in Chapter two. A set of GRG tests on samples from Snip, Aur's Louvicourt, Barrick Gold's East Malartic and Agnico-Eagle's La Ronde Division (AELRD) will be presented in Chapter three. Chapter four will focus on the study of gravity circuits at Louvicourt, AELRD, East Malartic, and Cambior's Chimo Mine. In Chapter five, simulation of the gravity circuit at AELRD will be presented and discussed. Finally, conclusions, recommendations and future work will be described in Chapter six.

## **CHAPTER 2**

### **LITERATURE REVIEW**

#### **2.1 Knelson Concentrator**

Knelson Concentrators Inc. started its business in 1980. Knelsons can be used in concentrating a very dense and very low grade phase or mineral from its gangue. The Knelson Concentrator has been successfully used in gold recovery from various ore types, from both placers and hard rock sources [Knelson, 1988, and 1992; Laplante, Shu and Marois, 1996; Luis, Meza, Willy Hartmann and Carlos, 1994; Hendriks and Chevalier, 1995; and Cloutt, 1995]. It has achieved worldwide acceptance, because of its remarkable ability to achieve very high gold recoveries over a wide size range. Its mechanical and operational simplicity and reliability also contribute significantly to its success.

The 7.5 cm unit, or LKC, was commercialized in 1988 and rapidly became a valuable laboratory tool for evaluating the performance of gravity circuits in gold plants and measuring the amount of gravity recoverable gold (GRG) in ores.

A schematic diagram of the LKC with a conventional bowl is shown in Figure 2-1. It uses a ringed bowl, called inner bowl, rotating clockwise in a pressurized water jacket. Within each ring there are holes through which high pressure water is injected tangentially from the outside of the inner bowl. Fluidization of the slurried feed takes place at the surface of each ring in which a gold concentrate bed gradually builds up.

Theoretically, the LKC achieves a centrifuge force sixty times that of gravity - i.e. 60Gs. In practice, the number of "Gs" varies from the high forties at the bottom ring to the low seventies at the top. The feed (minerals with slurring water) is added via a downcomer to the bottom of the inner bowl. The minerals are immediately imparted a high rotating speed. This velocity creates a significant centrifuge force which maximizes interaction

between particles. The most significant phenomenon is the percolation of the finer particles through the flowing slurry. This phenomenon is aided by the dispersive pressure created by the shear rates generated by the highly turbulent flow inside the Knelson.

The low density gangue particles are rejected by the fluidization water and flow of slurry on the surface of the riffles to the top of the bowl. The rejects are then collected in a circular launder and discharged. The unit is periodically stopped and the concentrate manually recovered (the process is automated in the production scale "CD" units).

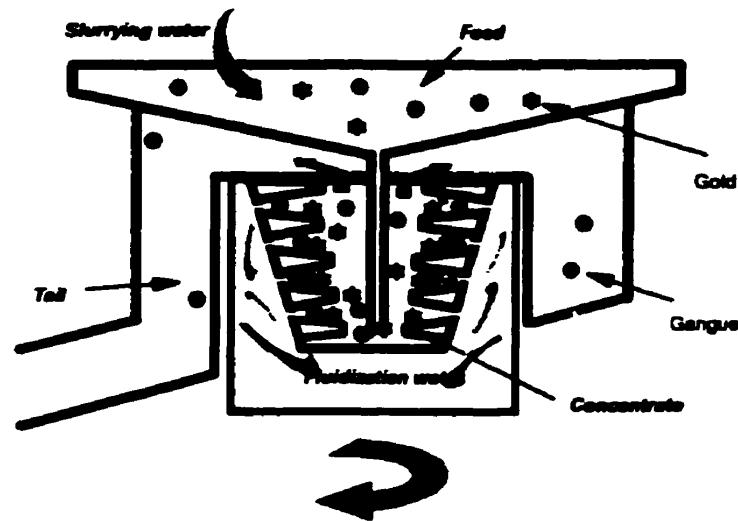


**Figure 2-1 A schematic diagram of the laboratory Knelson Concentrator with a conventional bowl**

It has been suggested that the feed slurry never attains the same speed as the bowl. If it did, it would be stagnant - i.e. separation would not happen at all [Knelson, 1988]. In the KC, the compaction of the concentrating bed is avoided by tangential injection of high pressure fluidized water, as illustrated by Figure 2-2.

The water assists in keeping particles shifting within the active concentrate bed; as



long as this action takes place, so does concentration of dense particles such as gold.

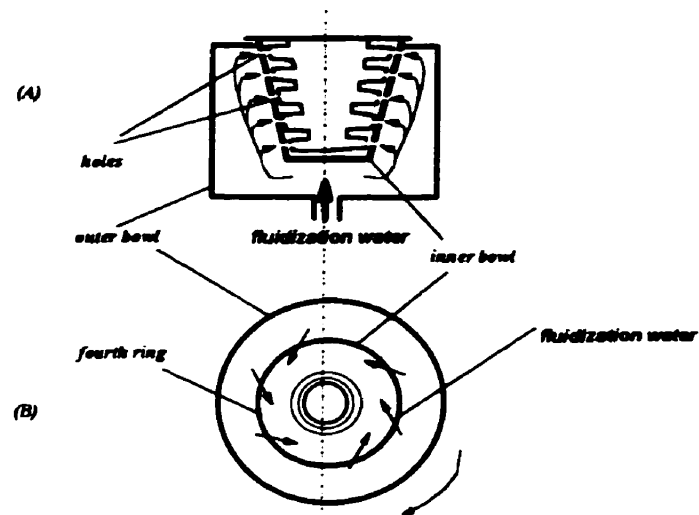


**Figure 2-2 The supply of fluidizing water**  
**(A) Cross-sectional view (B) Top view of the fourth ring**

Knelson claimed that this action takes place in most of the ring [Knelson, 1988]. Detailed photographic studies of the concentrate of individual rings suggest otherwise [Huang, 1996]. Huang's test work was performed at very high feed grade, 5% tungsten (used as a surrogate for gold). At the optimum fluidized water flow rate, concentrate within each ring was almost completely unfluidized (very small fluidized channels were observed at the water injection points). The concentrate of heavies laid at the surface of the rings (inner section, closest to the rotation axis) rather than at their bottom (outer section, closest to the wall of the bowl). Thus the role of fluidization water must be re-defined more accurately: clearly, it does not completely fluidize the rings, nor does it fluidize the flowing slurring (this is achieved by the rather turbulent upward flow of material). Fluidization water is most important in the critical zone between the non-fluidized portion of each ring (nearly all of its volume) and the flowing slurry. This active recovery zone must accommodate incremental concentrate, whilst rejecting fine light particles (that would easily percolate) and protecting

the accumulated concentrate from erosion by coarse or/and dense particles. Huang showed that for -212  $\mu\text{m}$  feeds, bed erosion problems were negligible. For a dense and coarse feed, -1.7 mm hematite, fluidization water could not protect the bed effectively, whereas, for coarse light gangue (-1.7 mm silica), this protection was effective for part of the loading cycle tested (long enough for very long recovery cycles with actual gold ores).

From a separation point, Knelson [1988] suggested that the fluidized particulate bed might make a small gold particle replace a large gangue mineral which has a lower density than that of gold. Huang found no evidence for this replacement. He rather proposed a model of concentrate build-up until it becomes too exposed to the flowing slurry, at which point erosion begins [Huang, 1996]. Larger gold particles, which have a high percolation velocity, are often concentrated in the bottom rings. Finer gold particles are harder to concentrate and are often recovered further up the rings.

At low feed rate and gangue density, it has been reported that GRG recovery is virtually independent of particle size [Liu, 1989; Laplante and Shu, 1993; Vincent, 1996]. Nevertheless, some studies with synthetic and natural feeds with LKCs and PKCs suggest that the unit's ability to recover GRG may have a size dependency. This has been verified with both the 7.6 and 76 cm Knelson [Laplante, Shu and Marois, 1996; Laplante, Vincent, Noaparast and Woodcock, 1995]. Increasing gangue density or feed rate can lower fine GRG recovery, because of its lower percolation velocity and high vulnerability to erosion from the concentrate bed [Laplante, Shu and Marois, 1996; Laplante, Huang and Harris, 1996].

A dip in recovery at intermediate particle sizes was also reported both for natural and synthetic feeds [Laplante, Shu and Marois, 1996; Laplante et al, 1995]. The original hypothesis for this phenomenon was linked to the flakiness of this material, but non-flaky synthetic feeds have reproduced the phenomenon [Lin, 1995], which refutes the flakiness theory and suggests a percolation problem which is consistent with known percolation studies

[Bridgwater and Ingram, 1971; Bridgwater, Sharpe and Stocker, 1969; Masliyah and Bridgwater, 1974]. As the coarsest tungsten or gold particles can displace gangue of equivalent particle size, and exhibit a very high recovery, percolation problems only affect recovery at intermediate size.

## **2.2 Applications of the 7.5 cm Knelson Concentrator**

The Knelson is capable of recovering finer gold than can be recovered by older gravity units such as jigs, spirals and sluices [Knelson, 1994, Laplante, 1993]. With the advent of the plant Knelson Concentrator (PKC), industrial gravity circuits were redefined in terms of how fine gold could be recovered. Thus arose the need to develop laboratory tools of at least similar capability to recover fine GRG, in order to characterize ores and plant performance adequately. Putz (1994) and Vincent (1996) discussed the rationale of using the LKC to evaluate circuit performance and determine if it is ore, equipment or flowsheet limited. Typically, the LKC is used as an instrument to measure the GRG content of samples 5 to 50 kg in size. Although this methodology is, strictly speaking, applied only to mineral samples, it can also be used to study gravity circuits, when applied to samples of feed, tails and concentrates from these circuits.

### **2.2.1 Measuring GRG in ore samples**

#### **Sampling and sample processing**

The GRG content represents GRG that can be recovered from an ore by gravity in a very small yield under ideal conditions [Laplante, 1996]. The amount of GRG in an ore is the most important factor in determining its potential for gravity recovery. Most of the GRG is liberated gold in the size range of 10 to 1000  $\mu\text{m}$ . GRG may also be gold not completely liberated from its gangue minerals which reports into the concentrate bed of Knelson. However, studies on table tails by Huang suggest that little GRG fits this category. Fine liberated gold, especially below 25  $\mu\text{m}$ , may not be gravity recoverable [Woodcock, 1994]. Huang used SEM studies to determine that almost all of the non-GRG gold in table tails was

indeed liberated below 25  $\mu\text{m}$ . Therefore, it may be concluded that the GRG content is mostly liberated gold and some coarse incompletely liberated gold with minor amounts of gangue minerals.

Considering the sampling error, Woodcock found that the biggest problem in laboratory test work aimed at measuring GRG content is the nugget effect in sampling and assaying, whilst natural gold traps in pilot grinding and gravity circuits constitute another bias. The nugget effect is a result of the low concentration of the valuable material coupled with the small number of particles that make up this concentration, thereby making it difficult to obtain a representative sample. If all the "nuggets" were to report to a concentrate to be fully assayed, then the nugget effect would not exist. This concentration is what the LKC-based methodology aims to achieve.

The procedure to characterize GRG in an ore sample consists of a three-step recovery, each successive step with the tails of the previous one at a finer grind. The first step is normally performed on a representative 40-60 kg sample at 100% -850  $\mu\text{m}$  (20 mesh), the second on 24 kg at 50% -75  $\mu\text{m}$  (200 mesh), and the third on 21 kg at 80% -75  $\mu\text{m}$  (200 mesh). The concentrate of each stage is fully assayed size-by-size (as is part of the tails), hence the claim that the nugget effect is eliminated [Woodcock, 1994; Laplante, Vincent and Luinstra, 1996].

### Industrial applications

Woodcock [1994] has tested nine ores and one grinding circuit, Les Mines Casa Berardi. The full Casa Berardi grinding circuit was adjusted to fit mass balance constraints; only minor adjustments were made to sized data. The ore contained 72% GRG, of which 88% was finer than 74  $\mu\text{m}$ . Gold was fine and the coarsest was liberated below 300  $\mu\text{m}$ . Woodcock also showed reasonable reproducibility for the GRG determination test, but with limited data. More will be presented in Chapter three.

As for the characterization of GRG, to study gold gravity circuits, samples of the relevant streams (typically the fresh feed and product of the grinding circuit, and feed, tails and concentrate of recovery units) are extracted and their GRG content determined size-by-size. Unlike the GRG test for ores, the samples are never ground, as the performance of circuit units should be based on the GRG available in its feed, rather than "potential" GRG that would be liberated by further grinding.

### **2.2.2 A methodology for studying gravity circuits**

The study of gold gravity circuits also suffers from the statistical problem of determining the behaviour of particles occurring at a very low frequency. This problem becomes particularly acute with increasing particle size [Laplante, 1992]. For example, a 100 gold particle sample, which yields a 10% fundamental sampling error, would require, at a grade of 15 g/t Au, only 5 kg of 300–425  $\mu\text{m}$  (40/50 mesh) material, but 1000 kg of 850–1200  $\mu\text{m}$  (14/20 mesh) fraction. A previous study concluded that gold content can be determined with reasonable accuracy overall and size-by-size below 300  $\mu\text{m}$  when processing samples of 5 to 15 kg for most applications [Laplante and Shu, 1992].

Again, the LKC is used, for the reasons described in the previous section. The application is more stringent in this case, as samples are processed only once: hence, it is critical to insure that the LKC recovers all GRG.

There is evidence, however, that the LKC becomes less efficient as gangue density increases [Laplante, Shu and Marois, 1996], or becomes too coarse [Putz, 1994]. This implies that the LKC methodology, when applied to samples more refractory to gravity recovery because of their gangue, must be refined: suitable feed preparation is required.

The first approach that was tested was to dilute high density samples with silica to lower their gangue density. The dilution ratio used was originally 4:1, with 212  $\mu\text{m}$  silica.

Subsequently, the dilution protocol was modified to use a 2:1 ratio with -75  $\mu\text{m}$  silica (silica flour). This approach always yields a lower density and finer gangue, and will be used for this work. Shu (1993), Putz (1994) and Huang (1996) showed that feed dilution will increase LKC recovery, especially below 75  $\mu\text{m}$ . Although dilution can minimize the effect of high density gangue at laboratory scale, it is unpractical at plant scale.

A second size preparation method, the removal of oversize (often mostly barren) was also used. Woodcock [1994] achieved an increase of gold recovery from 48% to 64% with removal of the +212  $\mu\text{m}$  fractions on a plant cyclone underflow (PCU) sample from Les Mines Casa Berardi. Other benefits of oversize removal include a higher grade concentrate, lower water consumption (lower fluidization water requirements), easier secondary upgrading and decreased circulating load [Laplante et al, 1994].

It is concluded that with LKC methodology at laboratory scale, oversize removal is the preferred method over dilution, which suffers the following drawbacks: (i) more mass must be processed, (ii) sample grade is lowered - i.e. by a factor of 3 with a 2:1 dilution ratio, and (iii) natural information is lost (e.g. the sample size distribution). Thus, whenever possible, oversize removal will be used to maximize LKC recovery in this work. Dilution will be used only when the size distribution of the original sample is too fine to benefit from oversize removal.

### **2.2.3 Predicting GRG Recovery**

#### **Behaviour of gold**

Gold, which has a hardness intermediate between that of lead and copper, should display an intermediate behaviour in grinding units. The main characteristic of gold is its malleability: gold is easily pounded into flaky shapes by grinding; these flakes can also fold into spherical and cylindrical shapes [Banisi, Laplante and Marois, 1991]. In laboratory studies, gold has been found to grind much slower than silica (used as a standard gangue), and flattens, to the extent that it can move into coarser size classes. Evidence of folding is not so

readily generated, as transfers to finer size classes can also be caused by breakage, but this phenomenon is supported by some photographic evidence [Banisi, Laplante and Marois, 1991] and a very large data base based of the grinding of lead (used as a surrogate for gold) [Noaparast, 1996]. At plant scale, gold grinds more slowly than most ores: at Hemlo Golden Giant, twenty times slower for the 850-1200  $\mu\text{m}$  fraction and six times slower at the 37-53  $\mu\text{m}$ . For typical circuits, more than 95% of the gravity recoverable gold that is ground to finer size classes is still gravity recoverable [Noaparast and Laplante, 1993]. In the absence of gravity, free gold disappears slowly from coarser size classes through grinding, and reappears in finer size classes.

Gold, particularly GRG, has a distinct behaviour in hydrocyclones, where it reports to the underflow stream even at very small size. Often, as much as 98 and even 99% of the GRG in a cyclone feed reports to its underflow, even if most of this GRG is finer than 100  $\mu\text{m}$  [Banisi, Laplante and Marois, 1991].

### Predicting GRG

Conditions specific to an ore can be investigated with a model of GRG recovery developed at McGill. This model makes it possible to estimate the performance of circuits with large gold circulating loads and relatively low unit recoveries, or with high recoveries on a bleed of the circulating load [Laplante, Woodcock and Noaparast, 1994].

The model represents gold liberation, breakage and classification behaviour and applies pre-concentration and recovery performance curves to gravity-recoverable gold to predict overall recovery.

For a circuit made of a single mill in closed circuit with recovery from the mill discharge, the model is based on the block diagram shown in Figure 2-3. Size-by-size recovery can be calculated as in equation 2-1.

$$\underline{D} = PR[I-HC(I-PR)]^{-1} \underline{F} \quad (2-1)$$

where  $\underline{D}$  is a column matrix of the free gold flowrate into the concentrate (its elements,  $d_i$ , sum up to the total gold recovery);  $P$  and  $R$  are diagonal matrices expressing the probability that free gold in size class  $i$  will first be fed (Pre-concentrated) to the separator, and then Recovered. Both are set when designing a gravity circuit by the selection and size of concentration equipment. The  $H$  matrix represents the breakage of GRG into finer size classes.  $C$  is the classification efficiency curve of the cyclones for GRG. The  $\underline{F}$  column matrix represents what amount of gold of the ore shows as GRG in each size class (in %, g/t or oz/st). This model will be used in Chapter 5, and input data described in detail.

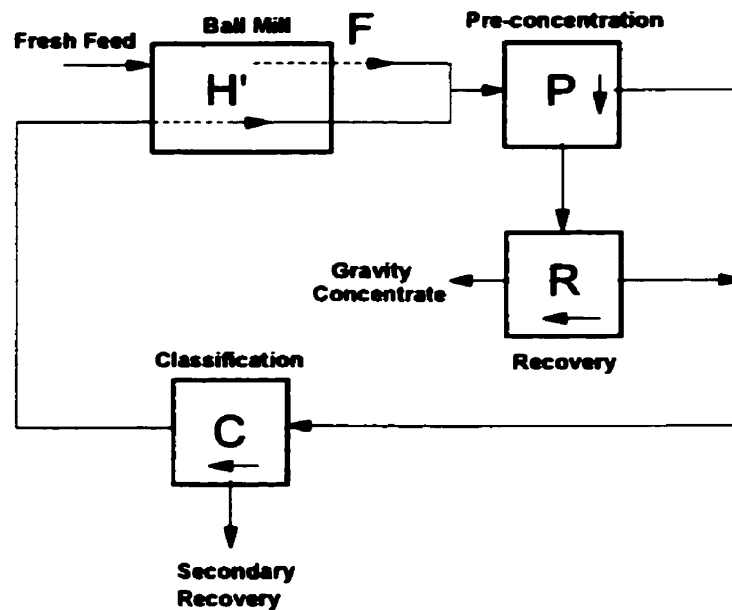


**Figure 2-3 Schematic of a gold recovery circuit within a grinding circuit**

[Laplante et al. 1994]

The model has been used for many case studies, such as Casa Berardi, AELRD, MSV, and Meston Resources [Laplante, Vincent., Noaparast, Woodcock, Boulet, Dubé and Robitaille, 1995; Laplante, Woodcock and Noaparast, 1994].



**2.3 Previous Studies of Gold Gravity Circuits with the LKC Methodology****2.3.1 Studying circuits with a low density gangue**

Most studies performed at McGill have focused on low density gangue applications, the more common and successful ones.

The data from Vincent's research work at Meston Resources, whose ore contains 3% sulphide [Woodcock, 1994], shows that 42% of the total gold in the sample of plant Knelson feed and 75% of the GRG was recovered. It is suggested that the 76 cm PKCs at Meston recovered at least 50% of the GRG in their feed over the full size range tested [Vincent, 1997]. Vincent reported that a 51 cm (20") Knelson at Aur's Aurbel mill with a throughput of 4-7 t/h yielded a GRG recovery between 70 and 93%, depending on throughput. At Hemlo, a 76 cm PKC was reported to recover 20-25% GRG with a throughput of 60 t/h [Vincent, 1997].

The link between unit and circuit performance is gold's circulating load, which can be very high. For instance, for an ore circulating load of 300%, the circulating load of gold can be as high as 2500% [Agar, 1993; Laplante, Liu and Cauchon, 1993]. For a unit processing the full circulating load, a stage recovery of 2% would yield a circuit recovery of 50%. This high "leverage" adds to the difficulty of measuring and predicting the performance of gravity circuits.

The LKC methodology was also applied to jig circuits. For Placer-Dome's South Porcupine mill, Putz reported a 40 - 50% GRG recovery with a circulating load of 2000% [Putz, 1994], for four Duplex jigs in parallel. Unit recovery was around 2%. Jig concentrates contained virtually no very fine ( $-37 \mu\text{m}$ ) gold. From detailed data at Cominco's Snip, Vincent indicated that jig performance was strongly linked to particle size. Virtually all gold recovered of the jig above  $150 \mu\text{m}$  was unliberated and rejected by the table. Jig recovery below  $75 \mu\text{m}$  was poor and almost no gold was recovered below  $25 \mu\text{m}$  [Vincent, 1997].

Stage recovery varied between 2 and 4%.

### **2.3.2 Studies of gravity circuits with a high density gangue**

Relatively few studies of gold gravity circuits or units processing high density gangues are available. Laboratory studies, however, indicate that high density gangues can reduce both the recovery and capacity of the Knelson. Laplante, Shu and Marois report that for a LKC treating a primary cyclone underflow sample from Hemlo Mines, recovery,  $R$ , is equal to:

$$R = 114.6 - 9.1 \pm 0.9 \cdot D - 0.14 \pm 0.03 D Q^4 \quad (2-2)$$

where  $D$  is the specific gravity of the gangue and  $Q$  the LKC dry feed rate in kg/min. The equation suggests a significant drop of recovery as gangue specific gravity increases from 2.8 to 4.0 (the range tested) at high feed rates. Thus, recovery can be maintained only if throughput is considerably decreased. Plant data support this, as reported by Putz for a flash flotation concentrate at Lucien Beliveau (1993). A 76 cm PKC was able to match the performance of the LKC, but only at a throughput of 1.5 t/h, considerably below the rated capacity of the unit, 35 t/h. When the 76 cm unit was replaced by a 51 cm PKC, circuit performance decreased significantly, even though the smaller unit is rated for 15 t/h, about ten times its feed rate at the time of the study.

### **2.3.3 Upgrading of primary concentrates**

Studies on primary gravity concentrates, which have a high density (even when extracted from a low density gangue ore), constitute an important source of information for the present work. Two types of studies have been performed at McGill university. First, primary concentrates have been processed with oversize removal or silica dilution, both to mimic eventual processing with a Knelson and to characterize the GRG content [Putz, 1994]. Second, Huang has studied the scavenging of GRG from table tails [Huang, 1996].

Primary concentrates are normally tabled to smelting grade, 40 - 80% Au. An alternative is to use a relatively small Knelson, such as a 19 or 30 cm unit, to perform the same task or scavenge gold from table tails. Liu (1989) indicated that the 19 cm Knelson previously used in the gold room at Meston Resources achieved about 90% recovery with two stages. The rougher stage achieved a 74% gold recovery with an upgrading ratio of 9.7; the scavenger stage achieved only 16% gold recovery of total feed, and decreased the overall upgrading ratio down to 5.9. The recovery of the 19 cm KC decreased with a increasing particle size [Liu, 1989].

Both Liu and Putz were capable of achieving very high recoveries, 89 - 95% when processing PKC concentrates with a LKC. In the normal Knelson-based gravity circuit, primary concentrates are normally upgraded with shaking tables. Whereas PKCs can recover fine and flaky gold effectively, tables can not, and their recovery suffers, especially below 212  $\mu\text{m}$ . Huang (1996) used a LKC to recover GRG from the -212  $\mu\text{m}$  fraction of selected of tails samples; recoveries of 60 - 91% were achieved.

In this work, both the methodology of Liu and Putz for the upgrading of primary Knelson concentrates and Huang for the scavenging of table tails will be tested on high density gangue samples.

## CHAPTER 3

# CHARACTERIZING ORES FOR GRAVITY RECOVERABLE GOLD

### 3.1 Introduction

In this chapter, the results of five GRG tests are presented. Of these, only the first, Snip2, was completed by the author. Others two, Aur2 and Est Malartic, were completed earlier, but never published. They are relevant to this work because of the high density of their gangue and the plant work presented in the next chapter. Permission to publish these results is gratefully acknowledged. Finally, the fourth, AELRD, was part of the first cluster of tests (Woodcock, 1994), and is included because of the substantial test work presented in chapter 4 and simulation presented in chapter five.

### 3.2 Cominco's Snip Operations

#### 3.2.1 Description of Snip

##### Information

The Snip gold mine was located on the Iskut River, about 40 km upstream of its confluence with the Stikine, and about 80 km east of the town of Wrangell, Alaska, USA. At the time of sampling, the mine was operated by Cominco Metals Ltd., as a joint venture between Cominco and Prime Resources Group Inc. The head grade of orebody was about 30 g/t with 8% sulphides. The overall gold average recovery was 91.6% in 1991. About 35% of the total gold was recovered in a concentrate grading about 45% Au by gravity. The balance was recovered into a flotation concentrate at an average grade of 300 g/t and a yield of 5%. Mining and milling throughput was 450 tpd in 1992. [Morrison and Hodson, 1992].

##### Flowsheet

As shown in Figure 3-1, the ore entering the mill is crushed to minus 7.6 cm (3 inch) in a 61 x 91 cm (24" x 36") jaw crusher, followed by secondary crushing to 100% minus 0.95 cm (3/8 inch) in a 130 cm (51 inch) shorthead cone crusher with a trommel screen in closed

## CHAPTER 3 CHARACTERIZING ORES FOR GRAVITY RECOVERABLE GOLD

19

circuit. The ore is then ground in a 2.4 x 3.7 m (8' x 12') ball mill, whose discharge is passed through a jig (double hutch Yuba-Richards). The concentrate of the jig goes to a concentrating table (Deister table with rubber sand deck) where coarse gold is extracted for smelting into bullion. The table tails, a gold-bearing sulphide, is returned to the ball mill. The light fraction of the jig is classified by a 50.8 cm (20 inch) of primary cyclone. The primary cyclone underflow is recycled to the ball mill and the overflow is classified in a secondary cyclone in closed circuit with a second ball mill (1.5 x 1.2 m) to achieve a fineness about 80% passing 75  $\mu\text{m}$  (200 mesh). This product is treated in a bank of flotation cells to produce a gold-bearing bulk sulphide concentrate. This concentrate is pressure filtered and bagged for sale (the concentrate is sent to a smelter in Japan). The flotation tailings go to a backfill circuit.

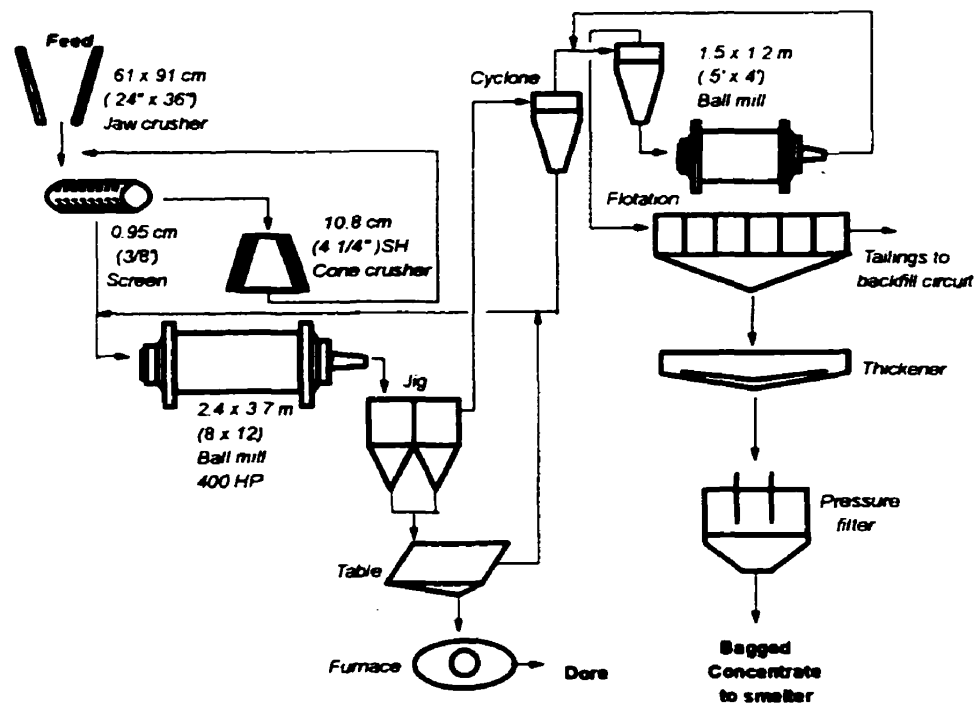


Figure 3-1 The flowsheet of Cominco's Snip gold operations

### **3.2.2 Materials and experiments**

A first GRG determination test ("Snip1") was performed by Woodcock (1994). A second test ("Snip2") was performed two years later in order to confirm the results of the first test, as part of the present work.

A general description of the test procedure of GRG characterization is shown in Figure 3-2. The sample was first dried, then crushed in a 25 cm (1 foot) Peacock cone crusher in closed circuit with a 41 cm Sweeco 850  $\mu\text{m}$  (20 mesh) screen. Crushing was considered complete when less than 1 kg of material remained on the screen. This oversize was then ground in a laboratory rod mill to pass 850  $\mu\text{m}$ .

The sample thus obtained, approximately 51 kg of minus 850  $\mu\text{m}$  (20 mesh) material, was processed with a LKC at a feed rate of 1 kg/min. A fluidizing water pressure of 21 kPa (3 psi) was used. During processing, six representative tail samples were collected at 7 minute intervals. At the end of the test, the bowl was removed and the concentrate was washed out, filtered and dried. The bulk tail settled for 12 hours, and was decanted, filtered and dried. From the dried bulk tail, a lot of 24 kg was split for the second stage and the rest was saved for further studies.

The second stage feed was ground in three laboratory rod mills (Research Hardware Model B-10 18 x 23 cm stainless steel) to 51% passing 75  $\mu\text{m}$ . The sample was then processed with the LKC at a feed rate of 570 g/min and 17 kPa (2.5 psi) of fluidizing water pressure. Six tails were cut during the test. Both concentrate and tails (the six cuts and bulk) were processed using the procedure presented above.

For the third stage, all the bulk tail of the second stage was ground to 81% -75  $\mu\text{m}$ , and processed with the LKC at a feed rate of 490 g/min and a 14 kPa (2 psi) fluidizing water pressure. Incremental tails samples and the concentrate were recovered.

For each stage, fractions of six tails samples totalling 600 g were combined, then wet screened at 25  $\mu\text{m}$  and dry screened from 25 to 850  $\mu\text{m}$ . The fractions coarser than 105  $\mu\text{m}$  were pulverized. The LKC concentrate, devoid of slimes, was dry screened directly. Finally, all size fractions for both concentrate and tails were analyzed for gold content at the Snip assay laboratory.

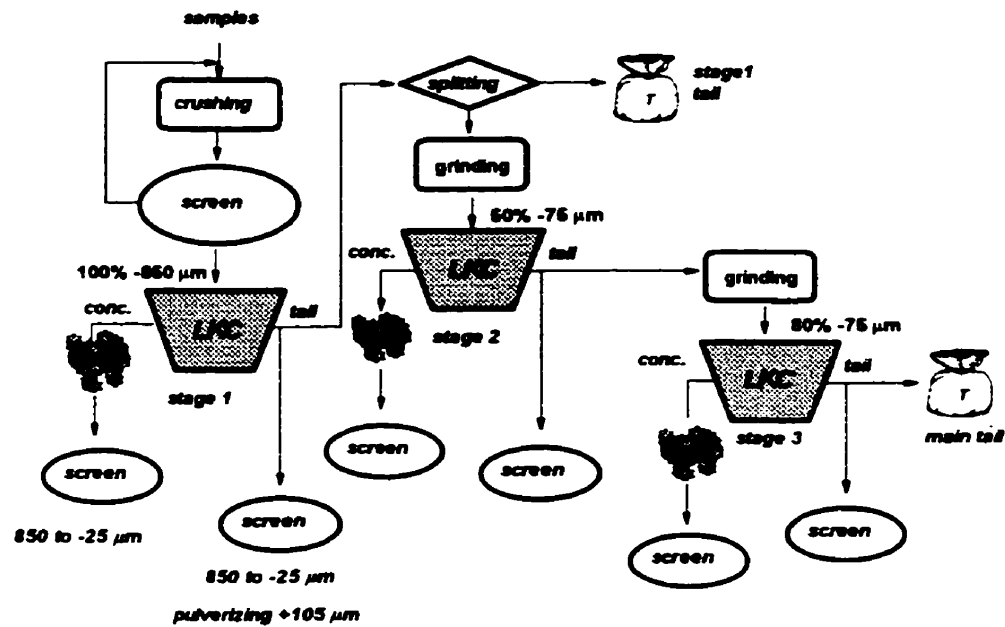


**Figure 3-2 Procedure for measuring GRG content with a LKC**

**3.2.3 Results and discussion**

Calculations

Stage recoveries were based on the concentrate and tail assays of each stage. The overall metallurgical balance was calculated from the concentrate assays of each stage and the final tail assays of the last stage (the most reliable ones because of the fineness of the material).

## Results and discussion

Figure 3-3 shows the size distribution of the feed to the three stages of the Snip2 test. The  $F_{80}$ s were 430, 170  $\mu\text{m}$  and 75  $\mu\text{m}$ .

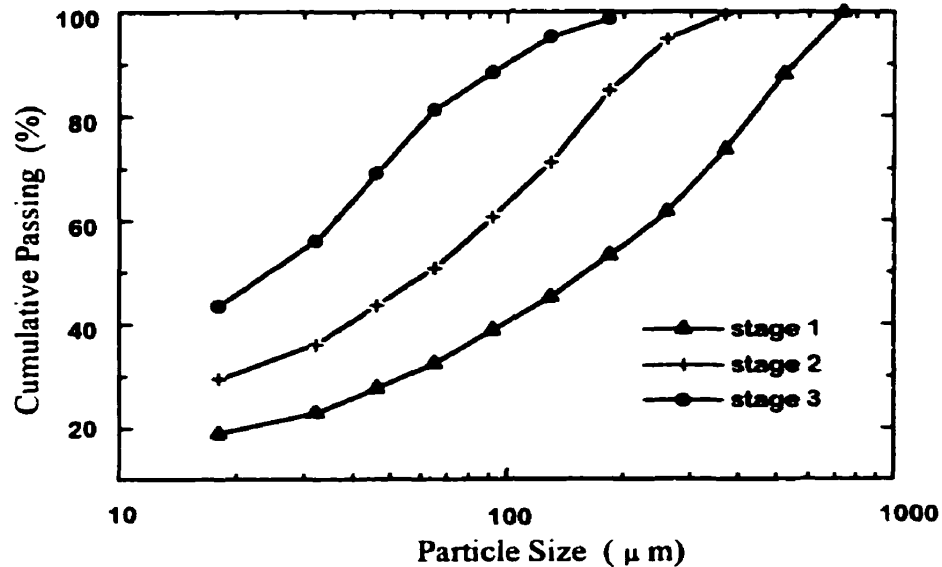


**Figure 3-3 Cumulative passing as a function of particle size for Snip2**

Figure 3-4 shows gold recovery as a function of particle size for the three stages. This diagram indicates that most gold in stage 1 was recovered in the particle size range of 25 to 150  $\mu\text{m}$ . The highest recoveries of the second stage were obtained between 25 to 105  $\mu\text{m}$ , those of the third stage below 75  $\mu\text{m}$ . The highest recoveries slightly shifted toward to the finer size from stages 1 to 3. Fine GRG which was locked in the first two stages was liberated by further grinding and recovered in the last stage. Gold recovery was extremely size dependent in stage 1 (on account of poor liberation in the coarse sizes and poor LKC performance below 25  $\mu\text{m}$ ), whereas it was virtually independent of particle size in stage three.



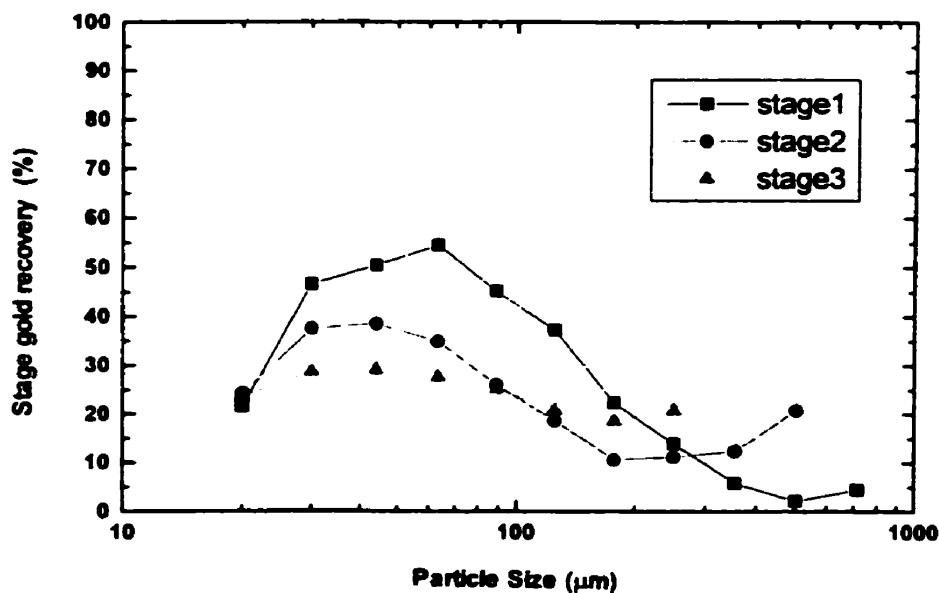


Figure 3-4 Size-by-size recoveries for each stage for Snip2

The cumulative stage-by-stage recovery is shown in Figure 3-5. In stage 1, the cumulative recovery was 22%, and increased by 20% in stage 2 to 42%. The overall GRG content still increased in the last stage to a total of 57% (detailed information can be found in Appendix A-1). Only 2% of gold was coarser than 300 µm; 42% of the total gold (74% of the GRG) was finer than 105 µm. Most of the GRG finer than 25 µm was recovered in stage 3, 12%, compared to only 2% in stage 1.

The  $F_{80}$ s for each stage of the Snip1 and Snip2 tests are shown in Figure 3-6. The differences are slight, and should not introduce significant variations in the GRG content.

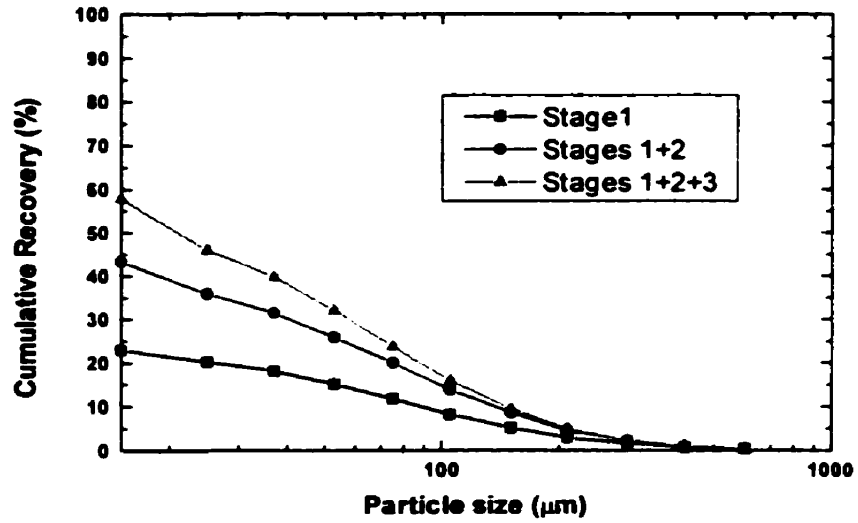


Figure 3-5 Cumulative gold recoveries for each of the three stages for Snip2

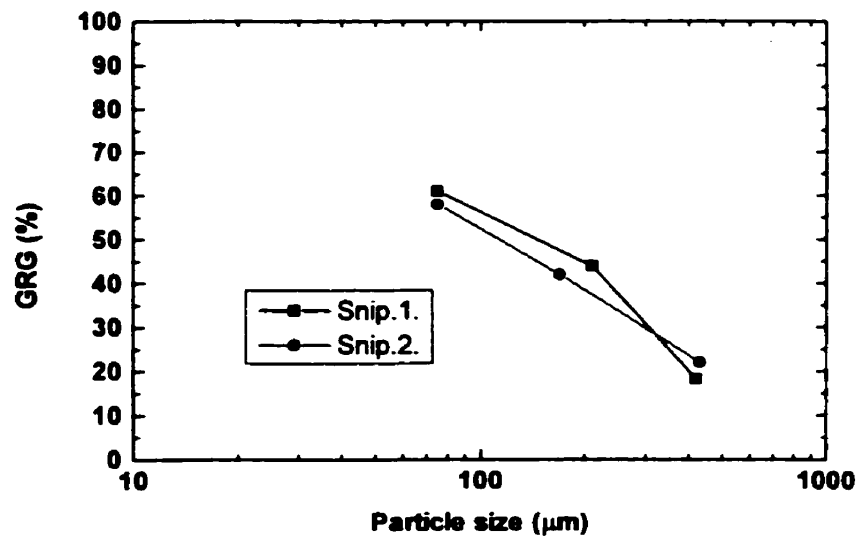
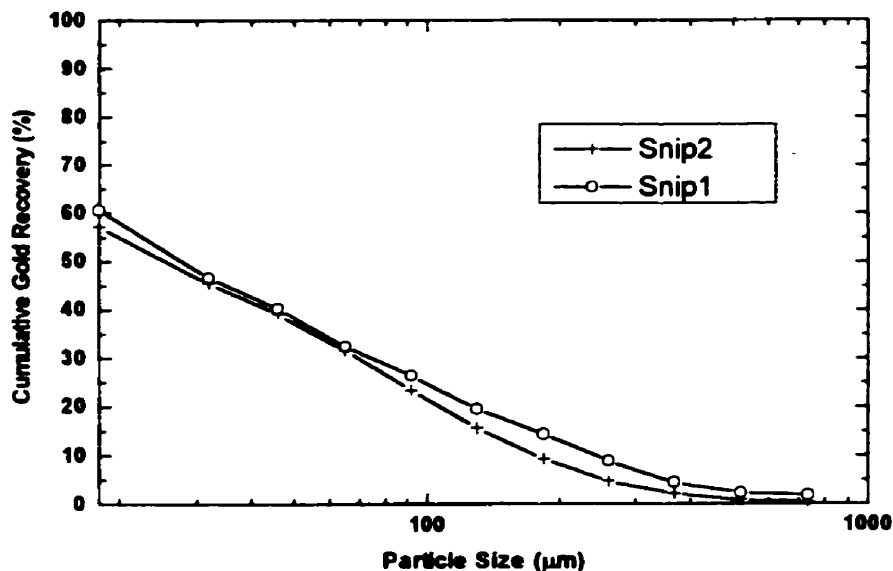


Figure 3-6 GRG content as a function of  $F_{90}$  for Snip1 and Snip2

Figure 3-7 compares the overall results of Snip1 and Snip2. There was slightly more GRG content in the first sample, 61% vs. 58%. It is quite apparent that the difference is in the coarse sizes, as was observed for the two MSV, Chimo and Hemlo samples [Laplante, 1996]. The higher GRG content of Snip 1 could be due to its higher gold content, 45 g/t vs. 27 g/t. Another possible explanation is that after the Snip1 test, the procedure was modified, using more feed mass to minimize the risk of overestimating GRG content: compare the 51 kg used for stage 1 of Snip2 to the 16 kg used for Snip1. This change would slightly decrease the amount of GRG measured. Nevertheless, differences are so small that for all practical purposes, test results can be considered identical. For samples taken more than two years apart, this is a strong validation of the reproducibility of the test.



**Figure 3-7 Size-by-size cumulative recoveries for Snip1 and Snip2**

Compared with the Snip samples, Hemlo Gold's Golden Giant ore, whose GRG is described in Figure 3-8 (the second test), shows a different behaviour. In the first stage, 47%

of gold was recovered, as was 20% in the second stage and only 10% in the last. In the four coarsest particle size classes, there was no apparent contribution from stages 2 and 3. About 90% of the total GRG was recovered in the first two stages, compared with 72% for Snip2. As discussed above, Hemlo's gold is coarser than Snip's, and liberates at a coarser grind. Primary gravity recovery takes place in the first of two grinding loops at Hemlo, an approach that yields acceptable results because of how easily GRG is liberated. The same approach would normally be unacceptable at Snip, whose GRG is liberated at a finer grind. Yet Figure 3-1 shows that gravity recovery does also take place in the first of two loops at Snip. It is probably because very little grinding is achieved in the second loop (on account of the much smaller ball mill), that Snip still achieves satisfactory gravity recoveries.

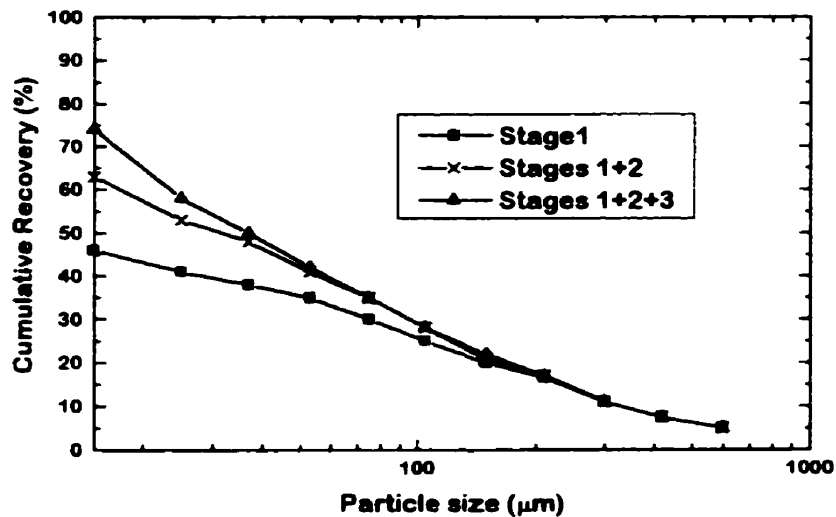


**Figure 3-8 Cumulative gold recovery as a function of particle size for Hemlo2**  
[Laplante et al., 1996]

Figure 3-9 shows that a repeat test was also carried out at Hemlo's Golden Giant (Hemlo1 and Hemlo2). The difference in GRG between the two samples is found at the coarse end, above 425 µm. The first Hemlo sample weighed only 8 kg, and contained very

## CHAPTER 3 CHARACTERIZING ORES FOR GRAVITY RECOVERABLE GOLD

little coarse gold; the difference would probably have been smaller had the first sample been of adequate size. Even Hemlo2 is not fully representative of the ore, where extremely coarse gold (particles in excess of 1 cm in size) is occasionally encountered. Such very coarse gold is statistically rare, and would require sample sizes of many tonnes to be adequately represented.

Since there is about 58% (Snip2) to 61% (Snip1) GRG content in the Snip gold ore and most of the GRG is in the finer size classes where jigs are well known not to perform well, a higher gravity recovery might be obtained by installing a centrifugal device, such as a Knelson. A potential of 40 - 45% recovery by gravity at Snip has been suggested [Laplante, 1996]. The projected increase in recovery is entirely in the fine range.

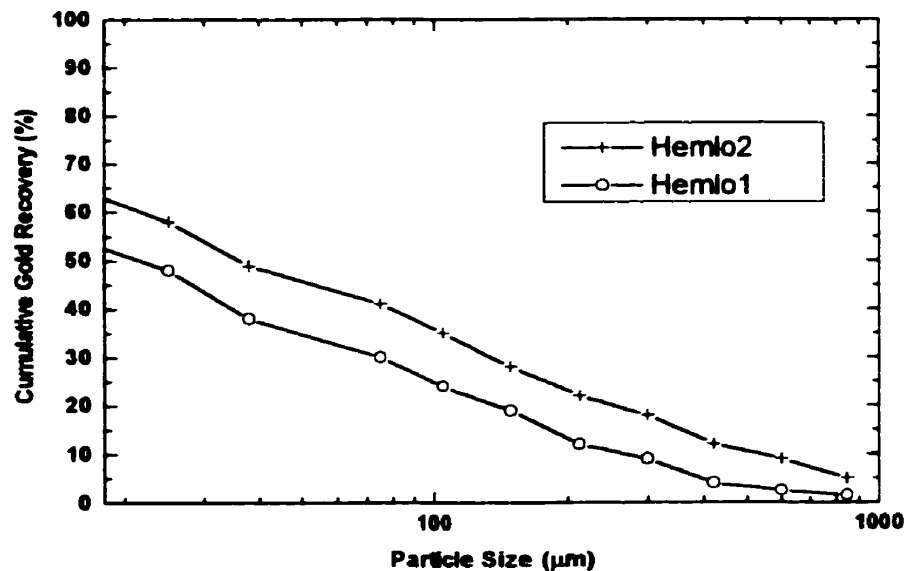


Figure 3-9 Comparison of the GRG content for both Hemlo1 and Hemlo2 [Laplante, 1996]

**3.3 Aur Louvicourt (Aur2)**

**3.3.1 Information**

The ore of Aur's Louvicourt contains 4.4% of Cu, 1.2% of Zn, 20% of Fe, 25 g/t of Ag, and 1.2 g/t of Au [Racine, 1995]. Mill throughput was 175 t/h as of January 1995. The most abundant gangue minerals are pyrite, chalcopyrite and some sphalerite. The circulating load of the grinding circuit also contains significant amounts of tramp iron (typical of SAG circuits). Gold is present mostly as aurian silver, or kustelite [Gasparrini, 1993], which is atypical; kustelite, as  $Ag_2Au$ , has a gold content of 45% Au, and a density of  $13.5 \text{ g/cm}^3$ . At Aur's Louvicourt, aurian gold has a gold content of 43% to 74% [Sinclair, 1995], which makes it intermediate between electrum (or argentinean gold) and kustelite, but closer to the latter. The lower gold content yields a specific density of 13.1 to 15.8, which is lower than that of electrum, and will hinder recovery, especially since gangue density is high.

A first GRG test was performed in 1994 (Aur1), which yielded 28% GRG at a head grade of 1.7 g/t. A second sample, Aur2, was analyzed in 1995, and will be the focus of this discussion. It was processed under the conditions shown in Table 3-1. The tests followed the procedure described in section 3.1.2.

**Table 3-1 Processing conditions of LKC for GRG measurement for Aur2**

	Feed rate (g/min)	Water pressure kPa (psi)	Feed mass (kg)	Fineness (%)	Feed grade (g/t)
Stage 1	1130	30 (4.4)	55	100% -850 $\mu\text{m}$	9.8
Stage 2	500	21 (3)	29	63% -75 $\mu\text{m}$	8.8
Stage 3	340	14 (2)	22	82% -75 $\mu\text{m}$	6.8

**3.3.2 Results and discussion**

Aur2 had 35% GRG with a fine GRG distribution, only 11% GRG coarser than 105  $\mu\text{m}$  (150 mesh). The recoveries from stages one to three were 11%, 16% and 11%,

respectively. The size-by-size cumulative recoveries for each stage are illustrated in Figure 3-10. The Aur2 sample had a head grade of 9 g/t, much higher than that of Aur1, which was more representative of the entire ore body. The test had been requested because it was felt that the much higher head grade would yield much more GRG. Evidently this was not the case.

Figure 3-10 shows that cumulative recovery increased significantly from stages 1 to 2, especially below 105  $\mu\text{m}$ . The contribution of stage 3 to the GRG content was modest. This might have been caused in part by the fineness of the feed in the second stage, 63% minus 75  $\mu\text{m}$ , as opposed the typical 50% (details are shown in Appendix A-2).

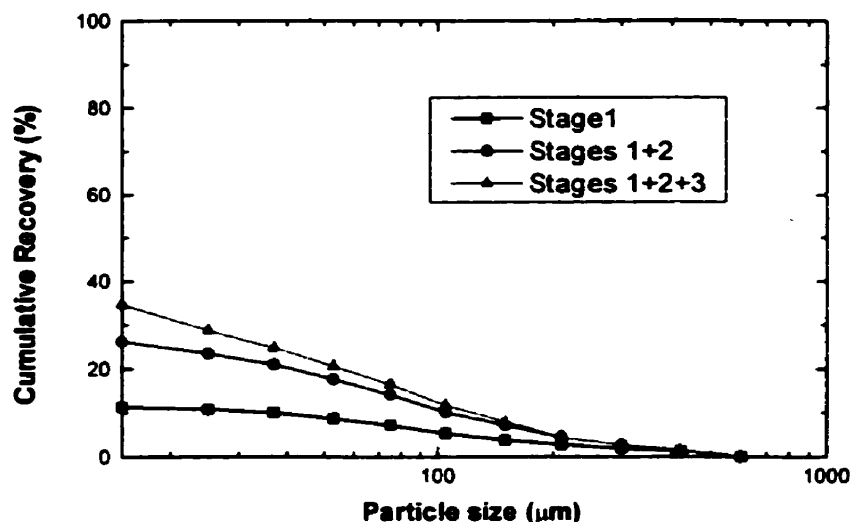


**Figure 3-10 Cumulative recovery for each of the three stages of Aur2**

Figure 3-11 shows that the Aur1 and Aur2 tests yielded similar results. Aur2 contained only slightly more GRG than Aur1, 35% vs. 27%, despite the significant difference in head grade, 9.3 (Aur2) vs. 1.7 g/t (Aur1).

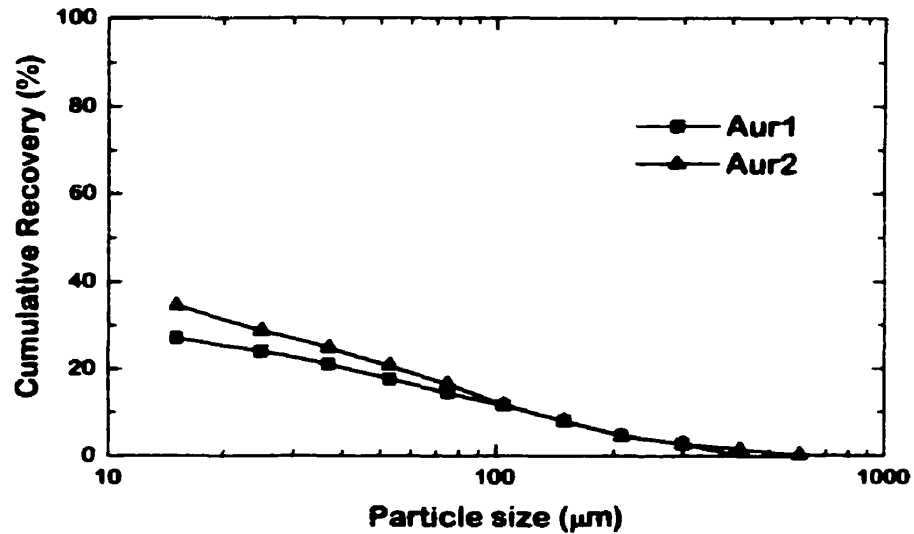


Figure 3-11 Comparison of GRG between Aur1 and Aur2

### 3.4 East Malartic

#### 3.4.1 Information

The East Malartic mill treats a massive sulphide copper/gold ore from the Bousquet 2 mine, to produce a gravity gold concentrate, a copper flotation concentrate and a gold precipitate [Hope, McMullen, and Green, 1993]. The current ore reserves total 9 million tonnes at 7 g/t (0.2 oz/st) gold and 0.7 % Cu. Ore from the high grade massive sulphide core has run over 2.5 % Cu and carried 1 oz/st of gold. Rimming of gold particles by fine mantles of hematite, or other iron oxides, is common and may cause some metallurgical difficulties, especially for flotation. The major copper minerals are chalcopyrite, bornite and tennantite.

A sample of rod mill discharge at East Malartic was sampled for GRG determination at McGill, using the procedure described in section 3.1.2. Tests were performed at conditions described in Table 3-2.



**Table 3-2 Processing conditions of LKC for GRG measurement for East Malartic**

	Feed rate (g/min)	Water pressure kPa (psi)	Feed mass (kg)	Fineness (%)	Feed grade (g/t)
Stage 1	940	28 (4)	52	100% -850 $\mu\text{m}$	20
Stage 2	320	21 (3)	20	64% -75 $\mu\text{m}$	7
Stage 3	330	14 (2)	17	78% -75 $\mu\text{m}$	6

**3.4.2 Results and discussion**

The test results indicate a GRG content of 78%, of which 43% was contained in one 0.43 g nugget. The 'nugget' effect raises a problem of statistical reliability. With it, the grade of the sample is 21 g/t, much higher than the typical head grade of the ore, 7 g/t [Hope and McMullen, 1993]. If the nugget is disregarded, the remaining sample grades 13 g/t, more in line with the average ore grade, and contains 61% GRG. The ore GRG content lies somewhere between 61 and 78% - i.e. very coarse gold is occasionally, but not systematically encountered in the circulating load [Laplante, 1995; Hayek, 1995; Vincent, 1996]. The presence of such coarse gold in the normal sample size used for the GRG test is only occasional. This can be illustrated if it is assumed that 20% of the gold is present as very coarse gold (particle mass: 0.4 g of pure gold), in an ore assaying 10 g/t (the average head grade at East Malartic at the time of sampling). This would correspond 5 nuggets per tonne, or an average of 0.25 nugget per 50 kg sample (i.e. the mass normally used for the test). If we assume a Poisson distribution, this corresponds roughly to four samples out of five without any coarse gold, and the fifth one with a single nugget. Thus the presence of a very coarse gold particle is the exception rather than the rule, and the actual GRG content of the ore is probably much closer to 61% (obtained when excluding the large nugget). The test data will now be presented without considering the nugget (details are shown in Appendix A-3).

Stage recoveries were 29% for the first stage and 16% for both the second and the last stage. As Figure 3-12 shows, about 87% of GRG was finer than 300  $\mu\text{m}$ . Therefore, treating the fine fractions becomes important. Primary cyclone underflow samples (the PKC feed) also contained GRG mostly below 300  $\mu\text{m}$  [Laplante, 1995].

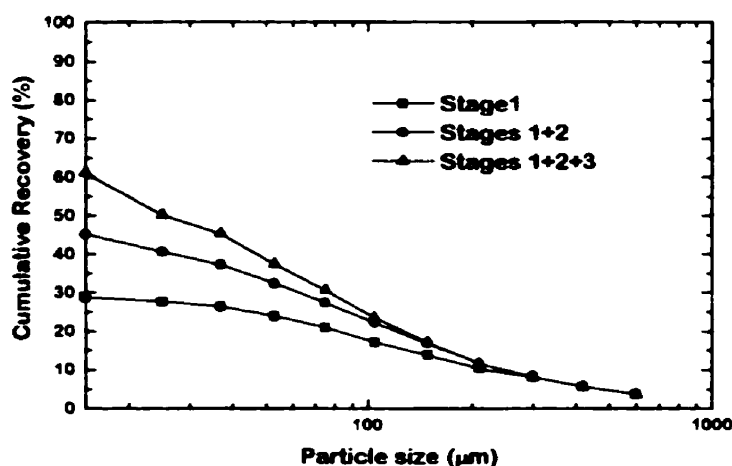


**Figure 3-12 Cumulative recovery for each of the three stages of Est Malartic**

The feed grades of each stage of the test were calculated to 12.5 g/t, 7.0 g/t and 5.9 g/t, respectively. Ideally, the tail grade of previous stage should be identical with that of the feed in the following stage. This is not the case for the tail of the first stage, 9.5 g/t, and the calculated head grade of the second, 7.0 g/t. This problem can be traced to some coarse gold in the tails of cycle one: 25% of the gold is coarser than 300  $\mu\text{m}$ , which causes a small nugget effect. This problem is less likely to arise with low gangue density ores, which generally contain less GRG in the first stage tails.

**3.5 Agnico-Eagle La Ronde Division**

**3.5.1 Introduction**

Woodcock (1992) characterized GRG in a sample of ball mill feed of Agnico-Eagle La Ronde Division (AELRD). The main characteristic of the ore is its high sulphide content (50%). The sample was processed under the conditions shown in Table 3-3.

**Table 3-3 Processing conditions of LKC for GRG measurement for AELRD**

	Feed rate (g/min)	Water pressure kPa (psi)	Feed mass (kg)	Fineness (%)	Feed grade (g/t)
Stage 1	593	35 (5)	25	100% -850 $\mu\text{m}$	7.1
Stage 2	172	28 (4)	9	45% -75 $\mu\text{m}$	9.1
Stage 3	212	14 (2)	5	78% -75 $\mu\text{m}$	10.1

**3.5.2 Results and discussion**

The AELRD ore contains 50% of GRG with a head grade of 10 g/t [Woodcock, 1993]. Figure 3-13 shows that the stage recoveries were 10, 27, and 34%, respectively. The mass used for the last two stages was much lower than what is now uses, 24 to 28 kg. This might have yielded a slight positive bias in recovery.

Only 13% of the gold in the -25  $\mu\text{m}$  fraction was recovered. This could be caused by a synergistic effect of a low GRG content below 25  $\mu\text{m}$  and the low Knelson recovery below 25  $\mu\text{m}$  with a high density gangue. However, gold present in the other size fractions was recovered very well. About 60% of the gold present is coarser than 25  $\mu\text{m}$ ; thus, the use of a gravity circuit to reduce the amount of gold reporting to the flotation circuit appears feasible.

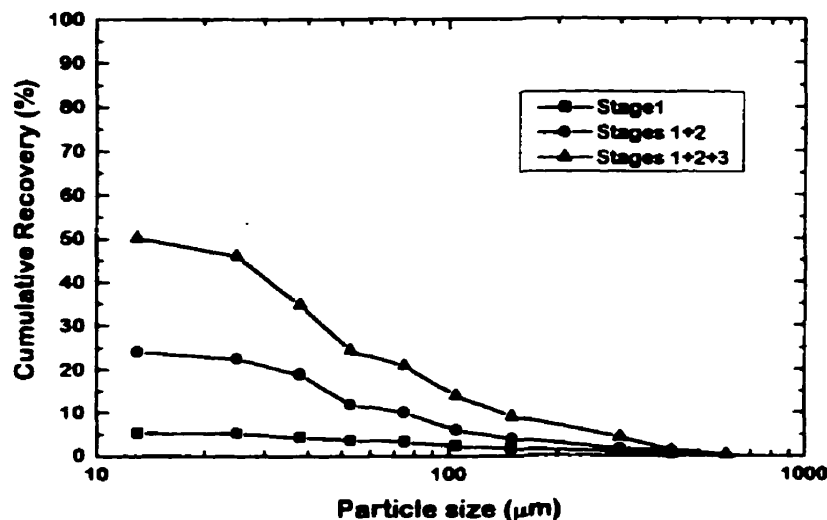


**Figure 3-13 Cumulative gold recovery as a function of particle size for AELRD**

The high gangue density has a negative impact on the overall recovery since all gravity concentration devices lose their effectiveness as gangue density increases [Burt, 1984]. Although the recovery is lower than most other gold ores amenable to gravity recovery, normally 60 - 95% GRG [Laplante, 1996], the gold that is recovered will not be subject to losses in the subsequent flotation and cyanidation processes, and will benefit from a higher economic return than gold in the flotation concentrate.

### 3.6 Discussion and conclusion

Based on thirty-eight samples tested at McGill, Laplante (1996) reported that the lowest GRG content was found to be 25% and the highest 94%. The average GRG content was 63% with a standard deviation of 19%. This places the Est Malartic ore above-average (if the nugget is included), Snip slightly below-average, AELRD well below-average, but still

treatable by gravity, and Aur Louvicourt in the group clearly refractory to gravity recovery.

Figure 3-14 compares the GRG of the four ores tested to Hemlo's. Aur2 contains the least GRG, and Hemlo2 the most, 73%. All curves, with the exception of AELRD, are roughly parallel, which suggests the relationship between gold particle size and GRG content which was reported by Laplante (1996).

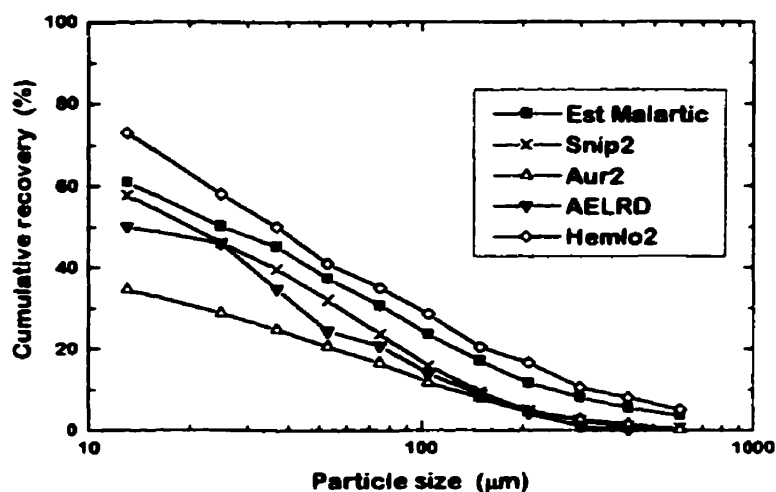


Figure 3-14 Comparison of the GRG in ores

A low GRG content can be related to (i) a low density for the gold-bearing species (i.e. kustelite, or aurian silver), (ii) massive sulphides yielding high density gangues, (iii) fine gold or gold intimately associated with sulphides. Generally, the coarser the gold, the more it is recovered in the first stage of the GRG test, such is the case for Hemlo2. When gold is fine, the recovery of the first stage will be low (e.g. Snip), particularly with high density gangues (Aur, AELRD).

## **CHAPTER 4**

### **STUDYING GOLD GRAVITY CIRCUITS**

#### **4.1 Introduction**

##### **4.1.1 Gravity circuits**

Gravity separation not only assists gold recoveries of flotation and cyanidation, but also decreases gold's circulating load. Ahead of flotation, increases of total gold recovery of 1 to 3% have been observed at Meston Resources [Laplante, 1994]. Without a gravity circuit, gold builds up to considerable circulating loads, such as 6700% in the primary cyclone underflow of Golden Giant [Banisi, Laplante and Marois, 1991] and 3700% in the secondary cyclone underflow of AELRD [Buonvino, 1993]. Gravity lowers the circulating loads considerably, especially when efficient circuits are used. This is the case at Meston Resources, which reported gold circulating loads of 500 - 600 % [Laplante, Shu and Marois, 1996].

In North America, the two units that dominate gold recovery in grinding and gravity circuits for primary gravity recovery are the KC and the jig. A general flowsheet of KC-based or jig-based gravity circuit is shown in Figure 4-1.

The SAG or rod mill and ball mill discharges feed the cyclone or cyclopak. Cyclone overflows go to flotation or cyanidation. Most of the underflow is fed to the ball mill but a bleed is processed by the gravity unit. Its concentrate is upgraded on a shaking table (e.g. Gemeni, Wilfley, Deister) to a smeltable grade and the tails return to the grinding circuit. The tails of the gravity unit are combined with the ball mill discharge for further classification. With jigs, an alternative is to treat the full ball mill discharge. With Knelsons, the feed is often, if not always, screened at cut sizes of 600 to 1700  $\mu\text{m}$ . The KC has now established itself as possibly the most logical choice for gold gravity recovery. Many plants, such as Hemlo's Golden Giant, which once boasted a jig, are now using Knelsons; others are contemplating the move. Vincent (1997) details a comparison of the two units. In this work,

only KC-based circuits will be investigated.

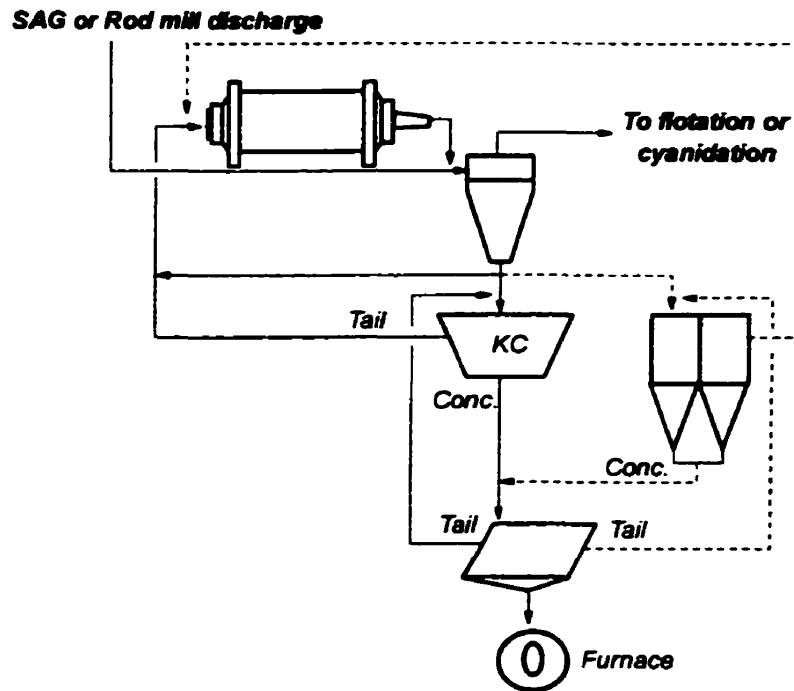


Figure 4-1 A general flowsheet of KC-based or jig-based gravity circuit

(- : Knelson; -- : jig)

#### 4.1.2 Objectives

The objectives of this chapter are:

- (i). to evaluate the performance of plant units using the LKC methodology;
- (ii). to extend the data base of plant Knelson performance; and
- (iii). to recommend modifications to existing flow sheets to increase their performance.

## 4.2 Aur Louvicourt

### 4.2.1 Introduction

The 76 cm CD Knelson used in Aur Resources's Louvicourt Project treated a bleed of the circulating load screened at 1.7 mm (10 mesh) feed. Failure of the circuit to recover significant gold led the Aur personnel to request McGill's assistance in assessing its

performance and recommending an appropriate course of action. Samples were extracted by Louvicourt personnel and sent to McGill for further processing.

#### 4.2.2 Materials and method

Samples of PKC feed (25 kg), concentrate (10 kg) and tails (17 kg) were received at McGill. Because of the low GRG content in the ore of Aur Louvicourt, the dilution method was ruled out, and fine screening was used to maximize LKC performance. Tests were conducted on the three samples - Knelson feed, concentrate, and tail, after oversize removal at 850  $\mu\text{m}$  (20 mesh) and 300  $\mu\text{m}$  (50 mesh).

All the samples were screened at 850  $\mu\text{m}$  (20 mesh) with a Sweeco screen. The oversize (+850  $\mu\text{m}$ ) was saved for further work. The undersize (-850  $\mu\text{m}$ ) was split in half: the first was processed with a LKC; the second was screened at 300  $\mu\text{m}$  (50 mesh) and processed with LKC. The unprocessed +300  $\mu\text{m}$  was saved for further studies. Tails, feed and then concentrate were processed in order to minimize contamination problems. The LKC concentrates and tails were processed as for previous tests (section 3.2.2). The concentrates and tails of LKC were analyzed for gold content at the Bourlamaque assay laboratory. Table 4-1 shows the LKC processing conditions and recovery.

**Table 4-1 Processing conditions and recovery of the LKC tests for Aur Louvicourt**

Product	Feed rate (g/min)	Water pressure kPa (psi)	Feed mass (kg)	Top size ( $\mu\text{m}$ )	Feed grade (g/t)	Recovery (%)
PKC Feed	516	28(4)	17	850	12	31
	460	21(3)	14	300	12	34
PKC Conc.	546	28(4)	6	850	1292	34
	430	21(3)	5	300	1325	58
PKC Tails	470	28(4)	8	850	11	35
	560	21(3)	6	300	17	34



### 4.2.3 Results and discussion

Overall recoveries are shown in table 4-1; with the exception of the -300  $\mu\text{m}$  PKC concentrate, all recoveries were in the low thirties.

Gold recovery is shown in Figure 4-2 as a function of particle size for the two PKC feeds. Low gold recoveries were obtained for both coarse (850  $\mu\text{m}$ ) and fine (300  $\mu\text{m}$ ) feeds. Recovery increased only modestly from 31% to 34% when the 300-850  $\mu\text{m}$  was removed. The highest recoveries for both tests took place between 53 and 150  $\mu\text{m}$ , where oversize removal increased recovery most.

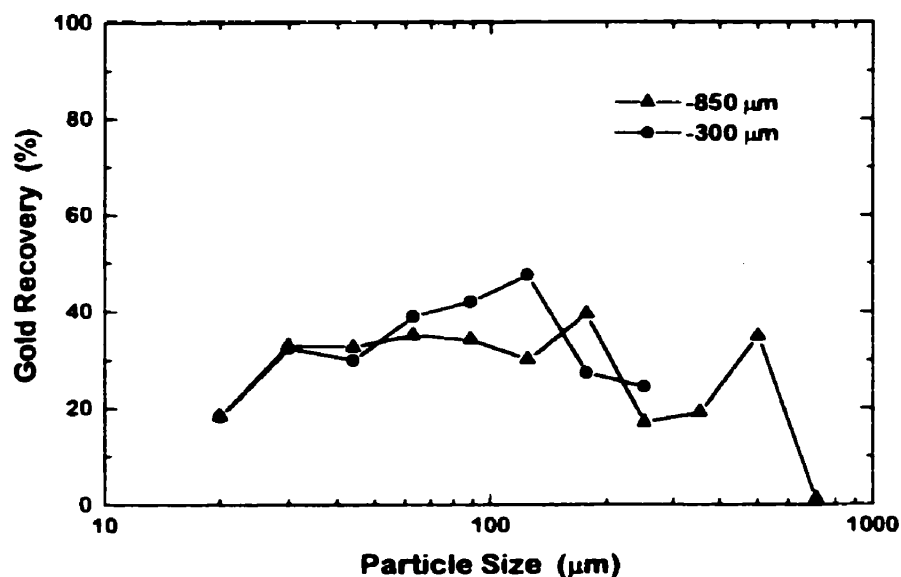


Figure 4-2 Size-by-size gold recoveries for PKC feeds of Aur Louvicourt

Figure 4-3 shows how the PKC concentrate samples responded. Although recovery increased significantly from 34% (-850  $\mu\text{m}$ ) to 58% (-300  $\mu\text{m}$ ) when the 300 - 850  $\mu\text{m}$  was removed, it remained well below PKC concentrate recoveries measured by Liu and Putz, 89 to 93%. This can be attributed to the low density of the gold bearing species, kustelite. The

highest recoveries were measured between 53 and 212  $\mu\text{m}$ , where oversize removal also had the most beneficial effect.

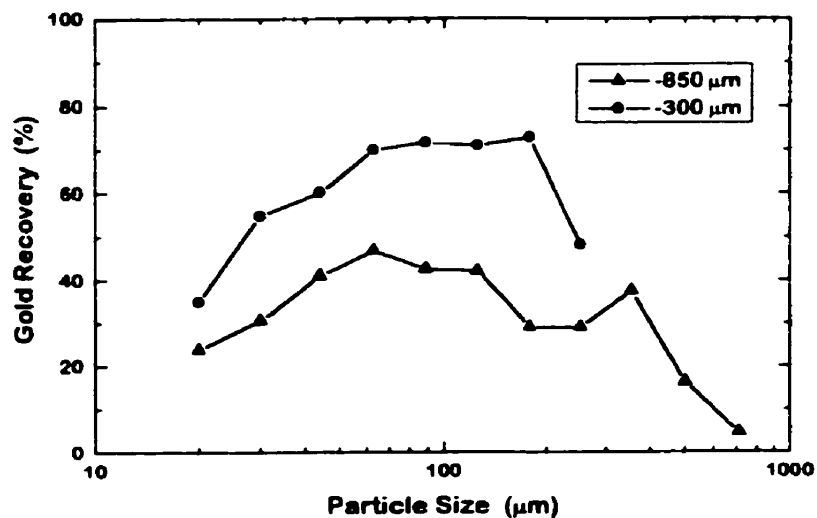


Figure 4-3 Size-by-size gold recoveries for PKC concentrates of Aur Louvicourt

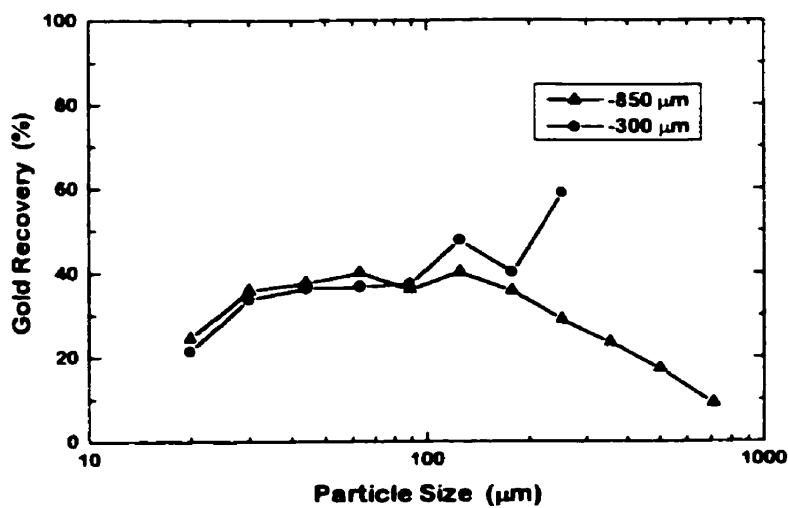


Figure 4-4 Size-by-size gold recoveries for PKC tails of Aur Louvicourt

For the PKC tails (size-by-size recovery is shown in Figure 4-4), LKC recovery was 35% for the -850  $\mu\text{m}$  and 34% for the -300  $\mu\text{m}$ . Recovery of the -850  $\mu\text{m}$  test was higher for the PKC tails, 35%, than the feed, 31%, because the mass processed by the LKC was lower, 7.9 kg vs. 16.8 kg. Some of the gold captured by the LKC was eroded from the concentrate bed, and this amount increased as more mass was treated [Huang, Laplante and Harris, 1993]. This would not be a significant factor for most ores, but it was amplified by the high gangue density and low kustelite density of the Louvicourt ore. When the +300  $\mu\text{m}$  fraction was removed, the recovery of the PKC feed and tails became identical, 34%.

For the PKC tails -300  $\mu\text{m}$  test, the size-by-size head assays below 75  $\mu\text{m}$  were significantly higher than those of the -850  $\mu\text{m}$ , or those of the -850 and -300  $\mu\text{m}$  test for the PKC feed (all these three data sets were in good agreement, as shown in Figure 4-5).

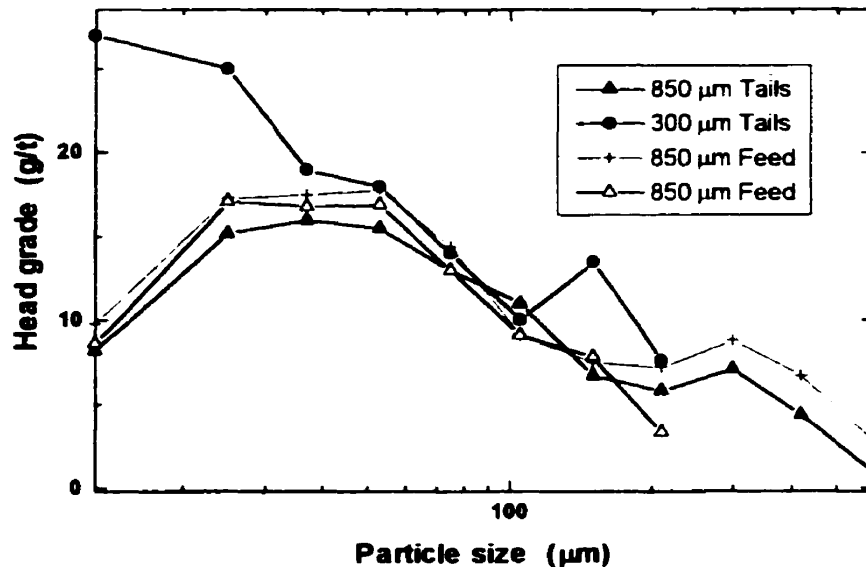


Figure 4-5 Size-by-size head grades of the PKC tail samples of Aur Louvicourt

This can be traced to the -300 μm LKC tails assays, which were very likely too high, and artificially reduced the recovery of this test. This explains why the recovery of the test, 34%, was less than that of the -850 μm test, 35% (removing the 300 - 850 μm fraction should increase recovery).

PKC performance can be calculated from the grade of its feed, concentrate and tails ( $G_f$ ,  $G_c$ , and  $G_b$ , respectively 12.5, 1292 and 11.2 g/t), the mass of concentrate,  $M_c$  (41 kg), its dry feed rate,  $Q_f$  (39 t/h), and cycle time,  $T_c$  (6 hours). Using the feed and concentrate grades:

$$R_{PKC} = \frac{M_c G_c}{Q_f T_c} \times 100 \% \quad \text{Eq. (4-1)}$$

Equation 4-2 yields, with the -850 μm data, a stage recovery for total gold of 1.8%.

Recovery based on fresh feed to the plant is calculated from the fresh feed grade,  $G_{ff}$  (1.2 g/t Au), and fresh feed rate,  $Q_{ff}$  (175 t/h):

$$R_{Total} = \frac{M_c G_c}{Q_{ff} T_c} \times 100 \% \quad \text{Eq. (4-2)}$$

Equation 4-3 yields, with the -850 μm data, a circuit recovery of 4.2% for total gold.

This is much lower than the GRG content of 27% of the Aur1 sample<sup>1</sup>. Further gains in recovery could be achieved with a finer PKC feed, but even doubling recovery would result in a low overall recovery below 10%, with little economic impact. Further, the poor recovery of the PKC concentrate, even without the +300 μm fraction, indicates that further upgrading

---

<sup>1</sup>The Aur2 sample is unrepresentative of the full ore body, as it originated from one very high grade stope.

to smeltable grade (to maximize the economic impact of gravity recovery) would be extremely difficult.

Based on these results, discontinuing gravity recovery at Louvicourt was recommended. It should be emphasized that this was the result of a number of unfavourable factors: the low gold grade of the ore, the high throughput of the mill, the low and relatively fine GRG content, and last but not least, the high density of the gangue and low density of the gold-bearing mineral.

### **4.3 Agnico-Eagle La Ronde Division**

#### **4.3.1 Introduction**

Based on work performed by Woodcock (1994), Laplante had suggested that a GRG recovery in the low thirties was a reasonable objective (1994). However, typical performance since the gravity circuits were implemented has been in the high teens, with an occasional excursion in the low twenties. This warranted additional work. Sampling of the unit was initiated to measure its efficiency. At the time of sampling, automatic flushing of the unit's concentrate had not yet been implemented, and a recovery cycle of three hours was used. One objective of the test work was to evaluate the impact of this prolonged cycle on PKC performance.

#### **4.3.2 Sampling procedure**

Samples of Knelson feed (cyclone underflow) and tails in the AELRD gold plant were extracted by AELRD personnel over the three-hour recovery cycle, as shown in Figure 4-6, during the summer of 1995. McGill received about 30 kg of dry cyclone underflow (as Knelson feed) and Knelson tails from each hour of the recovery cycle. The six samples were screened at 850  $\mu\text{m}$ ; the -850  $\mu\text{m}$  fraction was split into two parts: one part (about 15 kg) was used for direct processing with the LKC and the other one for a dilution test.

The dilution test was chosen because of the high density of the ore and the relatively

low mass of the +300 μm fraction in the PKC feed (which is screened at 850 μm). To minimize test work, only composite samples (from hour 1 to hour 3) of the cyclone underflow (PKC feed) and Knelson tails were processed with the LKC after 2:1 dilution with fine silica flour. The procedure for the diluted tests was as follows:

(i). For each hour, a 2.6 kg sample was extracted. Cyclone underflow (PKC feed) and PKC tails samples were then combined, yielding composite samples of 7.8 kg.

(ii). The composites were diluted with 2:1 ratio to obtain a total product weight of 23 kg.

(iii). The diluted and undiluted products were processed by LKC (details are in Table 4-2). Concentrates and tails were treated using the standard methodology. Size fractions were sent to the AELRD assay laboratory for gold determination.

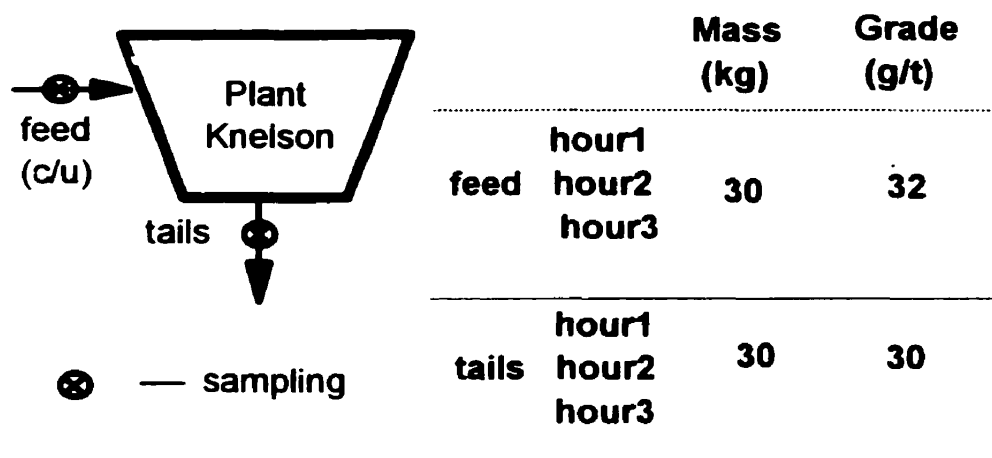


**Figure 4-6 Sampling of Agnico-Eagle La Ronde Division**

**4.3.3 Results and discussion**

The overall test results are shown in Table 4-3 (details are shown in Appendix B-2).

**Table 4-2 Processing conditions of LKC tests for AELRD**

Product		Feed rate (g/min)	Water pressure (kPa)	Sample mass (kg)
Cyclone Underflow (PKC feed)	hour 1	450	21	19
	hour 2	450	21	15
	hour 3	596	21	16
	Dilution	600	14	23
PKC tails	hour 1	470	21	15
	hour 2	490	21	19
	hour 3	520	21	15
	Dilution	600	14	23

**Table 4-3 LKC test results for AELRD**

Product	Grade (g/t)	%GRG	LKC Tail grade (g/t)
<b>Cyclone Underflow ( Plant Knelson Feed)</b>			
hour 1	31.6	48.4	16.4
hour 2	33.6	51.8	16.4
hour 3	33.7	48.4	17.6
Average	32.9	49.5	16.8
diluted	11.3	55.1	5.1
<b>Plant Knelson Tails</b>			
hour 1	26.1	41.4	15.4
hour 2	29.9	47.2	15.9
hour 3	32.9	51.4	16.1
Average	29.6	46.7	15.8
diluted	10.3	55.6	5.7

In the column of overall grade for the PKC feed, no trend is detected except for a small increase between the first and second hours. For the PKC tails, grades are lower and

increase from 26 to 33 g/t. The difference between feed and tail, which is indicative of recovery, decreases from 5.5 (hour 1) to 0.8 g/t (hour 3). This is a strong indication that PKC performance deteriorates significantly as the recovery cycle progresses. The average difference is 3.3 g/t. The same difference for the diluted composite samples should be one-third of this average since the dilution is a 2:1 silica : ore. This is indeed the case, 1.0 g/t, although the diluted grade in both cases is slightly superior to what it should be, but by only 0.3 - 0.4 g/t.

In the column of LKC recovery, or %GRG, there is a trend in the PKC tails data, as the GRG content increases from hours 1 to 3 (41.4 to 51.4%). For the feed, there is no such trend, which indicates that the increase in GRG content in the plant Knelson tail is not due to a change in mineralogy but to a drop in PKC performance as the recovery cycle progresses.

The diluted tests yield additional information, as they show how the density of the gangue can affect Knelson performance, not only at lab but also at plant scale. As expected, the relatively fine distribution of the feed limits the negative impact of the sulphides, and lab Knelson recovery increases only by 6%, from 49.5 to 55.1, with the cyclone underflow samples. For the plant Knelson tails, the increase is more important, 9% (from 46.7 to 55.6%), which can probably be explained by the more refractory nature of this material to gravity (since the PKC has recovered some of the GRG).

The effect of dilution on size-by-size gold recoveries for PKC feed and tails is shown in Figures 4-7 and 4-8, respectively. Dilution significantly increases recoveries in the fine particle size range, typically minus 75  $\mu\text{m}$ , for the PKC feed and even more for the tails. Since about half of the gold is finer than 75  $\mu\text{m}$ , the overall recovery increase in GRG content of diluted samples is about half that of the -75  $\mu\text{m}$ , - i.e. 5% for the PKC feed and 9% for the tails.



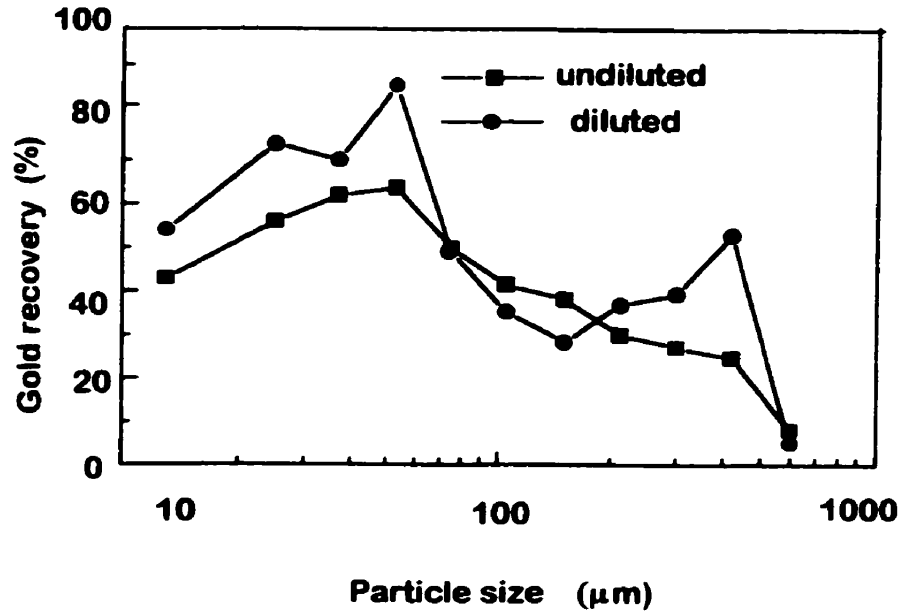


Figure 4-7 Size-by-size gold recoveries of diluted and undiluted PKC feed of AELRD

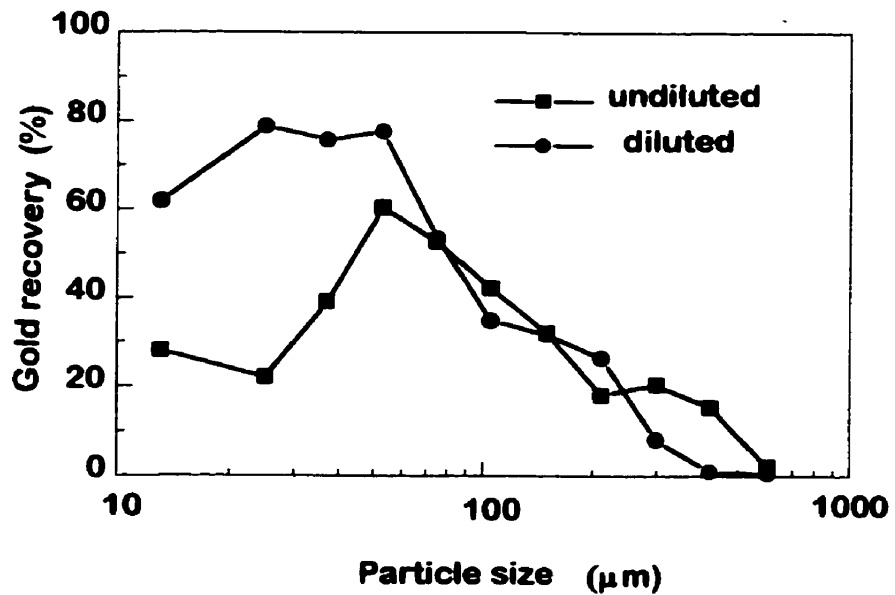


Figure 4-8 Size-by-size gold recoveries of diluted and undiluted PKC tail of AELRD

Ideally, the LKC tail gold grade of the PKC feed and tail should be identical, if the PKC recovers only GRG. This is tantamount to saying that the non-GRG content of the PKC feed and tails should be identical, and equal to the LKC tails gold grade (i.e. the LKC recovers all GRG and only GRG). This is not exactly the case, as the cyclone underflow averages 16.8 g/t, 1.0 g/t above the tails of the plant tails, 15.8 g/t. The difference is small and can not be explained by differences in size distribution or LKC operating conditions (feed mass or rate, fluidization water pressure). For the diluted samples, the difference is smaller (as expected), 0.6 g/t, and this time favours the PKC tails. The differences are probably the result of experimental and assaying error.

Total gold recovery can be calculated from the feed and tail grade of the PKC, since its yield is very small [Liu, 1989]:

$$R(\%) = \left(1 - \frac{G_t}{G_f}\right) \times 100 \% \quad \text{Eq. (4-3)}$$

This yields, for total gold, recoveries of 17, 11 and 2% for hours 1, 2 and 3, respectively. For GRG, the same equation is applied to GRG content (in g/t), rather than total gold. This yields recoveries of 30, 19 and -4% for the three hours. The last one is negative because the GRG content of the PKC tails exceeds that of its feed. This raises the issue of experimental error.

#### Experimental errors:

For the third hour of the cycle, GRG losses can be calculated from the grades of the PKC tails,  $G_t$  ( $30 \pm 0.5$  g/t) and feed,  $G_f$  ( $33 \pm 0.5$  g/t), and the GRG content of tails,  $R_t$  ( $41 \pm 2\%$ ), and feed  $R_f$  ( $48 \pm 2\%$ ), as shown in Equation 4-4.

$$L^{GRG} = 100 \times \frac{G_t R_t}{G_f R_f} \quad \text{Eq. (4-4)}$$

With these data a GRG recovery of 6% is calculated. Its variance,  $\sigma^2$ , can be calculated by Equation 4-5, which is a partial Taylor series [Chatfield, 1981]:

$$\sigma^2 = 0.25 \left[ \left( \frac{100 R_t}{G_f R_f} \right)^2 \cdot \left( \frac{-100 G_f R_t}{G_f^2 R_f} \right)^2 \right] + 4 \left[ \left( \frac{100 G_t}{G_f R_f} \right)^2 \cdot \left( \frac{-100 G_f R_t}{G_f R_f^2} \right)^2 \right] \quad \text{Eq. (4-5)}$$

This yields an experimental standard deviation,  $\sigma$ , of 6%. The standard deviation is greater than GRG recovery, 2%, which explains why a negative value can be calculated (-4% in this case).

Figure 4-9 illustrates PKC efficiency by representing the GRG content in its feed and tails over the full recovery cycle. Whilst the drop from the second to the third hour in efficiency between hours 1 and 2 is small, it is severe between hours 2 and 3, to the extent that the amount of GRG in the PKC tail slightly exceeds that of the feed (probably because of sampling, sample processing and assaying errors, as was demonstrated above). Thus, the recovery cycle should be shortened to a maximum of two hours, and possibly less. This is reflected by present practice at AELRD, a 45 minute cycle on weekdays and 60 minute cycle during weekends.

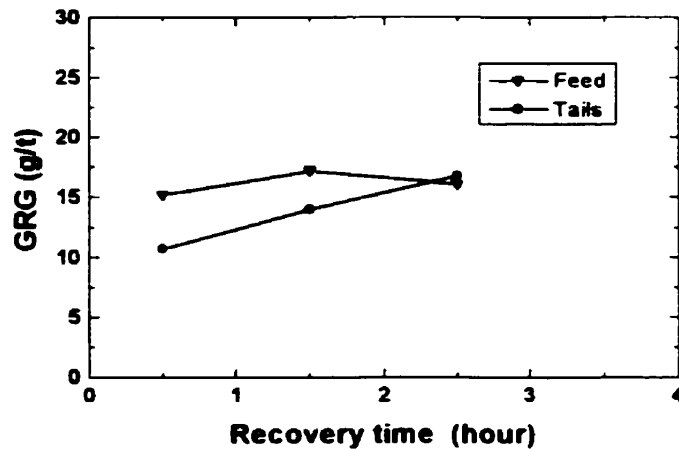


Figure 4-9 GRG content of PKC feed and tails over a three-hour recovery cycle of AELRD

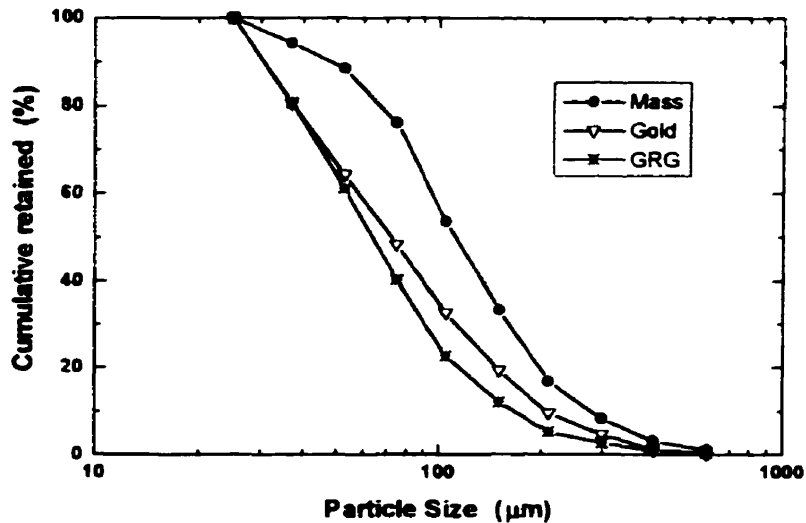


Figure 4-10 Size distributions of PKC feed of AELRD

To increase the low gravity recovery of gold, Figure 4-10 suggests the possible solution of oversize removal. Less than 6% of the GRG (10% of gold) is found in the coarsest 20% of the mass, the +212  $\mu\text{m}$  (70 mesh) fraction. Thus screening at or around 212  $\mu\text{m}$  would not only increase PKC recovery, but also upgrade the PKC feed.

#### 4.3.4 Conclusions

1. The AELRD data set is the first high quality sampling test of a Knelson-based gravity circuit treating a relatively coarse high density gangue with the laboratory Knelson methodology developed at McGill.

2. An illustration of the adequacy of the study is the reproducibility of the size-by-size grades of the laboratory Knelson for the plant unit feed and tails samples. There was also good reproducibility between undiluted and diluted samples.

3. Test work confirmed the presence of significant GRG, of which relatively little was recovered by the plant Knelson. Recovery dropped dramatically from the first to the third hour of the loading cycle, suggesting that frequent concentrate removal will be necessary.

4. The +212  $\mu\text{m}$  fraction of the plant Knelson feed contained a much lower GRG content than the -212  $\mu\text{m}$ . Feed grade and screening at a finer size would increase both the stage recovery of the Knelson and gold production by gravity.

5. Dilution of the Knelson feed yielded only a moderate increase in laboratory Knelson recovery, indicating that the effect of the high gangue density was somewhat limited, at least for the LKC.

## **4.4 Barrick's Est Malartic**

### **4.4.1 Introduction**

The Barrick's Est Malartic gold plant recovers both gold and copper. The presence of 0.7 to 1.5 % Cu, some of it bornite (a more potent cyanacide than chalcopyrite), required the removal of the copper ahead of cyanidation to minimize the copper concentration in the leach solution. It was found that most gold (up to 85 %) reported to the copper concentrate and with the normal 3-month smelter settlement terms, delayed payment for the gold had a negative impact on the cash flow. The coarse gold contained in the copper concentrate also decreased sampling accuracy and resulted in significant uncertainty in gold payments. Gravity concentration was thus considered necessary, and a Knelson based circuit was installed [Hope, McMullen, 1993].

The flowsheet of Barrick's Est Malartic is shown in Figure 4-11. The ore, which is directly crushed by a conventional three stage circuit consisting of a jaw and two cone crushers, is ground in an open circuit rod mill and a closed circuit ball mill to 80% passing 70  $\mu\text{m}$ . A portion of the classifying cyclone underflow is fed to a gravity concentration circuit

consisting of two 76 cm (30") Knelson concentrators operating continuously and two Gemini tables for final upgrading. The gravity circuit tailings are partially dewatered using cyclones before returning to the ball mill. The copper flotation circuit consists of a combination of Outokumpu high grade tank cells and conventional cells. The high grade tank cells are used in both roughing and cleaning duties while the conventional cells are used as scavenger and scavenger cleaners. The copper flotation tailing is thickened to 50% solids and cyanide leached for approximately 12 hours in open top agitators. Leaching is followed by solid/liquid separation and pulp washing on drum filters and gold recovery by zinc precipitation. The filter residue is treated in an INCO  $\text{SO}_2$ /air circuit to remove copper and cyanide prior to discharge to a flooded tailings area. A flooded tailings deposition scheme was adopted to eliminate the onset of acidification due to sulphide oxidation.

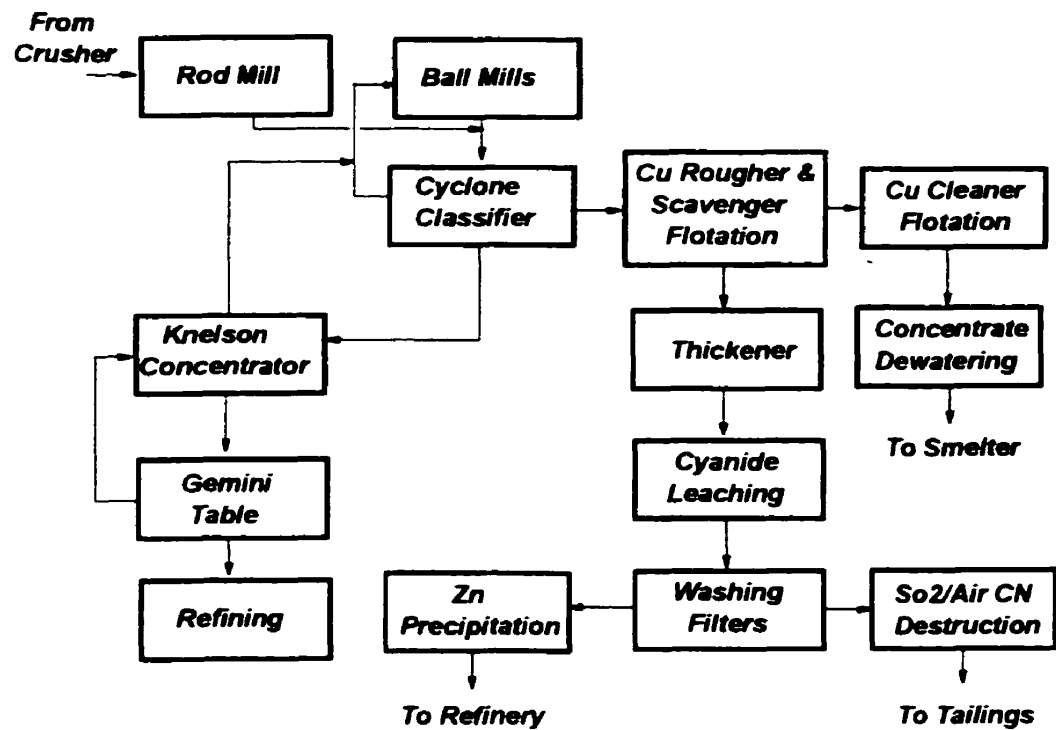


Figure 4-11 Block flowsheet of Barrick's Est Malartic

#### 4.4.2 Previous work on the 76 cm (30") CD Knelson

A first evaluation of Knelson performance was made by Vincent (1996); the Knelson-based methodology was applied to one feed and one tail sample. A gold recovery of 16% was estimated, with a GRG recovery of 57%. Because no concentrate sample had been extracted, size-by-size data proved unreliable, but suggested a decrease in recovery with decreasing particle size. To remedy this problem, a second survey, which included a PKC concentrate sample, was completed [Laplante, 1995]. Total gold recovery was estimated at 18 to 26%, and GRG recovery at 25 - 32%. As the feed rate to the unit might have decreased (from that of Vincent's work), there is not apparent discrepancy between the two data sets. Laplante (1995) estimated size-by-size total gold recovery, which was 14% for the  $-25 \mu\text{m}$  fraction and increased to 24 to 30% range for the  $+105 \mu\text{m}$  fraction. Data above  $105 \mu\text{m}$  were noisy because of the nugget effect and lower gold grades than in the finer size classes. A sample of the table tails was extracted as part of the same sampling effort, to estimate table efficiency and evaluate the potential for further recovery from the table tails with a PKC. This work will now be described.

#### 4.4.3 Materials and Method

##### Solid density measurement

Tramp iron with a density of  $7 \text{ g/cm}^3$  and pyrite with a density of  $5 \text{ g/cm}^3$  are recovered preferentially in the PKC concentrate, and increase the density of the table feed and tails. This density was determined using a 100 ml flask as a pycnometer; five measurements averaged  $3.5 \text{ g/cm}^3$ .

##### Sample preparation and tests with LKC

A composite sample (50 kg) of table tails from Barrick Est Malartic was received at McGill University. It was screened at  $850 \mu\text{m}$  (20 mesh). The undersize fraction was split into two. Part of the  $-850 \mu\text{m}$  sample was further screened at  $212 \mu\text{m}$  (70 mesh). Subsamples of the  $-850 \mu\text{m}$  and  $-212 \mu\text{m}$  fractions were processed with a LKC to determine GRG content at feed rate of 400 g/min and a fluidization pressure of 28 kPa (4 psi) for the

-850  $\mu\text{m}$  (20 mesh), and 28 kPa and 21 kPa (3 psi) for -212  $\mu\text{m}$  samples. All of the concentrate and samples of the tails were screened down to 25  $\mu\text{m}$  and the tails size fractions above 105  $\mu\text{m}$  were pulverized. All fractions were assayed at the Barrick Est Malartic laboratory.

#### 4.4.4 Results and discussion

Overall metallurgical balances, Table 4-4, show that the highest recovery, 91%, was achieved with the -212  $\mu\text{m}$  at a fluidization water pressure 28 kPa. Recovery at the same pressure for the -850  $\mu\text{m}$  was 76%. Both are high, when compared to the work of Huang, who measured table tails samples from eight Canadian plants, the recoveries of 30 -55% for -850 fractions, and 60 - 91% for -212  $\mu\text{m}$  fractions [Huang, 1996]. Agreement between the head grade of the two -212  $\mu\text{m}$  tests is good, 559 g/t vs. 565 g/t. The -850  $\mu\text{m}$  feed has a lower gold content, 339 g/t, because the 212 - 850  $\mu\text{m}$  fraction assays only 35 g/t, whereas the -212  $\mu\text{m}$  assays 492 g/t, in reasonable agreement with the head grade of the two -212  $\mu\text{m}$  tests. Laplante (1995) reported a Knelson concentrate assaying 14,600 g/t (-850  $\mu\text{m}$ ) at Est Malartic; the table tail grade of 339 g/t would correspond to a gold recovery of 98% for the Gemeni table, considerably higher than the 90% (at a concentrate grade of 85% Au) reported by Hope and McMullen (1993). This discrepancy may be the result of a lower table feed or concentrate grade, or unaccounted losses (in the middlings or magnetic product, for example). LKC recovery on the table tails is very high, which implies that scavenging additional gold from the Gemeni table tails is technically feasible. It is not likely that it would be economically justifiable, given the already high recovery of the table.

**Table 4-4 Table tails test results for Barrick's Est Malartic**

Product	Grade (g/t)	GRG (%)
-850 $\mu\text{m}$ at 28 kPa	339	76
-212 $\mu\text{m}$ at 28 kPa	559	91
-212 $\mu\text{m}$ at 21 kPa	565	69



The high GRG content of the Gemeni tails and its high recovery result likely from difficult PKC operations, on account of the coarseness (-1.7 mm) and high density of its feed. Consequently, only gold that is highly gravity recoverable is captured by the Knelson, and this gold is easily recovered again by gravity, either by the Gemeni table itself, or by the LKC from the Gemeni table tails.

Size-by-size recoveries of the three LKC tests are shown in Figure 4-12. The increased recovery of the -212  $\mu\text{m}$  test at 28 kPa (from 21 kPa) was not achieved in the fine sizes (-37  $\mu\text{m}$ ), where little gold is distributed, but in the 53 - 212  $\mu\text{m}$  fraction, presumably because of better fluidization of the PKC feed. The lowest recovery, 69%, was obtained with the -212  $\mu\text{m}$  test at 21 kPa, and was probably the result of an inadequate fluidization of the flowing slurry, as the recovery drop was most severe above 75  $\mu\text{m}$ . A similar drop in recovery had been reported by Laplante, Shu and Marois (1996), when fluidization water pressure was lowered below the optimum range.

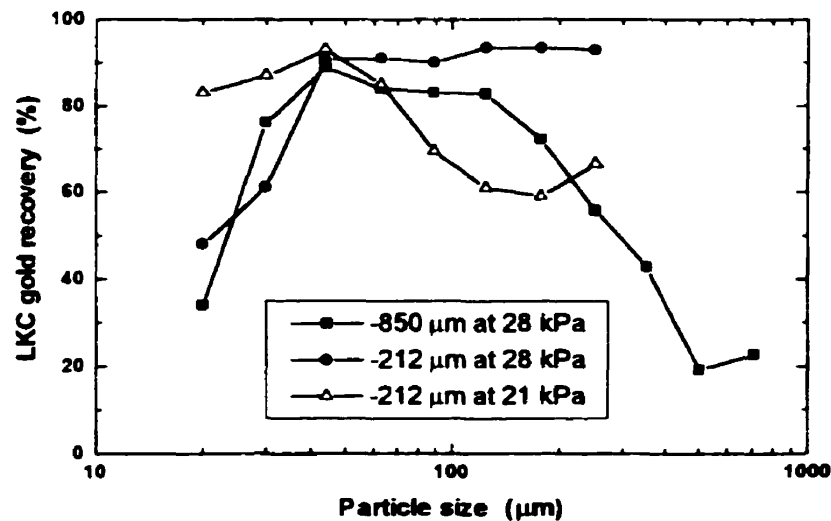
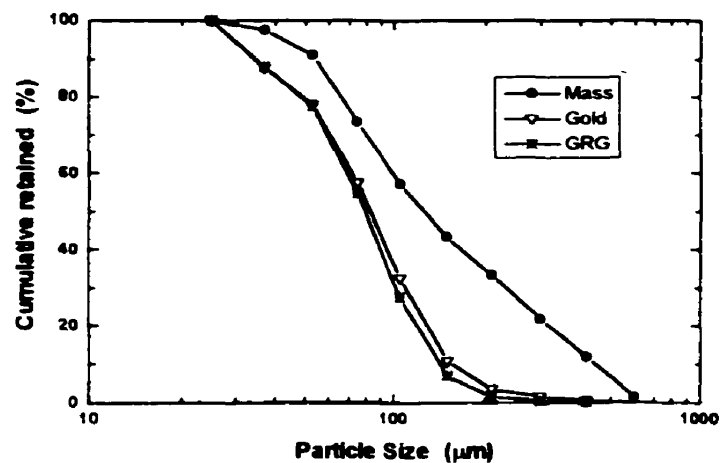


Figure 4-12 Size-by-size gold recovery of table tails of Barrick's Est Malartic

The lower fluidization pressure increases fines recovery (below 37  $\mu\text{m}$ ), but so little gold is finer than 37  $\mu\text{m}$  that the impact on overall gold recovery is negligible. There is an apparent inconsistency below 37  $\mu\text{m}$  for the two 28 kPa tests, as recovery curves cross at 25  $\mu\text{m}$ . How could the 25 - 37  $\mu\text{m}$  fraction recovery be higher with the -850  $\mu\text{m}$  feed? This can be traced to a suspicious assay for the LKC 25 - 37  $\mu\text{m}$  concentrate of the test at 28 kPa. The assay is too low, and results in a calculated head of 1474 g/t for this size class, compared to 2537 and 2368 g/t for the two other tests.

This short discussion highlights the importance of accurate assaying and the usefulness of multiple tests on the same feed. Reliable assaying is especially critical for LKC concentrate fractions, which can not be re-assayed (as they are completely assayed to eliminate the nugget effect). A similar situation had arisen for the fine fraction of the LKC tails for one of the Aur Louvicourt tests (Fig. 4-5).



**Figure 4-13** Size distributions of the table tails of Barrick's Est Malartic

Figure 4-13 shows that gold in the table tails is finer than its gangue, and narrowly distributed: only 3% is coarser than 300  $\mu\text{m}$  (but 24% of the gangue). An analysis of the PKC concentrate [Laplante, 1995] reported, for the same size classes, 14% of the gold in the

+300  $\mu\text{m}$ , and 8% below 37  $\mu\text{m}$ , for the PKC concentrate feeding the Gemeni table at the time of the table tails were sampled. Thus, gold in the Gemeni table tails is even more narrowly distributed than in its feed. This is largely because the Gemeni recovers coarse gold very efficiently. Above 212  $\mu\text{m}$ , the amount of GRG in the Gemeni table tails drops rapidly (Figure 4-12 -850  $\mu\text{m}$  test): this is mostly unliberated gold, probably associated with pyrite. Hope and McMullen (1993) had reported the same problem in the jigs that were replaced with the PKC, but to a much greater extent - i.e. jigs have an even higher tendency to recover coarse unliberated gold.

## 4.5 Cambior's Chimo Mine

### 4.5.1 Description of grinding and gravity circuit

In the grinding and gravity circuit of Chimo, shown in Figure 4-14, the SAG mill discharge is classified by cyclones. Part of the underflow is screened at 3.4 mm (6 mesh); the undersize is processed by a 76 cm (30") Knelson Concentrator. The tails of the KC feed a flash cell whose concentrate is further treated by a 51 cm (20") Knelson Concentrator. The screen oversize and the balance of the cyclone underflow flow by gravity to the SAG mill. The combined cyclone overflow goes to a conventional flotation circuit. The flash cell tail returns to cyclone.

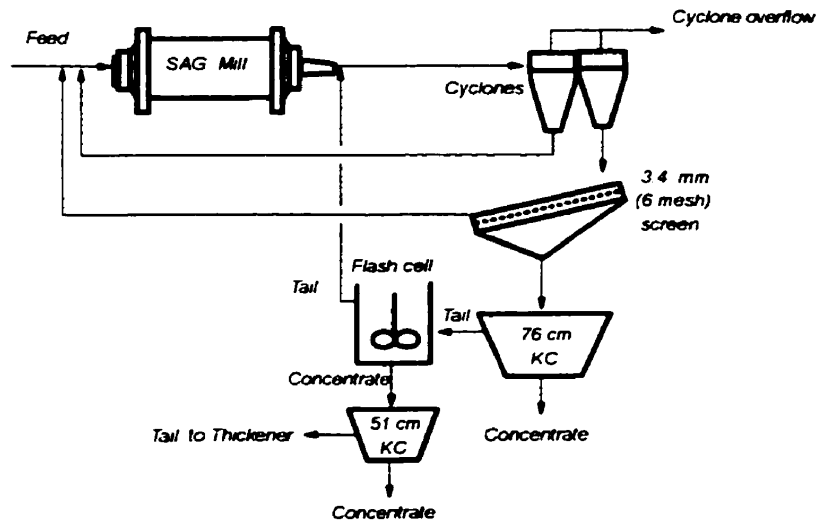


Figure 4-14 A flowsheet of the grinding and gravity circuit of Chimo Mine

**4.5.2 Sampling and processing with a laboratory Knelson**

Nine streams of the grinding and gravity circuit at Chimo were sampled; three for their size distributions (cyclone underflow, screen oversize and SAG mill discharge) and six for their GRG content (cyclone overflow, 76 cm KC feed and tail, 51 cm KC feed and tail, and flash cell tail). The sample mass varied between 4 and 20 kg.

Size distribution tests

Cyclone underflow (13 kg), SAG mill discharge (6 kg) and screen oversize (5 kg) were sequentially split, using a Jones riffle splitter, into two 600 g samples. Each sample was screened with the same screen set from 9,500 µm to -25 µm. The average size distributions obtained are shown in Figure 4-14.

LKC tests

The six LKC test samples were screened with a Sweeco at 850 µm, and the +850 µm fraction was stored for further studies. The -850 µm fraction was processed with a LKC under the conditions shown in Table 4-5 (details are shown in Appendix B-4). The LKC concentrate and tails were processed as for the previous tests (section 3.2.2), and the size fractions analyzed for gold content at the Bourlamaque assay laboratory.

**Table 4-5 Processing conditions with LKC for Chimo**

Product		Mass (kg)	Feed rate (g/min)	Water pressure (kPa)
Cyclone overflow		3.6	250	18
76 cm Knelson	Feed	10.8	480	21
	Tail	19.6	520	21
51 cm Knelson	Feed	6.0	300	18
	Tail	5.5	400	18
Flash cell tail		6.7	420	21

**4.5.3 Results and discussion**

Table 4-6 shows the overall results of LKC tests (details are shown in Appendix B-4). Perusal of the data identifies blatant inconsistencies. First, the cyclone overflow grade, 16 g/t, is much higher than what is routinely reported at Chimo, 1-3 g/t (the ore assays 2-5 g/t). Its GRG content, 76%, is also unrealistically high, as cyclone overflows typically contain 15 - 20% GRG. Both problems are caused by the high assays of the LKC concentrate size classes, which must be rejected as grossly overestimated.

**Table 4-6 Overall results of LKC tests for Chimo**

Product		Head Grade (g/t)	LKC Recovery (%)	LKC tail grade (g/t)
Cyclone overflow		15.8	76	3.9
76 cm Knelson	Feed	12.4	80	2.5
	Tail	5.9	62	2.3
51 cm Knelson	Feed	514	86	75
	Tail	73.9	35	48.7
Flash cell tail		3.5	73	1.0

A similar problem is encountered in the 51 cm PKC feed, whose head grade, 514 g/t, is far above reported values, typically around 50 - 100 g/t; its GRG content, 86%, is also excessive (values of 19 to 36% have been reported by Putz, 1994). Again, only very highly biased LKC concentrate assays can explain these data.

The 76 cm PKC feed and tail data are much more plausible: both are in the expected order of magnitude, with high but plausible GRG content (the GRG was measured twice for the ore, at 83 and 94%). Further, the LKC tail grades, 2.5 and 2.3 g/t, are very similar, as they should for the feed and tails of a PKC (as discussed in section 4.3.3). The size

distribution of the PKC feed and tails are also in good agreement (Appendix B-4), as PKC produces a very low yield.

The flash cell tails sample yields plausible GRG and size distribution data, as shown in Figures 4-15 and 4-16 (its size distribution compares well to that of the 76 cm PKC feed and tails). Whereas the 76 cm PKC can not reduce the quantity of non-GRG in its feed (the drop from 2.5 to 2.3 g/t is within experimental errors), the flash cell does so, to 1.0 g/t, as it floats gold-bearing sulphides. Size-by-size analyses show that flash cell dropped gold content below 300  $\mu\text{m}$ , as was reported by Putz' work [Putz, 1994]. About 50% of the total gold in the flash cell tail reported to the 300 - 850  $\mu\text{m}$  fraction.

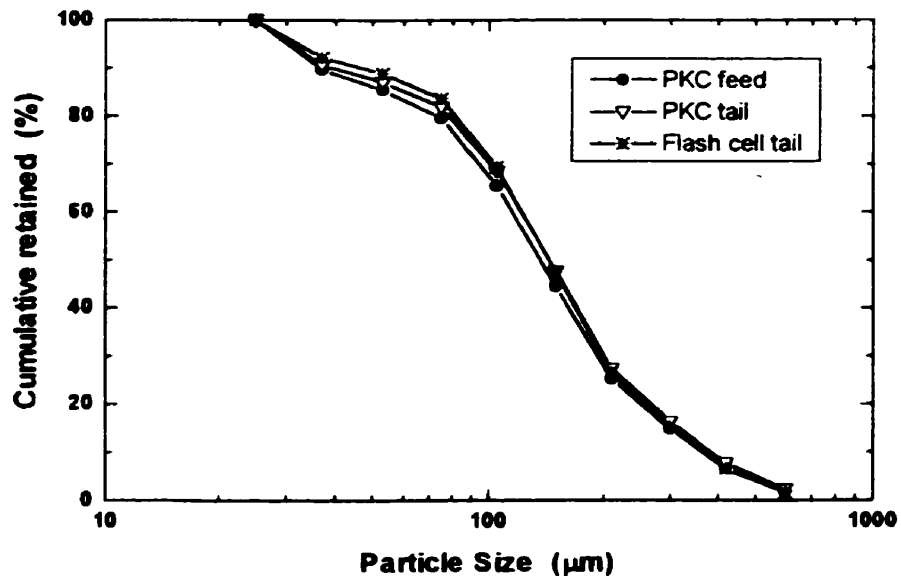


**Figure 4-15 Size distributions of PKC feed, tail and flash cell tail of Chimo Mine**

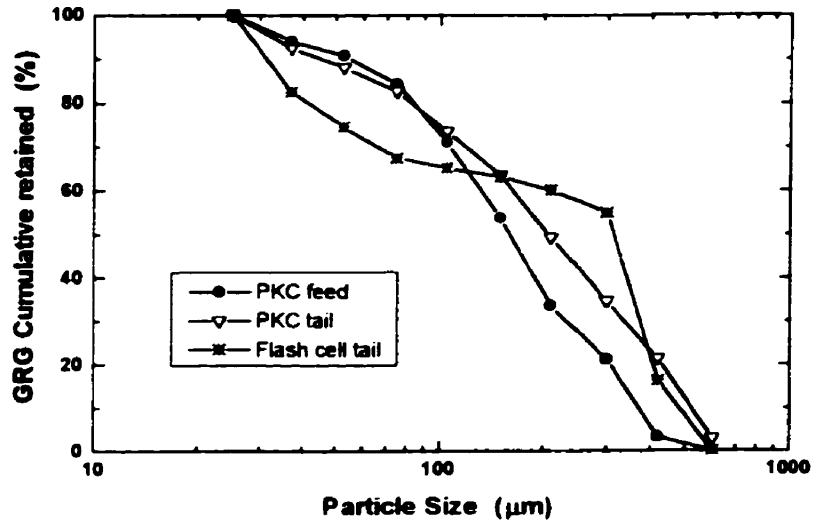


Figure 4-16 GRG content of PKC feed, tail and flash cell tail of Chimo Mine

The 76 cm PKC performance can be calculated from its feed and tail data (Equation 4-3, section 4.3.3). This yields a GRG recovery of 63.6%, and a total gold recovery of 6.5 g/t, or 52.4%. This recovery must correspond to the 15% gravity recovery recorded when the 51 cm PKC is not running. At an average feed grade of 4 g/t at 61 t/h for the mill, the 6.5 g/t recovered by the 76 PKC corresponds to 0.6 g/t of feed, which suggests that the 76 cm PKC is fed at:

$$\frac{0.6 \text{ (g/t)}}{6.5 \text{ (g/t)}} \times 61 \text{ (t/h)} = 5.6 \text{ (t/h)}$$

This is a very low feed rate for a 76 cm PKC with a low density gangue. A similar low feed rate was also reported in a recent survey of the circuit [Desharies, 1996]. The flow feed rate is also consistent with size distribution data, as mass balanced by NORBAL3 [NORBAL3, 1992; Appendix C]. This low feed rate decreases the ability of the PKC to recover gold and should be increased.

## CHAPTER 5

### SIMULATION OF GOLD GRAVITY RECOVERY AT AELRD

Laplante et al. (1994) proposed an algorithm to estimate gold recovery from a description of the grinding and classification behaviour of gold, coupled with an estimate of the GRG content of the ore and a measure or prediction of the efficiency of GRG recovery. All data were described size-by-size and merged in a relatively simple matrix algorithm. For a circuit such as AELRD's, schematized in Figure 5-1, with gold recovery from a bleed of the cyclone underflow, the following equation (5-1) is easily derived:

$$\underline{D} = PR [I - H(I - PR)]^{-1} C E \quad \text{Eq. 5-1}$$

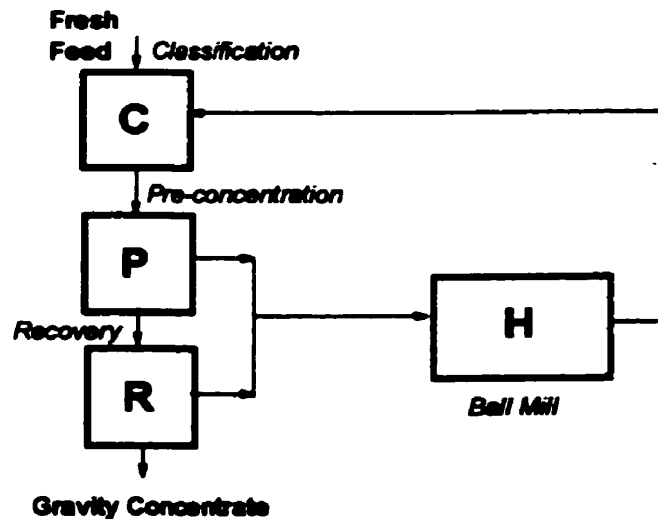


Figure 5-1 Schematic of a gold gravity circuit (recovery from cyclone underflow)

The variables of equation 5-1 are identical to those of equation 2-1 (section 2.2.1), and the result is in fact very similar, as only the location of the C matrix, which is nearly equal to unity (as 99% of GRG reports to the cyclone underflow), has changed. This reflects the fact that recovery from the mill discharge (Eq. 2-1) will yield similar results to the



## CHAPTER 5 SIMULATION OF GRAVITY RECOVERABLE

### GOLD AT AELRD

63

recovery from a cyclone underflow (Eq. 5-1). Thus, considerations other than metallurgy (i.e. layout and pumping) can dictate the location of the primary recovery unit.

Equation 5-1 will now be used to model gravity recovery on the basis of the Knelson results reported in Chapter 4 (section 4-3) and previously published data (Buonvino, 1993; Vincent, 1996; Woodcock, 1994). First, the  $E$  matrix will be that which Woodcock (1994) generated, as shown in Figure 3-13. The diagonal of the recovery matrix will be that which was generated at Est Malartic, and used to model Hemlo's gravity circuit (Laplante, Vincent and Luinstra, 1996). A second recovery matrix will also be used to simulate Knelson operation with a low density gangue. It is based on data from Meston Resources's 76 cm PKC operation (Laplante, Putz, Huang and Vincent, 1994). The main diagonal of the preconcentration matrix,  $P$ , is also shown in Table 5-1; it was estimated from the known circulating load, 800-1000%, of which the 76 cm PKC can only treat 10% at the fresh feed rate of 40 t/h for each of AELRD's two grinding lines.

**Table 5-1 R, P, and GRG matrix F (% of the total gold in feed) and main diagonal of C matrices**

Size ( $\mu\text{m}$ )	F	R (%)	P (%)	C (This work)	C (Vincent)
+600	0.0	20	7.5	0.998	0.999
420-600	0.1	20	10	0.998	0.999
300-420	1.0	20	10	0.998	0.999
212-300	3.2	20	10	0.998	0.999
150-212	4.9	20	10	0.998	0.999
105-150	4.9	20	10	0.990	0.995
75-105	6.9	20	10	0.990	0.995
53-75	3.7	16	10	0.990	0.995
37-53	10.3	14	10	0.980	0.990
25-37	11.3	12	10	0.960	0.980
-25	4.3	10	10	0.840	0.920

This value is slightly less for the 600-850  $\mu\text{m}$  fraction, which is partly rejected by the screen ahead of the Knelson. Finally, two classification matrices will be tested, that measured by Vincent at AELRD (1996), and one which reflects existing classification problems, with double the fraction of GRG reporting to the overflow. Both are shown in Table 5-1.

Since the H matrix is more difficult to extract from plant data, the grinding data from Buonvino (1993) will be used. The selection function of the ore is difficult to extract, as many of the coarser size classes present in the fresh feed are not in the mill discharge. Figure 5-2 shows the selection function of the ore for a limited size range, which has been extrapolated to cover the full size range of interest - i.e. 25 or 37  $\mu\text{m}$  to +850  $\mu\text{m}$ . Figure 5-2 also shows what the projected selection function of GRG would be, using the assumptions of Banisi, Laplante and Marois (1991) (presented in chapter 2). The relationship between the selection function of the ore and that of GRG is similar to that reported by Buonvino in AELRD's regrind mill, which then processed a sluice concentrate with a high GRG content.

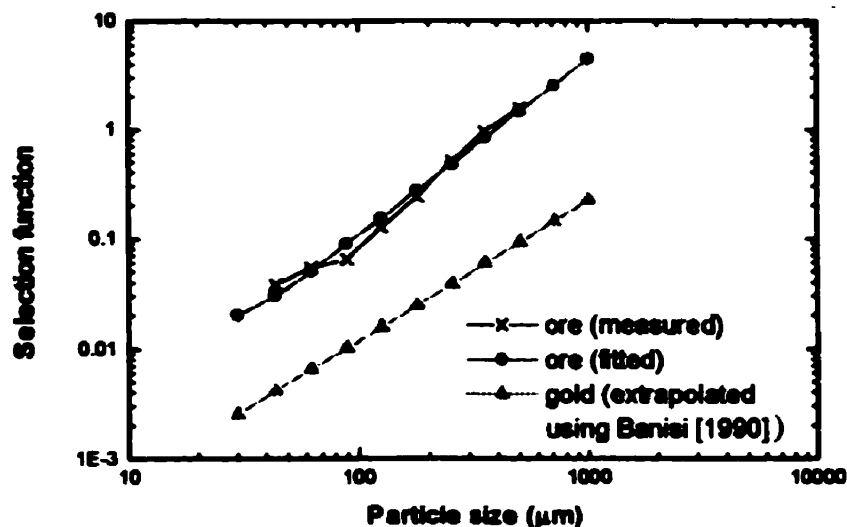


**Figure 5-2 Selection function vs. particle size**

From this information a first estimate of the H matrix, shown in Table 5-2, is computed using the algorithm proposed by Austin and Luckie (1984). The last three elements of the main diagonal must be corrected to account for GRG that becomes non-gravity recoverable without being ground because of excessive flaking, to values of 0.995, 0.99 and 0.98, respectively, as proposed by Laplante, Noaparast and Woodcock (1995). The elements below the main diagonal, which correspond to GRG being ground into finer size classes, must also be corrected for loss of gravity recoverability due to smearing, flaking, or breakage into very fine fragments. This is achieved with the equation (Eq. 5-2) proposed by Noaparast (1996):

$$R_{GRG} = 0.985 \left( 1 - e^{-0.693 \left( \frac{x}{22} \right)^4} \right) \quad \text{Eq. 5-2}$$

where x is particle size (the geomean of each size class, in  $\mu\text{m}$ ) and  $R_{GRG}$  is a correction factor. Further, for high density gangue ores, a more conservative estimate of recoverability will be used to account for the high gangue density, which may decrease the recoverability of fragments. Both estimates are shown in Table 5-3. Whereas the columns of the uncorrected H matrix (Table 5-2) sum up to unity (since the pan size fraction is included), those of the corrected H matrix do not, once each element below the main diagonal has been corrected with the factors of Table 5-3.

For the base case, the recovery data of Est Malartic, the poor classification function and the recoverability data of Noaparast will be used. Matrices will then be changed, only one at the time, to assess their impact on predicted recovery. More specifically, poor classification, poorer fragment recoverability, and better PKC performance (on account of low gangue density) will be simulated.

**Table 5-2 Uncorrected H matrix**

$\mu\text{m}$												
850	0.8094	0	0	0	0	0	0	0	0	0	0	0
600	0.1288	0.8710	0	0	0	0	0	0	0	0	0	0
420	0.0237	0.0904	0.9139	0	0	0	0	0	0	0	0	0
300	0.0106	0.0141	0.0617	0.9435	0	0	0	0	0	0	0	0
212	0.0074	0.0068	0.0085	0.0412	0.9631	0	0	0	0	0	0	0
150	0.0054	0.0048	0.0044	0.0051	0.0272	0.9759	0	0	0	0	0	0
105	0.0039	0.0035	0.0031	0.0028	0.0032	0.0178	0.9846	0	0	0	0	0
75	0.0028	0.0025	0.0022	0.0020	0.0018	0.0020	0.0114	0.9898	0	0	0	0
53	0.0022	0.0018	0.0016	0.0014	0.0012	0.0011	0.0012	0.0075	0.9935	0	0	0
37	0.0015	0.0014	0.0011	0.0010	0.0009	0.0008	0.0007	0.0008	0.0005	0.9959	0	0
25	0.0013	0.0009	0.0009	0.0007	0.0006	0.0006	0.0005	0.0004	0.0005	0.0031	0.9975	0
-25	0.0030	0.0028	0.0026	0.0020	0.0020	0.0018	0.0016	0.0015	0.0055	0.0010	0.0025	1

**Table 5-3 Correction factors for the H matrix**

Size ( $\mu\text{m}$ )	Noaparast's data	This work
+850	0.985	0.97
600-850	0.985	0.97
420-600	0.985	0.97
300-420	0.985	0.97
212-300	0.985	0.97
150-212	0.985	0.97
105-150	0.985	0.97
75-105	0.985	0.95
53-75	0.985	0.90
37-53	0.985	0.80
25-37	0.895	0.70
-25	0.371	0.30

## CHAPTER 5 SIMULATION OF GRAVITY RECOVERABLE GOLD AT AELRD

Simulation results are summarized in Table 5-4, which also includes plant recovery data for the first six months and the summer of 1996 [Robitaille, 1996], which experienced a sharp drop in gravity recovery (it has since climbed back to its original 18 - 21% levels). The low recovery of the summer 1996 was traced to a lower GRG content in the ore (Laplante, et al., 1997). This problem has since largely disappeared.

**Table 5-4 Measured and simulated recovery**

	Recovery (%)
Measured, Summer of 1996	12
Measured, before and after Summer of 1996	18-21
Simulated base case	22
Simulated, Vincent's classification matrix	28
Simulated, low density gangue performance (Meston)	27
Simulated, poorer fragment recoverability	21

The base case yielded a recovery of 22%, which is slightly higher than that measured in the plant, as it does not take table losses into account. When Vincent's classification matrix is used, the predicted recovery climbs to 28%, significantly higher than plant performance. Poorer classification has been used for the base case, because the classification circuit has been modified to accommodate gravity, and has yet to be optimized. This suggests that additional recovery gains can be achieved with improvements in classification.

Table 5-4 also shows that poorer fragment recoverability has little impact on total gold recovery, within the range it was tested. This is not the case for Knelson performance, as the recovery data of Vincent for the low gangue density Meston ore significantly increases predicted recovery. Clearly, the effect of gangue density on PKC performance has a significant effect of circuit recovery.

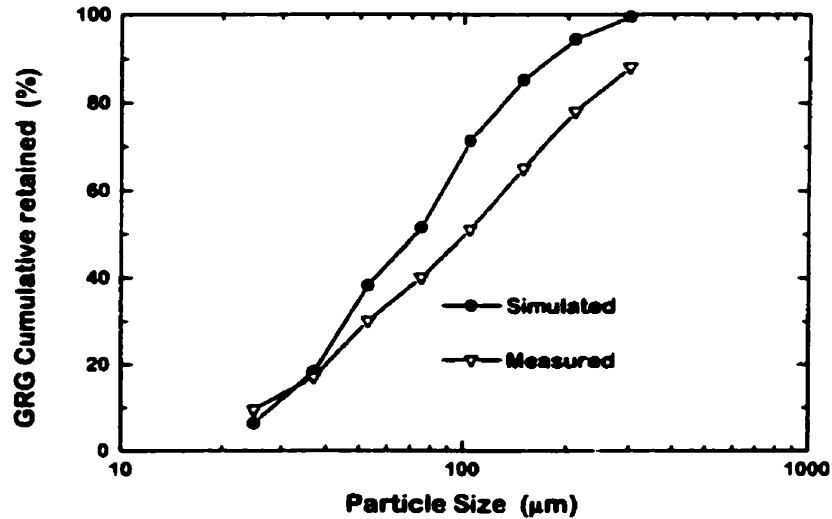


**Figure 5-3 Cumulative GRG size distribution of simulated and measured gravity stage recovery**

Figure 5-3 compares the simulated (base case) and measured size distribution of the Knelson concentrate (Huang, 1997). Agreement is not very good, mostly because there was no GRG measured above 300 µm in the original sample, which does not reflect the ore being mined today. As a result, the model can not generate the 12% +300 µm gold recovered in the Knelson concentrate with recently mined ore. The coarsening of GRG at La Ronde had been expected, as mining has proceeded from the outside to the core of the ore body over the past four years. A GRG test should be performed to obtain a more up-to-date estimate of the GRG distribution.

## CHAPTER 6

### CONCLUSIONS AND FUTURE WORK

#### 6.1 Summary and Conclusions

##### 6.1.1 Gravity recoverable gold

The distinct behaviour of gold in grinding circuits is dictated by its malleability and density, which influence all important mechanisms: breakage, classification and liberation. These will affect gold's residence time in the grinding circuit and its recovery by gravity [Banisi, 1991]. By far the most significant implication is that individual gold particles are recycled a large number of times (averages of up to 80 times have been measured) in the circulating load of grinding circuits, where gold primary gravity recovery normally takes place. As a result, gravity recovery performance depends mostly on the amount of GRG in the ore. A survey of forty ore types yielded an average of 63% GRG [Laplante, 1996], which suggests that most gold ores are amenable to gravity recovery. However, the present work clearly showed that gangue density also plays a critical role in determining how successful gravity recovery will be.

At the AELRD plant, the GRG content (50%) is below average, partially because of a very high sulphide content of 50%, mainly in pyrite with a specific gravity of five. Despite the dense gangue, the  $D_{50}^1$  of gold is three times smaller than that of the gangue [Buonvino, 1993], and gold builds up significantly in the circulating load. This indicates that much fine gold reports to the cyclone underflow and could eventually be recovered by the gravity.

At Aur's Louvicourt Mine, a very low GRG content (28 - 35%) was obtained, compared to the other ores discussed in Chapter 3. This indicates that the potential of gravity recovery is extremely low. Hindering gold recovery is the silver-rich gold bearing mineral,

---

<sup>1</sup>  $D_{50}$ , the cut point, or separation size of the cyclone, is often defined as that point on the partition curve for which 50% of particles in the feed of that size report to the underflow, i.e. particles of this size have an equal chance of going either with the overflow or underflow [Wills, 1988].

kustelite, with a density as low as 13.5 g/cm<sup>3</sup> (since gold and silver have very similar crystal structures and both are isometric with a face centred cubic lattice, there is no strictly defined composition for electrum, its gold to silver ratio, and specific density can vary). This is considerably below that of pure gold, 19.3 g/cm<sup>3</sup>, and makes gravity recovery difficult since the concentration criterion between kustelite and pyrite drops to 3.2 from a value of 4.8 for pure gold. Wills [1988] stated that the larger the concentration criterion, the easier the recovery by gravity. Nevertheless, Burt suggests that with a concentration criterion of 3.2 gravity recovery is still possible in the size range of interest (that is not to say that the relatively "soft" approach of treating only a bleed of the circulating load will be successful).

Snip's GRG is also characterized by its fineness. Laboratory tests show that 53% of the GRG (58% in Snip 2) is below 212 µm. GRG is relatively difficult to liberate, as 36% GRG was recovered in the second and third stages of the test, at finer grind. To compound the problem, Snip's fine gold is poorly recovered by the jig in the fine particle size range [Vincent, 1996]. The test work of Vincent suggested that an installation of a Knelson in the gravity circuit would increase the gravity recovery. Nevertheless, the Snip circuit still recovers about 38% of the gold, and 60% of the GRG.

At Barrick Gold's East Malartic, the ore contains at least 60% GRG, some of it very coarse. Plant data suggest that the very coarse gold is episodic; when absent, the size distribution of the GRG present in the circulating load is still coarser than that of Aur, Snip or AELRD.

### **6.1.2 Plant work**

At Aur Louvicourt, the plant Knelson achieved a stage recovery of 1.8% and a total gold recovery of 4.2%. The poor performance was predictable, given the low density of kustelite and the high gangue density. Although a finer PKC feed would boost recovery, it would still remain below that which is economical and upgrading would be difficult (as shown with LKC tests). An obvious conclusion is that the standard PKC is not suitable at



Louvicourt. A unit capable of a better performance, possibly a Knelson operating at a faster rotation velocity, would increase recovery, but it is unlikely that the increase would be high enough to make gravity economically justifiable.

At AELRD, the feed is of intermediate particle size ( $-850 \mu\text{m}$ ), but high gangue density, hence the plant gravity recovery, 20%, is only 40% of the measured GRG content. PKC performance was limited by an overload over a 3-hour recovery cycle. Previous studies indicated that the concentrate bed erodes faster for coarser and/or high density gangue than for fine and/or lower density gangue [Huang, 1996]. As discussed above (section 4.3), the recovery of PKC would be improved by diminishing the cycle time. In addition, since a GRC test at AELRD has shown that the ore contains a large amount of fine gold, removing the plus  $300 \mu\text{m}$  fraction from the PKC feed would also increase gravity recovery. Another increase in gravity recovery would result from decrease in the circulating loads, which would make it possible to treat a higher fraction of the circulating loads.

At Barrick Gold's East Malartic, the plant Knelson has a stage GRG recovery of 16% and most gold recovered by PKC is above  $300 \mu\text{m}$  [Vincent, 1996]. The dense concentrate is upgraded by a Gemeni table. It is known that tables do not effectively recover gold from primary concentrates in the fine particle size range and normally leave the fine gold in the table tail [Huang, et al., 1993]. Laboratory work shows that the 90% of the gold rejected by the table is finer than  $212 \mu\text{m}$ , compared to only 40% of the gangue. Because the PKC feed is both coarse and dense, it recovers only very highly recoverable GRG, which yields a high Gemeni table recovery above 95%, and a very high GRG content in the table tail, 91%. One conclusion is that difficult primary upgrading may result in easier cleaning, as the cleaner feed contains mostly gold very amenable to gravity recovery. On the down side, the gravity circuit recovers only 20% gold, from a GRG content above 60%.

At Chimo, the circuit survey was marred by assaying problems. Unfortunately, the high gangue density part of the survey, treating the flash flotation concentrate with a 51 cm

---

PKC, was the most affected.

### 6.1.3 Recovering gold from high gangue density ores

The surveys presented in this work point in the same direction: recovering gold from high density gangue is much more challenging than from their low density counter-parts. Work at Snip, Meston [Laplante, Huang and Noaparast, 1993], Hemlo [Laplante, 1996] indicates that at least 50% and as much as 70% of the GRG measured in the ore can be recovered by a conventional, Knelson-based gravity circuit: screening of 15 to 25% of the circulating load, at 850 to 1700  $\mu\text{m}$ , and processing the undersize with a PKC. This approach, when applied to high density ores, yields recoveries that total 30 to 40% of the GRG content (East Malartic, AELRD), or even much less (Louvicourt). Part of the problem is linked to the performance of the Knelson, which, at constant feed rate, is much lower with high density gangues, either at lab [Laplante, Shu and Marois, 1996] or at plant scale [Putz, Laplante and Ladouceur, 1993]. The test used to measure GRG in ores does not reflect this problem, as the LKC is not operated at high capacity, especially for the last two stages. Hence, it may not fully reflect the increased difficulty of recovering GRG from high density gangues. Whilst inserting a screen to remove the coarser size fraction (where little GRG is often found) prior to PKC in Les Mines Casa Berardi was recommended [Laplante, Putz, 1994], other work suggested using a higher rotating velocity KC to improve the recovery [Paventi, 1995].

## 6.2 Recommendations

Table 6-1 shows recommendations for the gold plants evaluated in this work. For AELRD and East Malartic, a finer feed and a shorter cycle are suggested. High density gangue and low density kustelite result in the recommendation of discontinuing gravity recovery at Aur Louvicourt. Increasing feed rate to the 76 cm PKC might increase gold gravity recovery at the Chimo Mine.

**Table 6-1 Recommendations for gold plants**

Gold Plant	Finer feed	Shorter cycle	Others
AELRD	Yes	Yes	-
Aur Louvicourt	-	-	Discontinue gravity
East Malartic	Yes	Yes	-
Chimo Mine	-	-	Increase feed rate to 76 cm PKC

### 6.3 Future Work

(1). Removing of the coarser size fractions, where most gold is not completely liberated, and shortening recovery cycles should increase recovery. This must be verified and documented.

(2). The variable speed LKC should be tested on gold ores with a high density gangue.

(3). Erosion of the Knelson Concentrate bed is closely linked to the size distribution and grade of the high density gangue minerals, typically sulphides. This should be further investigated at laboratory scale to determine the optimum screening size.

(4). There is evidence that kustelite might affect PKC performance even more so than that of the LKC. The GRG determination test, as it is presently designed, is incapable of detecting kustelite. A supplemental step should be included; it could be as simple as an atomic adsorption analysis of the gold and silver content of a fine fraction of the LKC concentrate. A high silver to gold ratio would identify the presence of kustelite.

## REFERENCES

Austin, L.G., Klimpel, R.R., and Luckie, P.T., 1984, "Process engineering of size reduction: Ball milling", Society for Mining Engineers, AIME Inc., New York.

Barisi, S., Laplante, A.R. and Marois, J., 1991, "The behaviour of gold in Hemlo mines Ltd. grinding circuit", CIM Bull., vol. 84 (955), pp. 72-78.

Bridgwater, J. and Ingram, N.D., 1971, "Rate of spontaneous inter-particle percolation ", Trans. Inst'n Chem. Engrs, vol. 49, pp. 163-169.

Bridgwater, J. Sharpe N.W. and Stocker, D.C., 1969, "Particle mixing by percolation", Trans. Inst'n Chem. Engrs, vol. 47, pp. T114-T119.

Buonvino, M., 1993, "A study of the Falcon concentrator", M. Eng. Thesis, McGill University, 152 pp.

Chatfield, C., 1981, "Statistics for technology - A course in applied statistics", Chapman and Hall, 2nd Ed., New York, 370 p.

Desharies, 1996, "Internal report on the grinding and gravity circuit at the Chimo Mine", 10 p.

Gasparini, C., 1993, "Gold and other precious metals - from ore to market", Springer - Verlag; Berlin, pp. 98-109.

Haque, K.E., 1987, "Gold leaching from refractory ores - literature survey", Mineral Processing and Extractive Metallurgy Review, No.2, pp. 235-253.

Hayek, C., 1995, "Identification B du cycle Knelson #2 (Alimentation/Rejet)", Internal technical report, Mine Est Malartic, 22 p.

Hope, G.H., McMullen J. and Green D., "Process advances at Lac Minerals Ltd. - Est Malartic Division", 1993, Proceedings - 25 Annual Meeting of the Canadian Mineral processors, The Canadian Institute of mining, Metallurgy and Petroleum, 13 p.

Huang, L., 1997, "Agnico-Eagle La Ronde survey", Technical report, 12 p.

Huang, L., 1996, "Upgrading of gold gravity concentrates: A study of the Knelson Concentrator", Ph.D. Thesis, McGill University, 200 p.

Knelson, B.V., "1988 - Centrifugal concentration and separation of precious metals", 1988, Gold Mining' 88, Ed. C.O. Brawner, pp. 303 - 317.

- Laplante, A.R., Huang, L. and Harris, G.B., 1996, "Defining overload conditions for the 7.6 cm Knelson Concentrator, using synthetic feeds", Trans. Inst. Min. Metall. (Section c: Mineral Process. Extr. Metall.), vol. 105, pp. c126 - c132.
- Laplante, A.R. & Shu, Y., Marois, J., "Experimental characterization of a laboratory centrifugal separator" 1996, Canadian Metallurgical Quarterly, Vol. 35, No. 1, pp. 23-29.
- Laplante, A.R., Huang, L., and Noaparast, M., and Nickoletopoulos, N., 1995, "A philosopher's stone: Turning tungsten and lead into gold -The use of synthetic ores to study gold gravity separation" Proceedings-27th Annual Meeting of the Canadian Mineral Processors, Ottawa, Ontario, Section 6, No. 28, pp. 379 - 394.
- Laplante, A.R., Putz, A. and Huang, L., May 1993, "Sampling and sample processing for gold gravity circuits," Professional Development Seminar on Gold Recovery by Gravity, McGill University, 22 p.
- Laplante, A.R., 1995, "Evaluation of gravity circuit at East Malartic", Technical report, September, 1995, Montreal, 29 p.
- Laplante, A.R., Huang, L. and Noaparast, M., 1993, "Report of the work performed for Meston Resources" Internal Report to Meston Resources, Montreal, 25 p.
- Laplante, A.R, Vincent, F. and Luisnta, W., 1996, "A laboratory procedure to determine the amount of gravity recoverable gold - a case study at Hemlo Gold Mines", Proceedings--28th Annual Meeting of the Canadian Mineral Processors, Ottawa, Ontario, pp. 69 - 82.
- Laplante, A.R., Putz, A., Huang, L. and Vincent, F., 1994, "Practical considerations in the operations of gold gravity circuits", Proceedings--26th Annual Meeting of the Canadian Mineral Processors, Ottawa, Paper 23, 21 p.
- Laplante, A. R. and Zhang, B., February 1996, "Report on two laboratory tests with table tails samples from East Malartic", Technical report, McGill University, 6 p.
- Laplante, A.R., 1993, "A comparative study of two centrifugal concentrators", Proc. 25th Annual Meeting of CMP, Ottawa, Paper 5, 18 p.
- Laplante, A.R., Vincent, F. Noaparast, M., Woodcock, 1995, "Predicting gravity separation gold recoveries", Proceedings of the XIX International Mineral Processing Congress, Vol. 4, Littleton, Colorado, USA, pp. 19-25.
- Laplante, A.R., 1996, "Characterization and behaviour of gold in grinding and gravity circuits", Final technical report for Snip operations, McGill University, 82 p.

- Laplante, A.R. and Shu, Y., January 1992, "The use of a laboratory centrifugal separator to study gravity recovery in industrial circuits", 24th Annual Meeting of the Canadian Mineral Processors Conference, Ottawa, paper No. 12.
- Laplante, A.R., Nov., 1996, "Characterization of gravity recoverable gold in a second sample of Agnico-Eagle La Ronde Division", Internal report, 8 p.
- Lin, J., 1995, "Variable speed Knelson Concentrator", A document for Ph. D. preliminary oral examination, McGill University, pp. 30 - 35.
- Liu, L., 1989, "An investigation of gold recovery in the grinding and gravity circuit at Les Mines Camchib Inc.", M. Eng. Thesis, McGill University, 180 p.
- Masliyah, J. and Bridgwater, J., 1974, "Particle percolation: a numerical study", Trans. Instn Chem. Engrs, vol. 52, pp. 31-42.
- Morrison, T.A., Hodson, T.W., 1992, "The Snip Mine Cominco Metals Ltd./Prime Resources Group Inc.", Presented at Minerals North 1992, Terrace, B.C..
- Noaparast, M., 1996, "The behaviour of malleable metals in tumbling mills", Ph. D. Thesis, McGill University, 350 p.
- Paventi, J., 1995, "Characterization of operation of a gravity circuit at Les Mines Casa Berardi", Research project report, McGill University, 45 p.
- Prasad, M.S., Mensah-Biney, R. and Pizarto, R.S., 1991, "Modern trends in gold processing - Overview", Minerals Engineering, Vol. 4, No. 12, pp. 1257-1277.
- Putz, A., Laplante, A.R. and Ladouceur, G., 1993, "Evaluation of a gravity circuit in a Canadian gold operation", Randol Gold Forum, Ed. Hans von Michaelis, Beaver Creek, pp. 145-149.
- Putz, A., 1994, "An investigation of the gravity recovery of gold", M.Eng. Thesis, McGill University, 230 p.
- Robitaille, J., 1996, Private communication, Agnico-Eagle La Ronde Division, Cadillac, Quebec.
- Sinclair, G., 1995, "Mineralogical study of mill products from the Louvicourt Mine-Part 4: mode of occurrence of gold and silver in a Knelson Concentrate" Report submitted to Aur Louvicourt Inc. by Min Scan Consultants Ltd., April 1995, 11p.

Spring, R., 1992, "NORBAL3 - software for material balance reconciliation", Noranda technology centre, Quebec, Canada, 62 p.

Vincent, F., 1998, "Comparing jig and Knelson concentrator performance for gold gravity recovery", M.Eng. Thesis in preparation, McGill University .

Wills, B.A., 1988, "Mineral processing technology", 4th edition, Pergamon press, London, pp. 357-358.

Woodcock, F., 1994, "Use of a Knelson unit to quantify gravity recoverable gold in an ore sample", M.Eng. Thesis, McGill University, 124 p.

Woodcock, F. and Laplante, A.R., 1993, "A laboratory method for determining the amount of gravity recoverable gold", Randol Gold Forum, Ed. Hans von Michaelis, Beaver Creek 1993, pp. 151-155.

**APPENDIX A**  
**Test results of gravity recoverable gold determinations**

**Appendix A-1 GRG tests of Snip2 Ball mill feed**

**Appendix A-2 GRG tests of Aur Louvicourt2**

**Appendix A-3 GRG tests of Barrick East Malartic**



**Appendix A-1**

**GRG tests at Snip2 Ball mill feed**

Date: August 6, 1995  
 Snip2 Ball Mill Feed, Stage #1, 3.0 psi, 955 g/min

Size (µm)	CONCENTRATE				TAILS				FEED			
	Weight (g)	% Weight	Grade (g/L)	Rec. (%)	Weight (g)	% Weight	Grade (g/L)	Rec. (%)	Weight (g)	% Weight	Grade (g/L)	Dist'n (%)
600	20.1	19.48	289.7	4.45	6069	11.90	20.6	95.55	6089	11.92	21.49	8.90
420	19.4	18.80	244.0	2.15	7293	14.30	29.5	97.85	7312	14.31	30.07	14.96
300	17.1	16.57	737.2	5.82	6145	12.05	33.2	94.18	6162	12.06	35.15	14.74
210	11.9	11.53	1477.0	13.96	4299	8.43	25.2	86.04	4311	8.44	29.21	8.57
150	11.3	10.95	2782.9	22.34	4156	8.15	26.3	77.66	4168	8.16	33.77	9.58
105	7.8	7.56	5472.6	37.20	3203	6.20	22.5	62.80	3210	6.28	35.74	7.81
75	5.6	5.43	9051.8	45.16	3274	6.42	18.8	54.84	3280	6.42	34.22	7.64
53	3.8	3.68	12321.1	54.51	2412	4.73	16.2	45.49	2416	4.73	35.55	5.84
37	2.6	2.52	15817.0	50.35	2458	4.82	16.5	49.65	2461	4.82	33.20	5.56
25	1.6	1.55	18770.0	46.58	2050	4.02	16.8	53.42	2052	4.02	31.42	4.39
-25	2.0	1.94	19071.3	21.56	9639	18.90	14.4	78.44	9641	18.87	18.35	12.04
Total	103.2	100.00	3117.1	21.88	50998	100.00	22.5	78.12	51101	100.00	28.77	100.00

Date: August 8, 1995  
 Snip(2) Ball Mill Feed, Stage #2, 2.5psi, 571 g/min

% -75 µm: 50.71

Size (µm)	CONCENTRATE				TAILS				FEED			
	Weight (g)	% Weight	Grade (g/L)	Rec. (%)	Weight (g)	% Weight	Grade (g/L)	Rec. (%)	Weight (g)	% Weight	Grade (g/L)	Dist'n (%)
600	0.00	0.00	0.00	0.00	0	0.00	0.0	0.00	0	0.00	0.00	0.00
420	1.05	1.06	551.40	20.77	93	0.39	23.7	79.23	94	0.39	29.58	0.46
300	8.10	8.14	407.60	12.39	1111	4.65	21.0	87.61	1119	4.66	23.80	4.38
210	15.00	15.07	463.70	11.24	2388	9.99	23.0	88.76	2403	10.01	25.75	10.17
150	21.53	21.63	557.00	10.59	3286	13.75	30.8	89.41	3308	13.78	34.22	18.61
105	16.78	16.86	813.60	18.66	2490	10.42	23.9	81.34	2507	10.45	29.19	12.03
75	12.79	12.85	1387.30	25.97	2385	9.98	21.2	74.03	2398	9.99	28.49	11.23
53	8.23	8.27	2002.20	34.92	1726	7.22	17.8	65.08	1734	7.22	27.22	7.76
37	6.80	6.83	2549.90	38.46	1778	7.44	15.6	61.54	1785	7.44	25.25	7.41
25	4.19	4.21	3678.50	37.55	1573	6.58	16.3	62.45	1577	6.57	26.03	6.75
-25	5.05	5.07	6212.60	24.33	7070	29.58	13.8	75.67	7075	29.48	18.22	21.20
Total	99.52	100.00	1354.78	22.17	23900	100.00	19.8	77.83	24000	100.00	25.34	100.00

Date: August 11, 1995  
 Smp Ball Mill Feed, Stage #3, 2.0 psi, 494 g/min  
 % - 75 µm: 81.20

Size (µm)	CONCENTRATE			TAILS			FEED					
	Weight (g)	% Weight	Grade (g/l)	Rec. (%)	Weight (g)	% Weight	Grade (g/l)	Rec. (%)	Weight (g)	% Weight	Grade (g/l)	Dist'n (%)
210	4.33	4.43	354.2	20.79	259	1.20	22.6	79.21	263	1.21	28.06	2.14
150	15.34	15.68	225.7	18.63	731	3.39	20.7	81.37	746	3.45	24.92	5.40
105	21.00	21.47	365.9	20.70	1457	6.76	20.2	79.30	1478	6.83	25.11	10.78
75	16.21	16.57	566.7	25.20	1567	7.27	17.4	74.80	1583	7.31	23.02	10.59
53	16.83	17.21	870.1	27.61	2612	12.12	14.7	72.39	2629	12.14	20.18	15.41
37	10.09	10.32	1265.6	29.06	2808	13.03	11.1	70.94	2818	13.02	15.59	12.77
25	6.09	6.23	1798.1	28.66	2726	12.65	10.0	71.34	2732	12.62	13.99	11.10
-25	7.92	8.10	3271.8	23.66	9392	43.58	8.9	76.34	9400	43.42	11.65	31.81
Total	97.81	100.00	861.4	25.02	21552	100.00	12.0	74.98	21650	100.00	15.90	100.00

SNIP, Second Sample, Overall Results

Size (µm)	First Stage: 100% - 850 µm		Second Stage: 51% - 75 µm		Third Stage: 81% - 75 µm		Total Recov. g/l	Total Recov. %
	Stage Recov.	Dist'n	Stage Recov.	Dist'n	Stage Recov.	Dist'n		
600	4.45	8.90	0.00	0.00	0.00	0.00	0.11	0.42
420	2.15	14.96	20.77	0.46	0.02	0.00	0.12	0.43
300	5.82	14.74	12.39	4.38	0.14	0.00	0.38	1.40
210	13.96	8.57	11.24	10.17	0.29	0.00	0.70	2.56
150	22.34	9.58	10.59	18.61	0.50	0.00	1.27	4.64
105	37.20	7.81	18.66	12.03	0.57	0.00	1.76	6.40
75	45.16	7.64	25.97	11.23	0.74	0.00	2.15	7.84
53	54.51	5.84	34.92	7.76	0.69	0.00	2.27	8.29
37	50.35	5.56	38.46	7.41	0.72	0.00	2.11	7.70
25	46.58	4.39	37.55	6.75	0.64	0.00	1.73	6.31
15	21.56	12.04	24.33	21.20	1.30	0.00	3.24	11.81
Total	22.94	100.00	26.52	100.00	5.61	100.00	15.86	57.79
O/A	22.94		20.44		14.41			
Yield Grade	0.0019		0.0041		0.0045			
Calc.:	28.77	g/l	25.34	g/l	15.90	g/l		
	27.44	g/l						

**Appendix A-2**  
**GRG tests at Aur Louvicourt2**

Date: November 13, 1995  
 Aur Louvicourt(2) , Stage #1, 4.4 psi, 1130 g/min

Size (µm)	CONCENTRATE			TAILS			FEED					
	Weight (g)	%Weight	Grade (g/L)	Rec. (%)	Weight (g)	%Weight	Grade (g/L)	Rec. (%)	Weight (g)	%Weight	Grade (g/L)	Dist'n (%)
600	16.90	14.07	11	0.30	4800	8.75	12.8	99.70	4817	8.76	12.79	11.46
420	17.75	14.78	388	6.96	6675	12.16	13.8	93.04	6693	12.17	14.79	18.41
300	17.75	14.78	159	5.17	5752	10.48	9.0	94.83	5770	10.49	9.46	10.15
210	13.37	11.13	329	10.05	4232	7.71	9.3	89.95	4245	7.72	10.31	8.14
150	14.70	12.24	350	11.51	4655	8.48	8.5	88.49	4670	8.49	9.58	8.32
105	10.89	9.07	719	20.59	4027	7.34	7.5	79.41	4038	7.34	9.42	7.07
75	9.75	8.12	1000	27.83	4213	7.68	6.0	72.17	4223	7.68	8.30	6.51
53	6.40	5.33	1138	24.27	3608	6.57	6.3	75.73	3614	6.57	8.30	5.58
37	5.58	4.64	1225	24.38	3365	6.13	6.3	75.62	3371	6.13	8.32	5.21
25	3.15	2.62	1239	15.45	2847	5.19	7.5	84.55	2850	5.18	8.86	4.70
-25	3.89	3.24	695	3.48	10707	19.51	7.0	96.52	10711	19.47	7.25	14.44
Total	120.13	100.00	481	10.74	54882	100.00	8.7	89.26	55002	100.00	9.78	100.00

Date: November 24, 1995  
 Aur Louvicourt(2), Stage #2, 3psi, 500 g/min

%-75 µm: 62.47

Size (µm)	CONCENTRATE			TAILS			FEED					
	Weight (g)	%Weight	Grade (g/L)	Rec. (%)	Weight (g)	%Weight	Grade (g/L)	Rec. (%)	Weight (g)	%Weight	Grade (g/L)	Dist'n (%)
600	1.59	1.25	9	0.46	82	0.29	38.0	99.54	84	0.29	37.45	1.25
420	7.31	5.76	14	2.10	548	1.93	8.7	97.90	555	1.94	8.77	1.95
300	13.89	10.95	137	11.42	1039	3.65	14.2	88.58	1053	3.69	15.82	6.66
210	11.20	8.83	209	17.40	911	3.20	12.2	82.60	922	3.23	14.59	5.38
150	19.22	15.16	243	15.79	1706	6.00	14.6	84.21	1725	6.04	17.14	11.82
105	19.67	15.51	187	10.52	2844	10.00	11.0	89.48	2864	10.03	12.21	13.97
75	19.67	15.51	289	21.88	3499	12.30	5.8	78.12	3519	12.32	7.38	10.38
53	11.81	9.31	439	25.44	2867	10.08	5.3	74.56	2879	10.08	7.08	8.15
37	10.12	7.98	515	26.81	2845	10.00	5.0	73.19	2855	10.00	6.81	7.77
25	5.97	4.71	777	29.54	2213	7.78	5.0	70.46	2219	7.77	7.08	6.28
-25	6.36	5.02	906	8.72	9883	34.76	6.1	91.28	9889	34.62	6.68	26.40
Total	126.81	100.00	309	15.66	28436	100.00	7.4	84.34	28563	100.00	8.76	100.00

Date: November 30, 1995  
 Aur Louvicourt(2), Stage #3, 2.0 psi, 340 g/min

%-75 µm: 81.72

Size (µm)	CONCENTRATE			TAILS			FEED					
	Weight (g)	% Weight	Grade (g/l)	Rec. (%)	Weight (g)	% Weight	Grade (g/l)	Rec. (%)	Weight (g)	% Weight	Grade (g/l)	Dist'n (%)
150	0.84	0.62	1799	51.13	62	0.29	23.3	48.87	63	0.29	47.04	1.99
105	10.08	7.49	153	10.70	926	4.29	13.9	89.30	936	4.31	15.40	9.71
75	35.60	26.46	44	6.18	2936	13.61	8.1	93.82	2972	13.69	8.53	17.08
53	26.20	19.47	49	5.62	2664	12.35	8.1	94.38	2690	12.39	8.50	15.41
37	24.56	18.25	71	9.63	2598	12.04	6.3	90.37	2623	12.08	6.91	12.21
25	19.32	14.36	142	19.93	2080	9.64	5.3	80.07	2099	9.67	6.56	9.28
-25	17.95	13.34	366	12.91	10311	47.79	4.3	87.09	10329	47.58	4.93	34.31
Total	134.55	100.00	126	11.43	21575	100.00	6.1	88.57	21710	100.01	6.83	100.00

Aur Louvicourt(2), Overall Results

Size (µm)	First Stage: 100% - 850 µm		Second Stage: 62.5% - 75 µm		Third Stage: 81.7% - 75 µm		Losses g/l	Total Recov. g/l	Total Recov. %
	Stage Recov. g/l	Dist'n	Stage Recov. g/l	Dist'n	Stage Recov. g/l	Dist'n			
600	0.30	11.46	0.46	1.25	0.00	0.00	0.004	0.0	
420	6.96	18.41	2.10	1.95	0.00	0.00	0.129	1.4	
300	5.17	10.15	11.42	6.66	0.07	0.07	0.118	1.3	
210	10.05	8.14	17.40	5.38	0.08	0.08	0.162	1.8	
150	11.51	8.32	15.79	11.82	0.16	0.16	0.327	3.5	
105	20.59	7.07	10.52	13.97	0.13	0.13	0.342	3.7	
75	27.83	6.51	21.88	10.38	0.20	0.20	0.448	4.8	
53	24.27	5.58	25.44	8.15	0.18	0.18	0.373	4.0	
37	24.38	5.21	26.81	7.77	0.18	0.18	0.387	4.2	
25	15.45	4.71	29.54	6.27	0.16	0.16	0.360	3.9	
15	3.48	14.44	8.72	26.40	0.20	0.20	0.553	6.0	
Total	11.4	100.00	16.7	100.00	1.37	1.37	3.203	34.6	
O/A	11.4		14.8	8.4	8.4				
Yield Grade	0.000018		0.000035		0.0062				
Calc.:	9.78	g/l	8.76	g/l	6.83	g/l			
	9.25	g/l							

**Appendix A-3**

**GRG tests at Barrick East Malartic**

Date: September, 1995  
 East Malarctic, Stage #1. 4 psi. 940 g/min. (with nuggets)

Size (µm)	CONCENTRATE				TAILS				FEED				
	Weight (g)	% Weight	Grade (g/L)	Rec. (%)	Weight (g)	% Weight	Grade (g/L)	Rec. (%)	Weight (g)	% Weight	Grade (g/L)	Rec. (%)	Dist'n (%)
850	0.76	0.63	548026	99.90	35	0.07	11.5	0.10	36	0.07	11650.38	0.10	38.92
600	18.80	15.50	1032	36.74	5132	9.83	6.5	63.26	5151	9.84	10.25	63.26	4.93
420	19.07	15.72	562	13.55	6175	11.82	11.1	86.45	6194	11.83	12.77	86.45	7.38
300	19.51	16.09	714	22.37	6180	11.83	7.8	77.63	6200	11.84	10.04	77.63	5.81
210	14.21	11.72	945	33.39	4651	8.91	5.8	66.61	4665	8.91	8.62	66.61	3.75
150	14.57	12.01	1314	37.40	4923	9.43	6.5	62.60	4938	9.43	10.37	62.60	4.70
105	10.53	8.68	1757	44.51	3910	7.49	5.9	55.49	3921	7.49	10.60	55.49	3.88
75	8.57	7.07	2427	47.09	3914	7.49	6.0	52.91	3923	7.49	11.26	52.91	4.12
53	5.79	4.77	2847	51.59	2787	5.34	5.6	48.41	2793	5.33	11.44	48.41	2.98
37	4.39	3.62	3173	39.25	2652	5.08	8.1	60.75	2656	5.07	13.36	60.75	3.31
25	2.25	1.86	3347	22.18	2036	3.90	13.0	77.82	2038	3.89	16.66	77.82	3.17
-25	2.83	2.33	2264	3.53	9832	18.82	17.8	96.47	9835	18.79	18.48	96.47	16.96
Total	121.28	100.00	4756	53.84	52229	100.00	9.5	46.16	52350	100.00	20.46	46.16	100.00

East Malarctic, Stage #1. 4 psi. 940 g/min

Size (µm)	CONCENTRATE				TAILS				FEED				
	Weight (g)	% Weight	Grade (g/L)	Rec. (%)	Weight (g)	% Weight	Grade (g/L)	Rec. (%)	Weight (g)	% Weight	Grade (g/L)	Rec. (%)	Dist'n (%)
600	19.56	16.13	1032	35.75	5167	9.89	7.0	64.25	5187	9.91	10.09	64.25	8.58
420	19.07	15.72	562	13.55	6175	11.82	11.1	86.45	6194	11.83	12.77	86.45	12.02
300	19.51	16.09	714	22.37	6180	11.83	7.8	77.63	6200	11.84	10.04	77.63	9.46
210	14.21	11.72	945	33.39	4651	8.91	5.8	66.61	4665	8.91	8.62	66.61	6.11
150	14.57	12.01	1314	37.40	4923	9.43	6.5	62.60	4938	9.43	10.37	62.60	7.70
105	10.53	8.68	1757	44.51	3910	7.49	5.9	55.49	3921	7.49	10.60	55.49	6.32
75	8.57	7.07	2427	47.09	3914	7.49	6.0	52.91	3923	7.49	11.26	52.91	6.71
53	5.79	4.77	2847	51.59	2787	5.34	5.6	48.41	2793	5.33	11.44	48.41	4.86
37	4.39	3.62	3173	39.25	2652	5.08	8.1	60.75	2656	5.07	13.36	60.75	5.39
25	2.25	1.86	3347	22.18	2036	3.90	13.0	77.82	2038	3.89	16.66	77.82	5.16
-25	2.83	2.33	2264	3.53	9832	18.82	17.8	96.47	9835	18.79	18.48	96.47	27.61
Total	121.28	100.00	1328	24.48	52229	100.00	9.5	75.52	52350	100.00	12.57	75.52	100.00



Date: September, 1995  
 East Malarctic, Stage #2, 3psi, 320 g/min

% - 75 µm: 64.42

Size (µm)	CONCENTRATE				TAILS				FEED			
	Weight (g)	% Weight	Grade (g/l)	Rec. (%)	Weight (g)	% Weight	Grade (g/l)	Rec. (%)	Weight (g)	% Weight	Grade (g/l)	Dist'n (%)
300	1.62	1.14	90	47.80	35	0.12	4.6	52.20	37	0.18	8.33	0.21
210	14.86	10.45	161	43.51	470	1.65	6.6	56.49	485	2.39	11.34	3.87
150	37.59	26.43	111	27.25	1924	6.77	5.8	72.75	1962	9.67	7.81	10.77
105	27.41	19.27	158	29.30	2103	7.40	5.0	70.70	2130	10.50	6.94	10.40
75	22.35	15.71	131	22.06	2580	9.07	4.0	77.94	2602	12.83	5.10	9.33
53	15.91	11.19	286	34.46	2296	8.07	3.8	65.54	2312	11.40	5.71	9.29
37	11.23	7.90	449	37.82	2259	7.94	3.7	62.18	2270	11.19	5.87	9.38
25	6.00	4.22	755	35.19	1713	6.02	4.9	64.81	1719	8.48	7.49	9.05
-25	5.26	3.70	1381	13.55	6757	23.76	6.9	86.45	6762	33.34	7.93	37.71
Total	142.23	100.00	249	24.86	20138	70.82	5.3	75.14	20280	100.00	7.01	100.00

Date: September, 1995  
 East Malarctic, Stage #3, 2.0 psi, 330 g/min

% - 75 µm: 78.29

Size (µm)	CONCENTRATE				TAILS				FEED			
	Weight (g)	% Weight	Grade (g/l)	Rec. (%)	Weight (g)	% Weight	Grade (g/l)	Rec. (%)	Weight (g)	% Weight	Grade (g/l)	Dist'n (%)
150	3.80	2.98	67	43.43	104	0.62	3.3	56.57	108	0.64	5.57	0.61
105	22.49	17.27	93	33.95	1044	6.26	3.9	66.05	1066	6.35	5.80	6.23
75	35.45	27.22	105	30.87	2437	14.62	3.4	69.13	2472	14.72	4.89	12.19
53	27.34	20.99	106	30.90	2152	12.91	3.0	69.10	2179	12.97	4.32	9.48
37	20.47	15.72	269	44.41	2231	13.38	3.1	55.59	2251	13.40	5.51	12.50
25	11.41	8.76	235	33.53	1685	10.11	3.2	66.47	1696	10.10	4.71	8.05
-25	9.20	7.06	1260	22.94	7016	42.09	5.6	77.06	7025	41.82	7.19	50.94
Total	130.24	100.00	221	29.01	16670	100.00	4.2	70.99	16800	100.00	5.90	100.00

East Malartic, Overall Results

Size ( $\mu\text{m}$ )	First Stage: 100% - 850 $\mu\text{m}$			Second Stage: 64.4% - 75 $\mu\text{m}$			Third Stage: 78.3% - 75 $\mu\text{m}$				Total Recov. g/l	Total Recov. %	
	Stage Recov.	Dist'n	Rec. g/l	Stage Recov.	Dist'n	Rec. g/l	Stage Recov.	Dist'n	Rec. g/l	Losses g/l			
600	35.75	8.58	0.38									0.383	3.6
420	13.55	12.02	0.20									0.204	1.9
300	22.37	9.46	0.26	47.80	0.21	0.01						0.272	2.6
210	33.39	6.11	0.26	43.51	3.87	0.12						0.373	3.5
150	37.40	7.78	0.36	27.25	10.77	0.20	43.43	0.61	0.015	0.020		0.584	5.5
105	44.51	6.32	0.35	29.30	10.40	0.21	33.95	6.23	0.124	0.241		0.688	6.5
75	47.09	6.71	0.40	22.06	9.33	0.14	30.87	12.19	0.220	0.493		0.759	7.1
53	51.59	4.86	0.31	34.46	9.29	0.22	30.90	9.48	0.171	0.383		0.708	6.7
37	39.25	5.39	0.26	37.82	9.38	0.25	44.41	12.50	0.324	0.406		0.837	7.9
25	22.18	5.16	0.14	35.19	9.05	0.22	33.53	8.05	0.158	0.313		0.523	4.9
15	3.53	27.61	0.12	13.55	37.71	0.36	22.94	50.94	0.683	2.295		1.162	10.9
Total	28.8	100.00	3.06	22.9	100.00	1.74	29.0	100.00	1.696	4.150		6.491	61.0
O/A	28.8			16.3			15.9						
Yield	0.0023			0.0070			0.0078						
Grade	12.5	g/l		7.0	g/l		5.9	g/l					
Calc.:	10.64	g/l											



**APPENDIX B**  
**Test results of the gravity circuit investigations**

- Appendix B-1 Aur Louvicourt**
- Appendix B-2 Agnico-Eagle La Ronde Division**
- Appendix B-3 Table tail at Barrick East Malartic**
- Appendix B-4 Cambior's Chimo**

**Appendix B-1**

**Aur Louvicourt**

Date: March 20, 1995  
 Aur Louvicourt, 30" Knelson Feed, 100% -20 mesh, 4 psi, 516 g/min

Size (µm)	CONCENTRATE				TAILS				FEED			
	Weight (g)	% Weight	Grade (g/l)	Rec. (%)	Weight (g)	% Weight	Grade (g/l)	Rec. (%)	Weight (g)	% Weight	Grade (g/l)	Dist'n (%)
600	5.83	5.71	2	1.18	349	2.09	2.8	98.82	355	2.11	2.79	0.47
420	8.07	7.91	179	34.91	612	3.66	4.4	65.09	620	3.69	6.67	1.97
300	11.81	11.57	129	19.10	896	5.36	7.2	80.90	908	5.40	8.78	3.79
210	10.99	10.77	107	17.04	954	5.71	6.0	82.96	965	5.74	7.15	3.28
150	12.81	12.55	346	39.51	1475	8.82	4.6	60.49	1488	8.85	7.54	5.34
105	11.56	11.33	432	30.03	1818	10.88	6.4	69.97	1830	10.88	9.09	7.91
75	12.49	12.24	976	34.21	2468	14.77	9.5	65.79	2480	14.75	14.37	16.96
53	11.41	11.18	1264	35.16	2293	13.72	11.6	64.84	2304	13.70	17.80	19.52
37	9.99	9.79	1379	32.73	2399	14.35	11.8	67.27	2409	14.33	17.47	20.02
25	4.70	4.61	1580	33.00	1300	7.78	11.6	67.00	1305	7.76	17.25	10.71
-25	2.40	2.35	1614	18.38	2150	12.86	8.0	81.62	2152	12.80	9.79	10.03
Total	102.06	100.00	640	31.06	16714	100.00	8.7	68.94	16816	100.00	12.50	100.00

Date: March 20, 1995  
 Aur Louvicourt, 30" Knelson Feed, 100% -50 mesh, 3 psi, 460 g/min

Size (µm)	CONCENTRATE				TAILS				FEED			
	Weight (g)	% Weight	Grade (g/l)	Rec. (%)	Weight (g)	% Weight	Grade (g/l)	Rec. (%)	Weight (g)	% Weight	Grade (g/l)	Dist'n (%)
210	31.26	25.30	18	24.42	670	4.95	2.6	75.58	701	5.14	3.29	1.36
150	27.04	21.88	121	27.33	1500	11.09	5.8	72.67	1527	11.18	7.84	7.07
105	16.81	13.60	423	47.58	1632	12.07	4.8	52.42	1649	12.08	9.06	8.83
75	14.58	11.80	864	42.05	2284	16.89	7.6	57.95	2299	16.84	13.03	17.69
53	13.58	10.99	1022	39.00	2087	15.43	10.4	61.00	2101	15.39	16.94	21.02
37	11.97	9.69	926	29.98	2194	16.22	11.8	70.02	2206	16.16	16.76	21.84
25	5.60	4.53	1215	32.45	1221	9.03	11.6	67.55	1227	8.99	17.09	12.38
-25	2.73	2.21	1115	18.32	1939	14.33	7.0	81.68	1942	14.23	8.56	9.81
Total	123.57	100.00	472	34.46	13526	100.00	8.2	65.54	13650	100.00	12.40	100.00

Date: March 21, 1995

Aur Louvicourt, 30" Knelson Concentrate, 100% -20 mesh, 4 psi, 546 g/min

Size (µm)	CONCENTRATE				TAILS				FEED			
	Weight (g)	% %Weight	Grade (g/l)	Rec. (%)	Weight (g)	% %Weight	Grade (g/l)	Rec. (%)	Weight (g)	% %Weight	Grade (g/l)	Dist'n (%)
600	11.85	9.65	174	4.53	207	3.63	209.8	95.47	219	3.76	207.86	0.60
420	13.21	10.76	2836	16.22	302	5.30	640.8	83.78	315	5.41	732.80	3.07
300	14.49	11.80	11694	37.50	404	7.08	699.0	62.50	418	7.18	1079.70	6.00
210	11.59	9.44	11751	29.01	391	6.86	852.2	70.99	403	6.91	1165.96	6.24
150	12.48	10.16	11925	29.03	490	8.59	742.4	70.97	502	8.63	1020.14	6.81
105	10.90	8.88	20596	41.99	499	8.75	621.6	58.01	510	8.75	1048.59	7.10
75	12.24	9.97	23795	42.51	688	12.07	572.6	57.49	700	12.02	978.52	9.11
53	12.39	10.09	34342	46.72	701	12.29	692.2	53.28	713	12.25	1276.62	12.10
37	12.55	10.22	34072	40.92	780	13.68	791.6	59.08	793	13.61	1318.59	13.89
25	6.39	5.20	58700	30.63	511	8.96	1662.6	69.37	517	8.88	2367.04	16.27
-25	4.71	3.84	71684	23.86	729	12.78	1477.6	76.14	734	12.60	1928.29	18.80
Total	122.80	100.00	20974	34.22	5702	100.00	868.1	65.78	5825	100.00	1291.92	100.00

Date: March 21, 1995

Aur Louvicourt, 30" Knelson Concentrate, 100% -50 mesh, 3 psi, 430 g/min

Size (µm)	CONCENTRATE				TAILS				FEED			
	Weight (g)	% %Weight	Grade (g/l)	Rec. (%)	Weight (g)	% %Weight	Grade (g/l)	Rec. (%)	Weight (g)	% %Weight	Grade (g/l)	Dist'n (%)
210	34.66	25.47	5772	48.07	355	7.67	608.7	51.93	390	8.18	1067.97	6.59
150	28.55	20.98	16931	72.69	387	8.36	469.2	27.31	416	8.72	1600.19	10.53
105	16.75	12.31	24046	70.90	442	9.55	374.0	29.10	459	9.63	1238.32	9.00
75	13.69	10.06	36958	71.64	662	14.29	302.8	28.36	675	14.17	1046.01	11.19
53	13.56	9.97	37876	69.88	694	15.00	319.0	30.12	708	14.85	1038.76	11.64
37	14.59	10.72	40449	60.16	784	16.94	498.5	39.84	799	16.76	1228.38	15.54
25	8.71	6.40	64982	54.74	515	11.13	908.6	45.26	524	10.99	1974.23	16.37
-25	5.55	4.08	76120	34.95	789	17.05	996.6	65.05	795	16.68	1521.34	19.14
Total	136.06	100.00	27079	58.35	4628	100.00	568.3	41.65	4764	100.00	1325.46	100.00

Date: March 16, 1995

Aur Louvicourt, 30" Knelson Tail, 100% -20 mesh, 4 psi, 470 g/min

Size ( $\mu$ m)	CONCENTRATE				TAILS				FEED			
	Weight (g)	% %Weight	Grade (g/l)	Rec. (%)	Weight (g)	% %Weight	Grade (g/l)	Rec. (%)	Weight (g)	% %Weight	Grade (g/l)	Dist'n (%)
600	6.60	6.44	2.0	9.09	132	1.70	1.0	90.91	139	1.76	1.05	0.17
420	9.32	9.09	22.4	17.33	262	3.37	3.8	82.67	271	3.44	4.44	1.37
300	13.06	12.74	57.4	23.53	435	5.59	5.6	76.47	448	5.68	7.11	3.62
210	11.32	11.04	72.0	28.96	476	6.12	4.2	71.04	487	6.18	5.77	3.20
150	12.32	12.01	139.2	35.67	703	9.03	4.4	64.33	715	9.07	6.72	5.47
105	11.02	10.75	331.8	40.15	826	10.61	6.6	59.85	837	10.62	10.88	10.36
75	11.32	11.04	474.4	36.15	1103	14.17	8.6	63.85	1114	14.13	13.33	16.90
53	10.33	10.07	619.6	40.03	1020	13.11	9.4	59.97	1030	13.07	15.52	18.18
37	9.46	9.22	666.0	37.66	1043	13.40	10.0	62.34	1052	13.35	15.90	19.03
25	4.65	4.53	740.8	35.89	628	8.07	9.8	64.11	633	8.02	15.17	10.92
-25	3.15	3.07	740.5	24.58	1155	14.83	6.2	75.42	1158	14.68	8.20	10.79
Total	102.55	100.00	302.4	35.26	7782	100.00	7.3	64.74	7805	100.00	11.15	100.00

Date: March 17, 1995

Aur Louvicourt, 30" Knelson Tail, 100% -50 mesh, 3 psi, 560 g/min

Size ( $\mu$ m)	CONCENTRATE				TAILS				FEED			
	Weight (g)	% %Weight	Grade (g/l)	Rec. (%)	Weight (g)	% %Weight	Grade (g/l)	Rec. (%)	Weight (g)	% %Weight	Grade (g/l)	Dist'n (%)
210	29.39	26.17	56	59.03	336	5.38	3.4	40.97	365	5.75	7.63	2.54
150	26.27	23.39	133	40.18	621	9.95	8.4	59.82	647	10.19	13.47	7.93
105	15.78	14.05	240	47.78	767	12.29	5.4	52.22	783	12.32	10.13	7.21
75	12.77	11.37	433	37.42	1052	16.85	8.8	62.58	1065	16.76	13.89	13.45
53	11.08	9.86	616	36.75	1030	16.50	11.4	63.25	1041	16.38	17.83	16.88
37	9.72	8.65	694	36.39	967	15.49	12.2	63.61	977	15.37	18.99	16.86
25	4.62	4.11	913	33.88	490	7.85	16.8	66.12	495	7.78	25.17	11.32
-25	2.69	2.39	2095	21.53	979	15.68	21.0	78.47	981	15.44	26.69	23.81
Total	112.32	100.00	337	34.46	6242	100.00	11.5	65.54	6354	100.00	17.31	100.00



**Appendix B-2**

**Agnico-Eagle La Ronde Division**

Date: October 4, 1995  
 Agnico-Eagle Cyclone underflow (PKC Feed) 1st hour, 3.0 psi, 450 g/min

Size (µm)	CONCENTRATE				TAILS				FEED			
	Weight (g)	% Weight	Grade (g/l)	Rec. (%)	Weight (g)	% Weight	Grade (g/l)	Rec. (%)	Weight (g)	% Weight	Grade (g/l)	Dist'n (%)
600	3.16	2.50	38.16	8.35	181	0.97	7.31	91.65	184	0.98	7.84	0.24
420	4.09	3.23	273.89	24.83	415	2.22	8.18	75.17	419	2.23	10.78	0.76
300	8.99	7.11	642.82	27.22	955	5.12	16.18	72.78	964	5.13	22.02	3.58
210	12.83	10.14	695.07	30.21	1578	8.46	13.05	69.79	1591	8.47	18.55	4.97
150	22.76	17.99	970.78	38.06	3057	16.38	11.76	61.94	3080	16.39	18.85	9.78
105	24.19	19.12	1349.61	41.53	3785	20.17	12.21	58.47	3789	20.16	20.75	13.25
75	25.05	19.80	1846.45	49.91	4205	22.53	11.04	50.09	4230	22.51	21.91	15.62
53	15.45	12.21	3911.35	63.66	2338	12.53	14.76	36.34	2353	12.52	40.34	16.00
37	6.47	5.11	9245.87	62.04	1105	5.92	33.12	37.96	1112	5.92	86.74	16.25
25	1.63	1.29	13896.19	43.82	371	1.99	78.26	56.18	373	1.98	138.69	8.71
-25	1.88	1.49	14632.53	42.76	694	3.72	53.07	57.24	696	3.70	92.46	10.84
Total	126.50	100.00	2271.50	48.42	18664	100.00	16.40	51.58	18790	100.00	31.58	100.00

Date: October 4, 1995  
 Agnico-Eagle Cyclone underflow 2hour, 3.0 psi, 450 g/min

Size (µm)	CONCENTRATE				TAILS				FEED			
	Weight (g)	% Weight	Grade (g/l)	Rec. (%)	Weight (g)	% Weight	Grade (g/l)	Rec. (%)	Weight (g)	% Weight	Grade (g/l)	Dist'n (%)
600	3.21	2.48	638.74	59.75	152	1.02	9.09	40.25	155	1.03	22.12	0.68
420	5.58	4.30	292.45	38.82	319	2.14	8.07	61.18	324	2.16	12.96	0.83
300	11.55	8.91	428.81	34.33	767	5.16	12.36	65.67	778	5.19	18.54	2.86
210	14.91	11.50	353.38	19.58	1258	8.46	17.21	80.42	1272	8.48	21.15	5.33
150	23.92	18.45	735.45	36.41	2448	16.46	12.55	63.59	2472	16.48	19.55	9.57
105	24.05	18.55	1073.56	40.73	3077	20.70	12.21	59.27	3101	20.68	20.44	12.56
75	23.81	18.37	2019.79	53.81	3562	23.96	11.59	46.19	3586	23.91	24.92	17.71
53	13.53	10.44	3763.64	63.46	1796	12.08	16.32	36.54	1810	12.07	44.33	15.90
37	5.36	4.13	8668.87	63.76	829	5.57	31.88	36.24	834	5.56	87.40	14.44
25	1.39	1.07	18642.76	54.06	285	1.92	77.20	45.94	287	1.91	167.23	9.50
-25	2.33	1.80	13936.56	60.69	378	2.54	55.68	39.31	380	2.53	140.78	10.60
Total	129.64	100.00	2014.65	51.76	14870	100.00	16.37	48.24	15000	100.00	33.64	100.00

Agnico-Eagle Cyclone underflow 3hour, 3.0 psi, 596 g/min

Size (µm)	CONCENTRATE				TAILS				FEED			
	Weight (g)	% Weight	Grade (g/l)	Rec. (%)	Weight (g)	% Weight	Grade (g/l)	Rec. (%)	Weight (g)	% Weight	Grade (g/l)	Dist'n (%)
600	4.43	3.48	26.40	7.92	136	0.89	10.00	92.08	140	0.91	10.52	0.28
420	6.61	5.19	378.63	46.93	313	2.04	9.04	53.07	320	2.06	16.68	1.02
300	12.40	9.74	281.11	21.63	739	4.81	17.09	78.37	751	4.85	21.45	3.08
210	14.95	11.74	434.24	22.43	1202	7.82	18.67	77.57	1217	7.85	23.77	5.54
150	23.21	18.23	606.48	29.74	2440	15.87	13.63	70.26	2463	15.89	19.22	9.06
105	23.11	18.15	1123.61	39.84	3229	21.01	12.14	60.16	3252	20.98	20.04	12.47
75	22.39	17.58	2115.25	51.28	3647	23.72	12.34	48.72	3669	23.67	25.17	17.67
53	12.12	9.52	4525.88	63.53	1929	12.55	16.32	36.47	1941	12.53	44.47	16.52
37	4.90	3.85	10628.70	62.48	901	5.86	34.70	37.52	906	5.85	91.98	15.95
25	1.42	1.12	18495.61	53.96	323	2.10	69.48	46.04	324	2.09	150.24	9.31
-25	1.80	1.41	10853.09	41.03	513	3.34	54.65	58.97	515	3.32	92.35	9.10
Total	127.34	100.00	1984.53	48.35	15373	100.00	17.56	51.65	15500	100.00	33.72	100.00

Date: October 20, 1995

Agnico-Eagle Cyclone Underflow (diluted with 2:1 fine silica), 2.0 psi, 600 g/min

Size (µm)	CONCENTRATE				TAILS				FEED			
	Weight (g)	% Weight	Grade (g/l)	Rec. (%)	Weight (g)	% Weight	Grade (g/l)	Rec. (%)	Weight (g)	% Weight	Grade (g/l)	Dist'n (%)
600	1.98	1.70	26.78	5.10	80	0.35	12.32	94.90	82	0.36	12.67	0.40
420	2.51	2.16	968.38	52.87	156	0.68	13.93	47.13	158	0.68	29.09	1.76
300	5.18	4.45	536.69	39.38	373	1.63	11.46	60.62	379	1.64	18.64	2.70
210	7.43	6.39	622.25	36.92	626	2.72	12.62	63.08	633	2.74	19.77	4.80
150	13.94	11.99	569.61	28.36	1214	5.28	16.52	71.64	1228	5.32	22.80	10.72
105	16.83	14.47	754.38	35.34	1493	6.50	15.56	64.66	1510	6.54	23.80	13.76
75	22.59	19.42	1022.06	49.03	2048	8.91	11.72	50.97	2070	8.96	22.74	18.04
53	17.17	14.76	1665.57	87.09	3007	13.08	1.41	12.91	3024	13.09	10.86	12.58
37	13.77	11.84	2140.76	69.94	4127	17.96	3.07	30.06	4141	17.93	10.18	16.14
25	6.77	5.82	2822.08	73.67	2809	12.22	2.43	26.33	2816	12.19	9.21	9.93
-25	8.13	6.99	1592.33	54.07	7050	30.67	1.56	45.93	7058	30.55	3.39	9.17
Total	116.30	100.00	1235.93	55.05	22984	100.00	5.11	44.95	23100	100.00	11.30	100.00

Agnico-Eagle KC Tail 1hour, 3.0 psi, 470 g/min

Size (µm)	CONCENTRATE				TAILS				FEED				
	Weight (g)	% Weight	Grade (g/t)	Rec. (%)	Weight (g)	% Weight	Grade (g/t)	Rec. (%)	Weight (g)	% Weight	Grade (g/t)	Rec. (%)	Dist'n (%)
600	2.59	2.03	7.42	2.09	132	0.89	6.83	97.91	134	0.90	6.84		0.24
420	3.73	2.93	127.82	15.21	286	1.92	9.30	84.79	290	1.93	10.83		0.80
300	8.44	6.63	253.43	20.45	731	4.92	11.38	79.55	739	4.93	14.14		2.67
210	13.50	10.61	293.90	18.03	1248	8.39	14.46	81.97	1261	8.41	17.45		5.63
150	23.93	18.80	587.49	31.97	2493	16.76	12.00	68.03	2517	16.78	17.47		11.24
105	24.98	19.63	997.11	42.09	3030	20.37	11.31	57.91	3055	20.37	19.37		15.13
75	26.70	20.98	1601.60	52.68	3479	23.40	11.04	47.32	3506	23.37	23.15		20.76
53	14.03	11.02	3031.70	60.43	1872	12.59	14.88	39.57	1886	12.57	37.33		18.00
37	5.87	4.61	2826.33	38.79	834	5.61	31.40	61.21	840	5.60	50.94		10.94
25	1.90	1.49	3064.68	22.00	296	1.99	69.77	78.00	298	1.99	88.87		6.77
-25	1.61	1.26	5339.11	28.14	473	3.18	46.42	71.86	475	3.16	64.38		7.81
Total	127.28	100.00	1271.81	41.40	14873	100.00	15.41	58.60	15000	100.00	26.07		100.00

Date: October 3, 1995

Agnico-Eagle KC Tail, 2hour, 3.0 psi, 490 g/min

Size (µm)	CONCENTRATE				TAILS				FEED				
	Weight (g)	% Weight	Grade (g/t)	Rec. (%)	Weight (g)	% Weight	Grade (g/t)	Rec. (%)	Weight (g)	% Weight	Grade (g/t)	Rec. (%)	Dist'n (%)
600	2.66	2.17	63.75	5.30	207	1.09	14.66	94.70	209	1.10	15.28		0.56
420	3.94	3.22	853.45	26.93	406	2.14	22.48	73.07	410	2.15	30.47		2.18
300	9.17	7.49	383.29	32.43	962	5.07	7.61	67.57	971	5.09	11.16		1.90
210	13.05	10.66	470.02	21.60	1599	8.43	13.92	78.40	1612	8.44	17.61		4.97
150	22.29	18.21	764.73	31.22	3170	16.70	11.85	68.78	3192	16.71	17.11		9.56
105	24.33	19.88	1201.78	37.48	3864	20.36	12.62	62.52	3889	20.36	20.06		13.65
75	24.38	19.92	2116.74	49.11	4431	23.35	12.07	50.89	4455	23.32	23.59		18.39
53	13.83	11.30	4225.08	61.14	2314	12.20	16.05	38.86	2328	12.19	41.05		16.73
37	5.63	4.60	8736.22	53.84	1106	5.83	38.12	46.16	1112	5.82	82.17		15.98
25	1.45	1.18	19792.45	67.62	368	1.94	37.30	32.38	370	1.94	114.73		7.43
-25	1.68	1.37	13235.70	44.94	550	2.90	49.51	55.06	552	2.89	89.64		8.66
Total	122.41	100.00	2202.64	47.18	18978	100.00	15.91	52.82	19100	100.00	29.92		100.00

Date: October 3, 1995

Agnico-Eagle KC Tail, 3hour, 3.0 psi, 520 g/min

Size (µm)	CONCENTRATE				TAILS				FEED			
	Weight (g)	% %Weight	Grade (g/l)	Rec. (%)	Weight (g)	% %Weight	Grade (g/l)	Rec. (%)	Weight (g)	% %Weight	Grade (g/l)	Dist'n (%)
600	2.56	1.93	398.38	32.64	158	1.10	13.32	67.36	161	1.11	19.46	0.65
420	4.37	3.29	282.95	24.12	337	2.35	11.53	75.88	342	2.36	15.00	1.07
300	9.69	7.29	615.86	43.30	766	5.33	10.20	56.70	776	5.35	17.76	2.89
210	13.47	10.13	334.98	20.02	1220	8.49	14.78	79.98	1233	8.50	18.28	4.72
150	23.64	17.78	597.22	30.06	2432	16.93	13.51	69.94	2456	16.93	19.13	9.84
105	27.10	20.38	995.46	41.33	3051	21.24	12.55	58.67	3078	21.23	21.20	13.68
75	27.66	20.80	1811.10	56.02	3221	22.42	12.21	43.98	3249	22.41	27.53	18.74
53	15.08	11.34	3498.17	65.60	1710	11.90	16.18	34.40	1725	11.89	46.62	16.85
37	6.28	4.72	7936.89	66.51	840	5.84	29.89	33.49	846	5.83	88.60	15.70
25	1.66	1.25	12615.91	54.41	283	1.97	62.01	45.59	285	1.96	135.21	8.07
-25	1.44	1.08	12407.67	48.06	349	2.43	55.27	51.94	351	2.42	105.98	7.79
Total	132.95	100.00	1845.30	51.40	14367	100.00	16.14	48.60	14500	100.00	32.91	100.00

Date: October 20, 1995

Agnico-Eagle KC Tail (diluted with 2:1 fine silica), 2.0 psi, 508 g/min

Size (µm)	CONCENTRATE				TAILS				FEED			
	Weight (g)	% %Weight	Grade (g/l)	Rec. (%)	Weight (g)	% %Weight	Grade (g/l)	Rec. (%)	Weight (g)	% %Weight	Grade (g/l)	Dist'n (%)
600	1.13	1.18	5.59	0.41	90	0.39	17.11	99.59	92	0.40	16.97	0.65
420	1.98	2.06	13.81	0.89	176	0.76	17.41	99.11	178	0.77	17.37	1.30
300	4.40	4.59	182.19	8.08	415	1.80	21.98	91.92	419	1.81	23.66	4.17
210	6.45	6.72	410.65	26.38	686	2.98	10.77	73.62	693	3.00	14.49	4.22
150	12.25	12.77	570.78	31.66	1326	5.77	11.38	68.34	1338	5.79	16.50	9.28
105	14.58	15.20	697.87	34.77	1620	7.04	11.78	65.23	1635	7.08	17.90	12.30
75	19.06	19.87	1211.04	53.50	2217	9.64	9.05	46.50	2236	9.68	19.30	18.13
53	14.97	15.61	1915.02	77.65	2896	12.59	2.85	22.35	2911	12.60	12.68	15.52
37	12.57	13.10	2368.12	75.70	4323	18.79	2.21	24.30	4335	18.77	9.07	16.52
25	5.17	5.39	3416.80	78.88	2673	11.62	1.77	21.12	2678	11.59	8.36	9.41
-25	3.36	3.50	3729.58	61.94	6582	28.61	1.17	38.06	6586	28.51	3.07	8.50
Total	95.92	100.00	1379.95	55.63	23004	100.00	4.59	44.37	23100	100.00	10.30	100.00

**Appendix B-3**

**Table tail at Barrick East Malartic**

Date: November 8, 1995  
 Barrick Table Tail, 100% -850 μm (20 mesh), 4 psi, 400 g/min.

Size (μm)	CONCENTRATE			TAILS			FEED					
	Weight (g)	% Weight	Grade (g/L)	Rec. (%)	Weight (g)	% Weight	Grade (g/L)	Rec. (%)	Weight (g)	% Weight	Grade (g/L)	Dist'n (%)
850	0.53	0.39	18.87	1.70	50	1.29	11.61	98.30	50	1.26	11.69	0.04
600	12.00	8.78	87.59	22.65	405	10.48	8.87	77.35	417	10.42	11.14	0.34
420	12.47	9.12	219.04	19.20	388	10.05	29.62	80.80	401	10.02	35.52	1.05
300	14.78	10.81	761.06	42.84	449	11.63	33.39	57.16	464	11.61	56.56	1.93
210	15.13	11.06	3700.32	55.68	382	9.88	116.81	44.32	397	9.92	253.50	7.41
150	18.72	13.69	11298.65	72.17	538	13.91	151.72	27.83	556	13.91	526.84	21.59
105	23.93	17.50	11732.31	82.75	623	16.12	93.96	17.25	647	16.17	524.62	25.00
75	21.03	15.38	11168.41	83.74	681	17.62	67.00	16.26	702	17.54	399.68	20.67
53	11.12	8.13	9784.02	83.59	255	6.60	83.70	16.41	266	6.66	488.84	9.59
37	6.46	4.72	14505.16	88.66	77	1.99	156.00	11.34	83	2.08	1268.71	7.79
25	0.48	0.35	35283.33	76.13	9	0.23	595.86	23.87	9	0.23	2368.25	1.64
-25	0.10	0.07	136430.00	34.06	8	0.20	3437.14	65.94	8	0.19	5145.56	2.95
Total	136.75	100.00	7541.09	75.98	3863	100.00	84.38	24.02	4000	100.00	339.31	100.00

Date: February 13, 1996  
 Barrick Table Tail, 100% -212 μm (70 mesh), 4psi, 400 g/min

Size (μm)	CONCENTRATE			TAILS			FEED					
	Weight (g)	% Weight	Grade (g/L)	Rec. (%)	Weight (g)	% Weight	Grade (g/L)	Rec. (%)	Weight (g)	% Weight	Grade (g/L)	Dist'n (%)
212	2.55	2.03	1889.51	93.10	10	0.40	34.56	6.90	13	0.48	401.80	0.34
150	40.35	32.20	7585.88	93.41	553	21.46	39.07	6.59	593	21.96	552.65	21.70
105	35.62	28.42	11841.94	93.57	727	28.24	39.89	6.43	763	28.25	591.01	29.86
75	25.96	20.71	12056.10	89.95	841	32.65	41.60	10.05	867	32.10	401.49	23.04
53	14.90	11.89	12496.43	91.02	328	12.76	55.95	8.98	343	12.72	595.88	13.55
37	5.57	4.44	21538.60	90.71	100	3.89	122.47	9.29	106	3.92	1249.44	8.76
25	0.29	0.23	38906.90	60.92	12	0.48	590.65	39.08	13	0.46	1476.40	1.23
-25	0.08	0.06	137300.00	47.89	3	0.12	4002.98	52.11	3	0.11	7481.98	1.52
Total	125.32	100.00	10964.96	91.01	2575	100.00	52.73	8.99	2700	100.00	559.22	100.00

Date: November 9, 1995  
 Barrick Table Tail (100% -70 mesh), 3psi, 400 g/min

Size ( $\mu$ m)	CONCENTRATE				TAILS				FEED			
	Weight (g)	% Weight	Grade (g/l)	Rec. (%)	Weight (g)	% Weight	Grade (g/l)	Rec. (%)	Weight (g)	% Weight	Grade (g/l)	Dist'n (%)
212	1.00	0.74	1884.40	66.61	9	0.33	106.51	33.39	10	0.35	286.64	0.18
150	33.28	24.77	6699.34	59.03	589	21.61	262.73	40.97	622	21.76	606.92	23.37
105	41.84	31.14	6407.35	60.83	763	27.98	226.32	39.17	804	28.13	547.78	27.27
75	34.40	25.60	8014.06	69.35	894	32.79	136.33	30.65	928	32.45	428.34	24.60
53	16.58	12.34	9558.78	85.46	347	12.71	77.83	14.54	363	12.70	510.72	11.47
37	6.85	5.10	20532.85	93.04	109	3.99	96.66	6.96	116	4.04	1307.35	9.35
25	0.34	0.25	84908.82	87.27	13	0.47	331.57	12.73	13	0.46	2537.38	2.05
-25	0.08	0.06	304562.50	83.24	3	0.12	1378.67	16.76	3	0.12	8043.56	1.72
Total	134.37	100.00	8333.41	69.28	2726	100.00	182.16	30.72	2860	100.00	565.11	100.00



**Appendix B-4**

**Cambior's Chimo**

<b>Sample ID: Chimo Grinding Circuit</b>			
<b>Date:</b>	<b>August 17, 1995</b>		
<b>Operator:</b>	<b>Bo Zhang</b>		
<b>screen opening</b>	<b>SAG mill discharge</b>	<b>Screen Oversize</b>	<b>Cyclone Underflow</b>
<b>µm</b>	<b>wt. dis.</b>	<b>wt. dis.</b>	<b>wt. dis.</b>
	<b>%</b>	<b>%</b>	<b>%</b>
9500	1.74	17.91	1.22
6700	1.52	24.63	2.14
4750	1.53	26.75	2.03
3350	1.40	23.07	2.42
2360	1.43	4.24	3.03
1680	1.24	0.85	2.61
1180	1.85	0.55	3.38
850	1.73	0.31	3.01
600	2.11	1.69	2.33
425	3.41		4.47
300	5.58		7.07
212	6.83		8.83
150	18.14		16.70
106	16.56		22.99
75	13.38		5.02
53	8.77		4.89
38	8.95		3.33
25	3.75		4.17
Pan	0.09		0.35
<b>Total</b>	<b>100.00</b>	<b>100.00</b>	<b>100.00</b>

Date: October 9, 1995  
 Chimo 20" kc feed, 6kg, 2.5 psi, 300 g/min

Size (µm)	CONCENTRATE			TAILS			FEED					
	Weight (g)	% Weight	Grade (g/L)	Rec. (%)	Weight (g)	% Weight	Grade (g/L)	Rec. (%)	Weight (g)	% Weight	Grade (g/L)	Dist'n (%)
600	1.28	0.93	3,964	73.53	22	0.38	82	26.47	24	0.39	293	0.22
420	3.20	2.38	27,964	88.65	95	1.63	123	11.35	99	1.65	1048	3.35
300	9.68	7.02	55,689	91.73	318	5.42	153	8.27	328	5.46	1794	19.05
210	14.64	10.61	59,115	89.02	521	8.89	205	10.98	535	8.92	1816	31.51
150	23.64	17.14	26,855	84.78	832	14.19	137	15.22	856	14.26	875	24.27
105	21.70	15.73	12,127	77.68	727	12.40	104	22.32	749	12.48	452	10.98
75	21.15	15.33	5,280	76.60	726	12.39	47	23.40	747	12.45	195	4.73
53	15.77	11.43	3,467	80.04	568	9.69	24	19.96	584	9.73	117	2.21
37	12.77	9.26	2,707	83.18	582	9.94	12	16.82	595	9.92	70	1.35
25	9.43	6.84	2,460	80.76	381	6.50	15	19.24	391	6.51	74	0.93
-25	4.59	3.33	4,674	49.80	1,089	18.58	20	50.12	1,093	18.22	39	1.39
Total	137.93	100.00	19,176	85.73	5,832	100.00	75	14.27	6,000	100.00	514	100.00

Date: October 9, 1995  
 Chimo 20" kc tail, 5.5kg, 2.5 psi, 400 g/min

Size (µm)	CONCENTRATE			TAILS			FEED					
	Weight (g)	% Weight	Grade (g/L)	Rec. (%)	Weight (g)	% Weight	Grade (g/L)	Rec. (%)	Weight (g)	% Weight	Grade (g/L)	Dist'n (%)
600	0.41	0.36	20	1.62	9	0.17	54.44	98.38	10	0.17	52.96	0.12
420	1.45	1.27	5,320	47.32	24	0.45	357.00	52.68	26	0.46	639.13	4.01
300	3.34	2.93	7,878	45.72	88	1.64	354.00	54.28	92	1.67	628.41	14.16
210	6.63	5.81	2,382	31.86	194	3.60	174.00	68.14	201	3.65	246.94	12.20
150	15.06	13.20	1,766	35.93	456	8.47	104.00	64.07	471	8.56	157.13	18.21
105	17.87	15.66	1,203	35.04	595	11.05	67.00	64.96	613	11.14	100.13	15.10
75	19.92	17.46	811	32.28	753	13.98	45.00	67.72	773	14.05	64.74	12.31
53	17.39	15.24	558	39.00	660	12.25	23.00	61.00	677	12.31	36.74	6.12
37	14.65	12.84	454	37.20	661	12.27	17.00	62.80	675	12.28	26.48	4.40
25	9.01	7.90	519	38.07	423	7.85	18.00	61.93	432	7.85	28.46	3.02
-25	8.37	7.34	1,053	20.97	1,523	28.29	21.80	79.03	1,532	27.85	27.43	10.34
Total	114.10	100.00	1,261	35.41	5,386	100.00	48.74	64.59	5,500	100.00	73.89	100.00

Date: October 10, 1995

Chimo 30" kc feed, 10.8kg, 3.0 psi, 482 g/min

Size (µm)	CONCENTRATE				TAILS				FEED			
	Weight (g)	% %Weight	Grade (g/l)	Rec. (%)	Weight (g)	% %Weight	Grade (g/l)	Rec. (%)	Weight (g)	% %Weight	Grade (g/l)	Dist'n (%)
600	2.80	3.04	9	2.10	205	1.91	5.75	97.90	207	1.92	5.79	0.89
420	6.65	7.21	529	62.36	531	4.96	4.00	37.64	538	4.97	10.49	4.17
300	9.84	10.67	2,000	85.41	862	8.05	3.90	14.59	872	8.06	26.43	17.02
210	11.00	11.93	1,212	64.17	1,119	10.45	6.65	35.83	1,130	10.46	18.38	15.34
150	18.89	20.49	1,160	90.70	2,041	19.07	1.10	9.30	2,060	19.07	11.73	17.84
105	18.96	20.56	993	87.41	2,260	21.11	1.20	12.59	2,279	21.10	9.45	15.91
75	13.30	14.42	1,081	86.80	1,508	14.08	1.45	13.20	1,521	14.08	10.89	12.23
53	5.71	6.19	1,266	85.23	626	5.85	2.00	14.77	632	5.85	13.42	6.26
37	2.31	3.16	1,214	80.99	461	4.30	1.80	19.01	464	4.30	9.41	3.22
25	1.47	1.59	2,450	86.03	258	2.41	2.30	13.97	260	2.41	16.37	3.14
-25	0.68	0.74	4,240	53.47	836	7.81	3.00	46.53	837	7.78	6.44	3.98
Total	92.21	100.00	1,182	80.48	10,708	100.00	2.47	19.52	10,800	100.00	12.54	100.00

Date: October 10, 1995

Chimo 30" kc tail, 19.6kg, 3.0 psi, 524 g/min

Size (µm)	CONCENTRATE				TAILS				FEED			
	Weight (g)	% %Weight	Grade (g/l)	Rec. (%)	Weight (g)	% %Weight	Grade (g/l)	Rec. (%)	Weight (g)	% %Weight	Grade (g/l)	Dist'n (%)
600	5.05	5.59	401.43	70.39	474	2.43	1.80	29.61	479	2.44	6.01	2.47
420	8.03	8.89	1,673.50	89.65	1,034	5.30	1.50	10.35	1,042	5.32	14.38	12.88
300	10.17	11.26	941.40	58.27	1,672	8.57	4.10	41.73	1,682	8.58	9.77	14.11
210	10.76	11.92	977.40	80.91	2,157	11.06	1.15	19.09	2,168	11.06	6.00	11.17
150	17.38	19.25	598.10	44.35	3,952	20.26	3.30	55.65	3,970	20.25	5.90	20.13
105	17.63	19.52	408.10	59.34	4,108	21.06	1.20	40.66	4,126	21.05	2.94	10.42
75	12.48	13.82	529.40	55.03	2,633	13.50	2.05	44.97	2,646	13.50	4.54	10.31
53	4.91	5.44	803.33	69.80	1,004	5.15	1.70	30.20	1,009	5.15	5.60	4.85
37	2.25	2.49	1,410.00	67.54	693	3.55	2.20	32.46	695	3.55	6.76	4.03
-37	1.64	1.82	3,351.00	49.09	1,781	9.13	3.20	50.91	1,783	9.10	6.28	9.62
Total	90.30	100.00	801.39	62.16	19,510	100.00	2.26	37.84	19,600	100.00	5.94	100.00

Date: September 7, 1995  
 Chimo cyclone overflow, 2.5psi, 3.6kg, 250 g/min

Size ( $\mu$ m)	CONCENTRATE				TAILS				FEED			
	Weight (g)	% Weight	Grade (g/l)	Rec. (%)	Weight (g)	% Weight	Grade (g/l)	Rec. (%)	Weight (g)	% Weight	Grade (g/l)	Dist'n (%)
150	3.95	6.11	757.71	99.41	18	0.50	1.00	0.59	22	0.60	138.57	5.28
105	5.18	8.02	63.00	82.28	117	3.30	0.60	17.72	122	3.39	3.24	0.70
75	9.53	14.75	81.25	77.44	410	11.56	0.55	22.56	420	11.62	2.38	1.75
53	10.79	16.70	215.50	89.17	403	11.37	0.70	10.83	414	11.47	6.30	4.57
37	11.33	17.53	456.20	90.01	478	13.48	1.20	9.99	490	13.56	11.73	10.07
25	14.70	22.75	543.80	90.05	411	11.59	2.15	9.95	426	11.79	20.86	15.57
-25	9.14	14.14	2569.40	66.91	1709	48.19	6.85	33.09	1718	47.58	20.59	62.05
Total	64.62	100.00	669.28	75.86	3546	100.00	3.88	24.14	3611	100.00	15.79	100.00

Date: September 8, 1995  
 Chimo Unit Cell Tail, 3psi, 6.7kg, 420 g/min

Size ( $\mu$ m)	CONCENTRATE				TAILS				FEED			
	Weight (g)	% Weight	Grade (g/l)	Rec. (%)	Weight (g)	% Weight	Grade (g/l)	Rec. (%)	Weight (g)	% Weight	Grade (g/l)	Dist'n (%)
600	1.95	2.32	7.0	2.53	113	1.70	4.66	97.47	115	1.71	4.70	2.28
420	5.90	7.01	476.0	86.98	323	4.89	1.30	13.02	329	4.91	9.81	13.64
300	9.41	11.18	713.0	87.60	576	8.70	1.65	12.40	585	8.73	13.09	32.37
210	10.61	12.60	85.0	54.69	747	11.29	1.00	45.31	758	11.31	2.18	6.97
150	17.44	20.72	30.0	38.86	1372	20.74	0.60	61.14	1389	20.74	0.97	5.69
105	18.05	21.44	19.0	34.27	1462	22.10	0.45	65.73	1480	22.09	0.68	4.23
75	12.28	14.59	32.0	48.19	939	14.19	0.45	51.81	951	14.20	0.86	3.45
53	4.77	5.67	280.0	83.68	346	5.22	0.70	16.32	350	5.23	4.23	6.26
37	2.30	2.73	603.0	87.19	226	3.42	0.90	12.81	229	3.41	6.95	6.72
25	1.23	1.46	1256.0	77.76	147	2.23	3.00	22.24	149	2.22	13.38	8.40
-25	0.24	0.29	6210.0	63.00	365	5.51	2.40	37.00	365	5.45	6.48	10.00
Total	84.18	100.00	206.2	73.34	6616	100.00	0.95	26.66	6700	100.00	3.53	100.00

## **APPENDIX C**

**Mass balance of size distributions at the gravity circuit of Chimo Mine**

Residual sum of squares: 14.48856

Final Results

Stream	Absolute Solids	Meas	Pulp Mass Flowrate		
	Flowrate		Calc	S.D.	Adjust
1 Feed	60.56	61.0	60.6	2.0	-0.4
2 SAG disc	179.35		179.3		
3 Cyclone U1	50.19	50.0	50.2	5.0	0.2
4 Cyclone U2	69.93	50.0	69.9	50.0	19.9
5 Screen O/S	7.50	6.0	7.5	10.0	1.5
6 Screen U/S	62.43		62.4		
7 KC30 Tails	62.43		62.4		
8 Cell Conc.	1.32	1.3	1.3	0.5	0.0
9 Cyclone O/	59.23		59.2		

Stream	Relative Solids
	Flowrate
1 Feed	100.00
2 SAG disc	296.17
3 Cyclone U1	82.88
4 Cyclone U2	115.47
5 Screen O/S	12.39
6 Screen U/S	103.09
7 KC30 Tails	103.09
8 Cell Conc.	2.18
9 Cyclone O/	97.82

Fractional Size Distribution Data

Size	Meas	SAG disc			Meas	Cyclone U1		
		Calc	SD.	Adj.		Calc	SD.	Adj.
20 mesh	12.43	13.10	0.5	0.7*	19.84	19.65	0.5	-0.2
30 mesh	2.11	1.50	0.5	-0.6*	2.33	2.50	0.5	0.2
40 mesh	3.41	2.98	0.5	-0.4	4.47	4.59	0.5	0.1
50 mesh	5.58	4.74	0.5	-0.8*	7.07	7.31	0.5	0.2
70 mesh	6.83	5.99	0.5	-0.8*	8.83	9.06	0.5	0.2

Size	Meas	Cyclone U2			Meas	Screen O/S		
		Calc	SD.	Adj.		Calc	SD.	Adj.
20 mesh	19.84	19.50	0.5	-0.3	98.31	98.32	0.5	0.0
30 mesh	2.33	2.05	0.5	-0.3	0.90	0.95	0.5	0.0
40 mesh	4.47	4.34	0.5	-0.1	0.60	0.61	0.3	0.0
50 mesh	7.07	6.90	0.5	-0.2	0.10	0.10	0.1	0.0
70 mesh	8.83	8.77	0.5	-0.1	0.00	0.00	0.1	0.0

Size	Meas	Screen U/S			Meas	KC30 Tails		
		Calc	SD.	Adj.		Calc	SD.	Adj.
20 mesh	9.90	10.03	0.5	0.1	10.10	10.03	0.5	-0.1
30 mesh	1.70	2.18	0.5	0.5	2.20	2.18	0.5	-0.0
40 mesh	4.50	4.78	0.5	0.3	4.80	4.78	0.5	-0.0
50 mesh	7.30	7.72	0.5	0.4	7.70	7.72	0.5	0.0
70 mesh	9.40	9.82	0.5	0.4	9.90	9.82	0.5	-0.1

Size	Meas	Cyclone O/		Adj.
		Calc	SD.	
20 mesh	0.00	-0.00	0.1	-0.0
30 mesh	0.00	0.00	0.1	0.0
40 mesh	0.00	0.00	0.1	0.0
50 mesh	0.00	0.00	0.1	0.0
70 mesh	0.10	0.11	0.1	0.0